

Computer Program for Deflection Chart of Simply Supported Prestressed Railway Girder



Addis Ababa University
Addis Ababa Institute of Technology
School of Graduate Studies
School of Civil and Environmental Engineering
Railway Civil Engineering

By: Fiseha Nega

January, 2016



Computer Program for Deflection Chart of Simply Supported Prestressed Railway Girder

By: Fiseha Nega

A thesis submitted to school of graduate studies, Addis Ababa University, Addis Ababa Institute of Technology in partial fulfillment of the requirement for the degree of M.Sc. Railway Civil Engineering

Advisor: - Dr. Essayas G/Yohannes (Ass. Professor)

January, 2016
Addis Ababa University
Addis Ababa
Ethiopia

CERTIFICATION

I, the undersigned below, certify that I read and hereby recommend for the acceptance by the Addis Ababa University a dissertation entitled: **Chart Development for the Estimation of Deflection in Prestressed Railway Girder**: in partial fulfillment of a degree of Masters of Science in Railway Civil Engineering.

Dr. Essayas G/Yohannes (Ass. Professor)

Thesis Advisor

Date: _____

Chart Development for the Estimation of Deflection in Prestressed Railway Girder

A thesis submitted to the school of graduate studies, Addis Ababa University, Addis Ababa Institute of Technology in partial fulfillment of the requirements for the degree of masters of Science in Railway civil engineering.

Date defended: _____

Members of Examining Board:

- 1. _____
-- (Chairman) (Signature)

- 2. _____
-- (Thesis Advisor) (Signature)

- 3. _____
-- (Internal examiner) (Signature)

- 4. _____
-- (External examiner) (Signature)

DECLARATION

Fiseha Nega declares that this thesis; titled as **Chart Development for the Estimation of Deflection in Prestressed Railway Girder** is my original work. This thesis is my individual work and it has not been presented before for any other institute and I will not present it to any other university for similar or any other degree award.

Signature_____.

Abstract

Light rail transit has been under construction in the city for the last two years and it crosses many intersection and roundabouts. Most of the time the rail crosses the road with elevated bridge using a prestressed girder but due to design limitation the span of the bridge is limited and this leads to a number of closely spaced piers in the city centers which interferes with the traffic flow and causes more traffic congestion to the ever growing city of Addis Ababa. Traffic congestion around intersection and round about is the major problem in big cities like Addis Ababa. Therefore when other infrastructure interferes with the existing flow the problem is worse. And one of the main factors that limit the span of the structure is deflection requirement. Therefore being able to assess and know the deflection of prestressed girder as precisely as possible will indeed help in designing an economical large span girders.

In designing prestressed girder, calculating deflection the necessary and rigorous step which one has to calculate at the end of the design process and tell whether the design girder is within the allowable limit or not. If it is not the designer has to change the cross sectional dimension and repeat the whole step once again. But if the designer can certainly know the deflection of that structure in advance of those steps he/she can eliminate such iteration.

Therefore this thesis intended to develop a program that plot a deflection chart for simply supported prestressed railway girder.

MATLAB programing language has been used to develop the program of deflection calculation and to plot the chart. Microsoft excel has also been used to develop a deflection calculation template for checking purpose.

Mainly AAHSTO LRFD Bridge specification, American Concrete Institute (ACI) publications and American Railway Engineering and Maintenance-of-way Association (AREMA) has been used in this thesis but other important material has also been referred when needed.

The findings were one can control the deflection or camber of the prestressed member with the magnitude of the applied load and varying the eccentricity of the tendon profile both at the support and at the mid-span. However the deflection vs. span length chart will show some unexpected behavior after a certain span length. It suddenly changes is dimension and direction in unanticipated manner. And this leads to the development of another chart “the design chart” which tells the minimum prestressing force needed and the working range of a certain geometric section for a given load. And from this we notice that for a given load and a given cross-sectional geometry a prestressed member has not only a maximum span length limit but also a minimum span length limit in order to serve the intended function without failure.

Acknowledgment

First and foremost, praises and thanks to God, the almighty, for providing me the capability to proceed successfully. The thesis appears in current form due to assistance and guidance of several people. I would like to thank offer my sincere thanks to all of them.

I would like to express my deep and sincere gratitude to my research supervisor, Dr. Essayas G/Yohannes, Assistant Professor and Head of School of civil and environmental engineering, for giving me the opportunity to do the research and providing invaluable guidance throughout the research, starting from giving me the core idea of this research. His dynamism, vision, sincerity and motivation have deeply inspired me. The way he simplifies the difficulties I face with in some minutes of discussion that I was mourning about a week and so was a great relief for me and an access road in advancing and progressing in this thesis. He has thought me some courses since I was under grad student and he was an inspiration to most of us to engage and entertain in structural engineering. It was a great honor and privilege to work and study under his guidance. I would like also thank him for his friendship, empathy, and great sense of humor.

I am greatly thankful to my cousin Getahun Melesse (B.Sc. Electrical Engineering), for his guidance and help in every step of the development of MATLAB programming and for answering my silly and frequent questions without boredom and with great motivation.

I would like to offer my sincere thanks to my brother Fetene Nega (M.sc Civil Engineering), for inspiring me in with his great strength and motivational speech. And for helping me a lot in stationary works.

I am extremely grateful my family for their understanding, love, prayers, caring and scarifying for educating and preparing for my future.

The last but not the least my special thanks go to my friends. In helping me in a lot of preparation of paper work, for their comments and insights and their challenging questions to shape and modify my program.

Table of Content

| | |
|--|------|
| Abstract | i |
| Acknowledgment | ii |
| Table of Content | iii |
| List of Table | vi |
| List of Figures | vii |
| List of Abbreviation | viii |
| 1 Introduction | 1 |
| 1.1 Background | 1 |
| 1.2 Statement of the Problem..... | 2 |
| 1.3 Objective | 3 |
| 1.3.1 General Objective | 3 |
| 1.3.2 Specific Objective..... | 3 |
| 2 Literature Review | 4 |
| 2.1 Prestressed Concrete | 4 |
| 2.1.1 Introduction to Prestress Concrete | 4 |
| 2.1.2 Materials for Prestressed Concrete | 6 |
| 2.1.3 Prestress Loss..... | 7 |
| 2.1.4 Tendon Profile (Eccentricity/e)..... | 8 |
| 2.1.5 Minimum Prestressing Force and Maximum Eccentricity | 11 |
| 2.2 Deflection in Reinforced Concrete Beam | 12 |
| 2.2.1 Material properties | 12 |
| 2.2.2 Short-term Deflection..... | 15 |
| 2.2.3 Long – Term Deflection..... | 16 |
| 2.2.4 Temperature-induced deflections..... | 16 |
| 2.3 Deflection of Prestressed Concrete Beam..... | 17 |
| 2.3.1 Prestressing Reinforcement | 17 |
| 2.3.2 Loss of prestress..... | 17 |
| 2.3.3 General approach to curvature and Deflection | 20 |
| 2.3.4 Short-term deflection and camber evaluation in prestressed beams | 24 |
| 2.3.5 Long-term deflection and camber evaluation in prestressed Beams. | 27 |

| | | |
|-------|--|----|
| 2.3.6 | Effect of Tendon Profile on Deflection | 31 |
| 2.4 | Allowable Limit According to AREMA MRE volume 2..... | 34 |
| 2.4.1 | Deflection and Camber | 34 |
| 2.4.2 | Minimum Concrete Cover | 34 |
| 3 | Methodology..... | 35 |
| 3.1 | Camber due to prestressing Tendon..... | 35 |
| 3.2 | Short Term Deflection | 35 |
| 3.3 | Long Term Deflection..... | 36 |
| 3.4 | Geometry..... | 36 |
| 3.5 | Loading | 38 |
| 4 | Analysis | 39 |
| 4.1 | Factors affecting Deflection..... | 39 |
| 4.2 | Loading | 39 |
| 4.2.1 | Self-weight (Wdl) | 39 |
| 4.2.2 | Super imposed Dead Load | 40 |
| 4.2.3 | Live Load | 41 |
| 4.2.4 | Impact Load | 44 |
| 4.3 | Geometry..... | 44 |
| 4.3.1 | Precast Section | 44 |
| 4.4 | Material Property | 51 |
| 4.4.1 | Concrete | 51 |
| 4.4.2 | Prestressing Tendon | 51 |
| 4.5 | Eccentricity and Minimum prestressing reinforcement..... | 52 |
| 4.5.1 | Eccentricity | 52 |
| 4.5.2 | Minimum Prestressing reinforcement..... | 53 |
| 4.6 | Deflection of Prestressed Beam | 54 |
| 4.6.1 | Section Stress | 54 |
| 4.6.2 | Deflection Calculation | 55 |
| 4.6.3 | Example 4.1 | 59 |
| 5 | Result and Discussion..... | 67 |
| 6 | Conclusion..... | 73 |
| 7 | Topics for Further Study..... | 74 |

| | | |
|---|---|-----|
| 8 | Reference | 75 |
| | Appendix A: code for MATLAB Program Language | 76 |
| | Appendix B: Sample Charts plotted using the program | 96 |
| | AASHTO/PCI I beam Type I | 96 |
| | AASHTO/PCI I beam Type II..... | 102 |
| | AASHTO/PCI I beam Type III | 108 |
| | AASHTO/PCI I beam Type IV | 114 |
| | AASHTO/PCI I beam Type V..... | 120 |
| | AASHTO/PCI I beam Type VI..... | 126 |
| | User Defined I beam..... | 132 |

List of Table

| | |
|--|----|
| Table 2-1 Standard Tensile Strength of prestressing bar | 7 |
| Table 2-2 Types of loss in pre-tensioned and post-tensioned members | 7 |
| Table 2-3 PCI suggested multipliers to be used for calculating long term camber and deflection. | 28 |
| Table 4-1 Summary of Super Imposed Dead Load | 40 |
| Table 4-2 Calculation of moments on short, simple span from Table 15-1-6 of AREMA MRE. | 41 |
| Table 4-3 Maximum moments, shears and pier Reaction for Cooper E 80 Live load or alternate load (9) | 42 |
| Table 4-4 Maximum Live load moments for cooper E80 and cooper E 60 live load..... | 43 |
| Table 4-5 section properties of AASHTO I beam type I..... | 45 |
| Table 4-6 section properties of AASHTO I beam type II..... | 46 |
| Table 4-7 section properties of AASHTO I beam type III | 46 |
| Table 4-8 section properties of AASHTO I beam type IV | 47 |
| Table 4-9 section properties of AASHTO I beam Type V | 48 |
| Table 4-10 section properties of AASHTO I beam type VI | 49 |

List of Figures

| | |
|--|----|
| Figure 2-1 Magnel Diagram (5)..... | 10 |
| Figure 2-2 Critical Points on Magnel Diagram (5)..... | 10 |
| Figure 2-3 stress under the application of different loading..... | 22 |
| Figure 2-4 strain under the application of different loading..... | 22 |
| Figure 2-5 Deflection versus time due to prestress and transverse loads..... | 23 |
| Figure 2-6 Moment curvature diagram according to ACI 435..... | 23 |
| Figure 2-7 Camber of beam with straight tendon (2)..... | 31 |
| Figure 2-8 Camber of a beam Trapezoidal or Draped Tendon..... | 31 |
| Figure 2-9 camber of parabolic tendon central anchors (2)..... | 32 |
| Figure 2-10 Camber of parabolic tendon eccentric anchors (2)..... | 32 |
| Figure 2-11 camber of slopping tendon eccentric anchor (2)..... | 33 |
| Figure 2-12 camber of parabolic and straight tendon central anchor (2)..... | 33 |
| Figure 2-13 Camber of parabolic and straight tendon eccentric anchor (2)..... | 33 |
| Figure 3-1 AASHTO/PCI I Beams..... | 37 |
| Figure 3-2 User Defined I beam based AASHTO I beam..... | 38 |
| Figure 3-3 Copper E-80 (EM 360) Axle load Diagram (9)..... | 38 |
| Figure 4-1 Copper E-80 (EM 360) Axle load Diagram (9)..... | 41 |
| Figure 4-2 AAHSTO I beam Type II composite section..... | 45 |
| Figure 4-3 AAHSTO I beam Type II composite section..... | 46 |
| Figure 4-4 AAHSTO I beam Type III composite section..... | 46 |
| Figure 4-5 AAHSTO I beam Type IV composite section..... | 47 |
| Figure 4-6 AAHSTO I beam Type V composite section..... | 48 |
| Figure 4-7 AAHSTO I beam Type VI composite section..... | 49 |
| Figure 4-8 Deflection Chart for AASHTO Type 6 I beam..... | 66 |
| Figure 5-1 Typical deflection vs. Span Length Chart..... | 69 |
| Figure 5-2 Allowable eccentricity and minimum prestressing force vs. span length for type 6 AASHTO I beam for $P_i = 1.25 \cdot P_{imin}$ | 70 |
| Figure 5-3 Allowable eccentricity and minimum prestressing force vs. span length for type 6 AASHTO I beam for $P_i = P_{imin}$ | 71 |

List of Abbreviation

| | |
|-----------------------------------|---|
| <i>ac</i> | :-area of concrete |
| <i>acc</i> | :-area of concrete for composite section |
| <i>Aps</i> | :- area of prestressing reinforcement |
| <i>Apsmin</i> | :- minimum area of prestressing reinforcement |
| <i>C</i> | :-cubic strength of prestressed concrete |
| <i>Cs</i> | :-cubic strength of cast in-situ concrete |
| <i>ec</i> | :- eccentricity at mid span |
| <i>Ecp</i> | :- elastic modulus of prestressed concrete |
| <i>Ecs</i> | :- elastic modulus of cast in-situ concrete |
| <i>edg</i> | :- cantilever length for edge beam |
| <i>ee</i> | :- eccentricity at support |
| <i>emaxc</i> | :- maximum eccentricity at midspan corresponding to Pimin |
| <i>emaxm</i> | :- maximum allowable eccentricity at midspan |
| <i>emaxs</i> | :- maximum allowable eccentricity at support |
| <i>eminm</i> | :- minimum allowable eccentricity at midspan |
| <i>emins</i> | :- minimum allowable eccentricity at support |
| <i>Ep</i> | :- elastic modulus of prestressing reinforcement |
| <i>fbem</i> | :- bottom midspan stress at service |
| <i>fbim</i> | :- bottom midspan stress at transfer |
| <i>fbis</i> | :- bottom support stress at transfer |
| <i>fbsm</i> | :- bottom midspan stress at erection |
| <i>fbss</i> | :- bottom support stress at erection |
| <i>fck</i> | :- characteristic compressive strength of concrete |
| <i>fct</i> | :-compressive strength of concrete at transfer |
| <i>fcw</i> | :-compressive strength of concrete at service |
| <i>fpe</i> | :- effective tensile strength of tendon |
| <i>fpew</i> | :- tensile strength of tendon at service |
| <i>fpi</i> | :- applied tensile strength of tendon |
| <i>fpit</i> | :- tensile strength of tendon at transfer |
| <i>fpk</i> | :- tensile strength of tendon |
| <i>fpv</i> | :- characteristic tensile strength of tendon |
| <i>fr</i> | :- modulus of rupture of concrete |
| <i>f_{tem}</i> | :-top mid span stress at service |
| <i>f_{tim}</i> | :-top mid span stress at transfer |
| <i>f_{tis}</i> | :-top support stress at transfer |
| <i>f_{t_{sm}}</i> | :-top mid span stress at erection |

| | |
|------------|---|
| f_{tss} | :-top support stress at erection |
| f_{tt} | :- tensile strength of concrete at transfer |
| f_{tw} | :- tensile strength of concrete at service |
| H | :- total Depth of a section |
| I_c | :- cracked moment of inertia |
| I_e | :- effective moment of inertia |
| I_f | :- impact factor |
| I_g | :-gross moment of inertia |
| I_{gc} | :-gross moment of inertia for composite section |
| L | :- span length |
| l_e | :- effective length |
| l_{ef} | :- transformed effective length |
| M_{dl} | :- moment due to dead load |
| M_{ll} | :- moment due to live load |
| M_{sl} | :- moment due to live load |
| M_{tot} | :- total load due to all applied gravity load |
| n_p | :- modular ratio between prestressing reinf and prestressed concrete |
| n_s | :- modular ratio between prestressed concrete and cast in-situ slab |
| P_e | :- effective prestressing force |
| p_{ff} | :- ratio of applied prestress force to the minimum prestressing force |
| P_i | :-initial prestressing force |
| P_{imin} | :- minimum prestressing force at transfer |
| P_{min} | :- minimum prestressing force |
| prl | :-prestress loss |
| ts | :- cast in-situ slab thickness |
| w_{dl} | :- self weight per meter length |
| w_{ll} | :-live load per meter length |
| w_{sd} | :- super imposed load per meter length |
| y_b | :- distance from the neutral axis to bottom section of precast beam |
| y_{bg} | :- distance from the neutral axis to bottom section of composite beam |
| Y_c | :- height of neutral axis from bottom section |
| y_t | :- distance from the neutral axis to top section of precast beam |
| y_{tg} | :- distance from the neutral axis to top section of composite beam |
| y_{ts} | :- distance from the neutral axis to top of cast in-situ slab |
| z_b | :- section modulus at bottom section of precast beam |
| z_{bp} | :- section modulus at bottom section of composite beam |
| z_{bs} | :- section modulus at bottom section of cast insitu slab |
| z_t | :- section modulus at top section of precast beam |
| z_{tp} | :- section modulus at top section of composite beam |
| γ_c | :- unit weight of concrete |

| | |
|--------------|--|
| δdl | :- deflection due to dead load |
| δi | :- deflection due to prestressing force |
| δll | :- deflection due to live load |
| δnes | :- net deflection at erection just after super-imposed dead load |
| δnfl | :- net deflection at service just after super-imposed dead load |
| δnt | :- net deflection at transfer |
| δsl | :- deflection due to superimposed live load |
| η | :- the ratio of effective stress to initial stress |

1 Introduction

1.1 Background

Each day, millions of commuters, tourists and students around the globe rely on regional rail transit as their primary source of transportation to and from city centers. This light rail is growing. Over the past several decades, the rapid expansion in city suburbs and a more environmentally conscious public have led city officials to believe that light rail can help alleviate traffic congestion and pollution. In addition, dozens of metropolitan areas across the country also see rail transit as a form of public transportation that can encourage economic development-if light-rail stations are strategically placed and city officials and private developers cooperate with one another.

Addis Ababa is also currently engaged in building This Light Rail Transit (LRT). The LRT, which has a total length of 34.35 km, has two routes – a 16.9-km section running from north to south, and a 17.35-km section stretching from east to west. The two sections run parallel for 2.7 km. The LRT will have a total of 41 cars, each with the capacity to carry 286 passengers at a time. This will enable the LRT to provide transportation to 15,000 people an hour, in one direction, and 60,000 in all four directions.

Addis Ababa’s Light Rail Uses Semi-exclusive: A light rail transit alignment that is in a separate right-of-way or along a street or railroad right-of way where motor vehicles, pedestrians, and bicycles have limited access and cross at designated locations only.” In this case we use Bridges to overpass intersection and roundabouts, to increase the span and to use the depth of the girder effectively, Addis Ababa LRT uses prestressed concrete girder.

Prestressed Concrete is a concrete in which internal stress of suitable magnitude and distribution are introduced so that the stresses resulting from external loads are counteracted to a desired degree. In reinforced concrete the prestress is commonly introduced by tensioning the steel reinforcement. Concrete is a building material that is strong but relatively weak in tension. So prestressing is introduced to overcome this problem. In prestressed concrete construction, steel tendons are stretched and anchored at each end so that compressive forces are applied to the concrete. The forces are transmitted from the tendons to the concrete either by the bond between the concrete and the tendon (pre-tensioning) or by embedded anchorage (post-tensioning), depending on the method of prestressing.

1.2 Statement of the Problem

Addis Ababa is a capital and the largest city of Ethiopia and it is the country's commercial, manufacturing, and cultural center. There are a large number of cars that uses the city's roads in a daily basis. Nowadays the number of car is increasing dramatically with the number of population that is why it became common to see traffic congestion everywhere in the city especially at cross section and roundabouts. The Addis Ababa LRT system has been under construction to minimize transport problem. The LRT passes all three modes of construction at different sites of the city, i.e. Underground, Aboveground and at grade. When the LRT pass through intersection and roundabouts it usually uses aboveground mode of construction (Bridge).

Prestressed girder is being used for construction of the bridge. However due to design limitation, difficulty of construction, and difficulty of hauling heavy pre-cast girder, and various factors the span of the prestressed girder is limited to a length of 40m, this leads to more closely spaced piers in the road. These piers become obstruction to the flow of traffic on the road, which causes more traffic congestion on the intersection and through roads where the rail track passes. And the main reason behind limited depth span is deflection requirement of prestressed girder. And the first step to achieve the possibility of designing large span prestressed girder is determining the deflection requirement of prestressed girder as precisely as possible. An accurate and precise determination of a beam like structure helps the designer to limit the span of the structure based on the allowable deflection for that specific intended purpose.

In designing prestressed girder, calculating deflection the necessary and rigorous step which one has to calculate at the end of the design process and tell whether the design girder is within the allowable limit or not. If it is not the designer has to change the cross sectional dimension and repeat the whole step once again. But if the designer can certainly know the deflection of that structure in advance of those steps he/she can eliminate such iteration.

Therefore this thesis intended to develop a program that plot a deflection chart for simply supported prestressed railway girder.

1.3 Objective

1.3.1 General Objective

The general objective of this thesis is to develop an empirical chart for the estimation of long term and short term deflection in prestressed railway girder based on the method recommended by ACI-435.

1.3.2 Specific Objective

The specific objectives of this thesis are

- To ease the calculation of deflection in prestressed girder
- To help the designer to certainly know the deflection of the selected beam prior to detail design and rigorous calculation.
- To question the ACI-435 method of deflection calculation (As the code itself questions it.) One can use another method or simulation technique to find the deflection of a specified beam and can compare it to the estimated deflection by ACI-435 method as it will be provided in the chart.
- For preliminary design of prestressed railway girder.
- To determine the working range of a given section.
- To increase the adaptation and use of prestressed girder design in the country

2 Literature Review

2.1 Prestressed Concrete

2.1.1 Introduction to Prestress Concrete

2.1.1.1 *Prestressed concrete*

Prestressing is more a philosophy than a specific technique. It means preparing a structure to receive a load by applying a pre-emptive countervailing load. For instance, if it is known that a column will be deflected 100 mm to the left by applied loads, the designer can arrange to bend it 50 mm to the right; the column then only has to be designed to resist a deflection of +/- 50 mm, rather than the full 100 mm. (1)

Prestressed concrete is basically concrete in which internal stresses of a member a suitable magnitude and distribution are introduced so that the stresses resulting from external loads are counteracted to a desired degree. In reinforced concrete members, the prestress is commonly introduced by tensioning the steel reinforcement. (2)

The tensile strength of plain concrete is only a fraction of its compressive strength and the problem of it being deficient in tensile strength appears to have been the driving factor in the development of the composite material known as "reinforced concrete". (2)

The development of early cracks in reinforced concrete due to incompatibility in the strains of steel and concrete was perhaps the starting point in the development of a new material like "prestressed concrete". The application of permanent compressive stress to a material like concrete, which is strong in compression but weak in tension, increases the apparent tensile strength of that material, because the subsequent application of tensile stress must first nullify the compressive prestress. (2)

- Prestressing can be either Pre-tensioned or Post-Tensioned based on method(system) of prestressing
 - *Pre-tensioning*:- A method of prestressing concrete in which the tendons are tensioned before the concrete is placed. In this method, the prestress is imparted to concrete by bond between steel and concrete. (2)
 - *Post-tensioning*:- A method of prestressing concrete by tensioning the tendons against hardened concrete. In this method, the prestress is imparted to concrete by bearing. (2)

Note: - Tendon is stretched element used in a concrete member of structure to impart pre-stress to the concrete. Generally, high-tensile steel wires, bars cables or strands are used as tendons. (2)

- Based on the interaction of tendon and concrete they may be classified as Bonded and Non-bonded

- *Bonded Prestressed concrete*: - Concrete in which prestress is imparted to concrete through bond between the tendons and surrounding concrete. Pre-tensioned members belong to this group (2).
- *Non-bonded Prestressed concrete*: - A method of construction in which the tendons are not bonded to the surrounding concrete. The tendons may be placed in ducts formed in the concrete members or they may be placed outside the concrete section. (2)
- Based on the allowable tensile strength of concrete in the design they may be classified as
 - *Full prestressing*: - Prestressed concrete in which tensile stresses in the concrete are entirely obviated at working loads by having sufficiently high prestress in the members. (2)
 - *Limited or partial prestressing*: - The degree of prestress applied to concrete in which tensile stresses to a limited degree are permitted in concrete under working loads. In this case, in addition to tensioned steel, a considerable proportion of un-tensioned reinforcement is generally used to limit the width of cracks developed under service loads. (2)
- Based on the tendon profile they can be classified as
 - *Axial prestressing*: - Members in which the entire cross-section of concrete has a uniform compressive prestress. In this type of prestressing, the centroid, of the tendons coincides with that of the concrete section. (2)
 - *Eccentric prestressing*: - A section at which the tendons are eccentric to the centroid, resulting in a triangular or trapezoidal compressive stress distribution. (2)
 - *Concordant prestressing*: - Prestressing of members in which the cables follow a concordant profile, In the case of statically indeterminate structures, concordant prestressing does not cause any change in the support reactions. (2)
 - *Non-distortional prestressing*: - In this type, the combined effect of the degree of pre-stress and the dead-weight stresses is such that the deflection of the axis of the member is prevented. In such cases the moments due to prestress and dead-weight exactly balance resulting only in an axial force in the member. (2)
 - *Uniaxial, biaxial and triaxial prestressing*: - The terms refer to the cases where concrete is prestressed (i) in only one direction, (ii) in two mutually perpendicular directions and (iii) in three mutually perpendicular directions. (2)
 - *Circular prestressing*: - The term refers to prestressing in round members, such as tanks and pipes... (2)

2.1.1.2 Advantage of Prestressing

- Tension and cracking under service loads may be avoided or reduced to a low level,

depending on the magnitude of the prestressing force. Avoiding of tensile cracks increase the efficiency of utilization the section compared to reinforced concrete. (3)

- Downward deflections of beams and slabs under service loads may be avoided or greatly reduced. (3)
- Fatigue resistance (i.e. the ability to resist the effect of repeated live loading due to, for instance, road and rail traffic) is considerably enhanced. (3)
- Enable Segmental forms of construction in which different members of a structure are constructed separate and joined to become a monolithic structure. (3)
- Very high strength steel may be used to form the tendons this results in lighter and slender members than is possible with reinforced concrete. The two structural features of prestressed concrete, namely high-strength concrete and freedom from cracks, contribute to the improved durability of the structure under aggressive environmental conditions. Prestressing of concrete improves the ability of the material for energy absorption under impact loads. (2)
- Beam and slab sections may be smaller than in reinforced concrete, due mainly to the capacity to reduce deflection. In the long-span range, prestressed concrete is generally more economical than reinforced concrete and steel. (3)
- Prestressed concrete possess improved resistance to shearing forces, due to the effect of compressive prestress, which reduces the principal tensile stress. The use of curved cables, particularly in long-span members, helps to reduce the shear forces developed at the support sections. (2)
- A prestressed concrete flexural member is stiffer under working loads than a reinforced concrete member of the same depth. However after the onset of cracking, the flexural behavior of a prestressed member is similar to that of reinforce concrete member. (2)

2.1.2 Materials for Prestressed Concrete

2.1.2.1 Concrete

Prestressed concrete requires concrete which has a high compressive strength at a reasonably early age, with comparatively higher tensile strength than ordinary concrete. Low shrinkage, minimum creep characteristics and a high value of Young's modulus are generally deemed necessary for concrete used for prestressed members. Many desirable properties, such as durability, impermeability and abrasion resistance, are highly influenced by the strength of concrete. The minimum 28-day cube compressive strength prescribed in the Indian standard code IS: 1343-1980 is 40 N/mm² for pre-tensioned members and 30 N/mm² for post-tensioned members. (2)

2.1.2.2 High Tensile Steel

For prestressed concrete members, the high-tensile steel used generally consists of wires, bars, or strands. The higher tensile strength is generally achieved by marginally increasing the carbon content in steel in comparison with mild steel. High-tensile steel usually contains 0.6 to 0.85 per cent carbon, 0.7 to 1 percent manganese, 0.05 percent of sulphur and phosphorus with traces of silicon. (2)

The following are standard tensile strength of tendon as N Krishna Raju put it in prestressed concrete fourth edition book by referring the Indian standard

| Nominal Diameter (mm) | Tensile strength (minimum) (N/mm ²) | Elongation (%) |
|-----------------------|---|----------------|
| 2.50 | 2010 | 2.50 |
| 3.00 | 1865 | 2.50 |
| 4.00 | 1715 | 3.00 |
| 5.00 | 1570 | 4.00 |
| 7.00 | 1470 | 4.00 |
| 8.00 | 1375 | 4.00 |

Table 2-1 Standard Tensile Strength of prestressing bar

2.1.3 Prestress Loss

The initial prestress in concrete undergoes a gradual reduction with time from the stage of transfer due to various causes. This is generally referred to as 'loss of pre-stress'. A reasonably good estimate of the magnitude of loss of prestress is necessary from the point of view of design. Types of prestress loss in pre-tensioned and post-tensioned members are summarized as follows. (2)

| Types of Loss | Pre-Tensioned Member | Post-tensioned Member |
|---------------|---------------------------------|--|
| No | | |
| | Elastic deformation of concrete | No loss due to elastic deformation if all wires are simultaneously tensioned, However if the wires are successively there will be loss |
| 1 | Relaxation of stress in steel | Relaxation of stress in steel |
| 2 | Shrinkage of concrete | Shrinkage of concrete |
| 3 | Creep of concrete | Creep of concrete |
| 4 | | Friction |
| 5 | | Anchorage Slip |

Table 2-2 Types of loss in pre-tensioned and post-tensioned members

In addition to the above, there may be losses of prestress due to sudden changes in temperature, especially in steam curing of pre-tensioned units. The rise in temperature causes a partial transfer of prestress (due to the elongation of the tendons between adjacent units in the long-line process) which may cause a large amount of creep if the concrete is not properly cured. (2)

The details of the prestress loss will be presented in *section 2.3.2*

2.1.4 Tendon Profile (Eccentricity/e)

Eccentricity is the distance of the tendon from the neutral axis. The combination of prestress force and eccentricity greatly affect the deflection of a member. In fact designing prestressed member is all about finding the combination of prestressing force and the corresponding eccentricity at a section for a given loading.

Once the section modulus of a beam is defined the next step is determine what combination of prestress force, P and eccentricity, e, to use at that section. Taking each stress limit in turn: (4)

a. Tensile Stress at transfer (top section)

$$-f_{tt} \leq \frac{P_i}{A_c} - \frac{P_i * e}{Z_t} + \frac{Mg}{Z_t} \quad \text{Equation 2-1}$$

Solving for e

$$e \leq \frac{Z_t * f_{tt}}{P_i} + \frac{Z_t}{A_c} + \frac{Mg}{P_i} \quad \text{Equation 2-2}$$

Solving for p

$$p_i \geq \frac{-f_{tt} + Mg/Z_t}{1/A_c - e/Z_t} \quad \text{Equation 2-3}$$

$$\frac{1}{P_i} \geq \frac{1/A_c - e/Z_t}{-f_{tt} - Mg/Z_t}$$

b. Compressive Stress at Transfer (Bottom Section)

$$f_{ct} \geq \frac{P_i}{A_c} + \frac{P_i * e}{Z_b} - \frac{Mg}{Z_b} \quad \text{Equation 2-4}$$

Solving for e

$$e \leq \frac{Z_b * f_{ct}}{P_i} - \frac{Z_b}{A_c} + \frac{Mg}{P_i} \quad \text{Equation 2-5}$$

Solving for p

$$p_i \leq \frac{f_{ct} + Mg/Z_b}{1/A_c + e/Z_b}$$

$$\frac{1}{P_i} \geq \frac{1/Ac + e/Zb}{f_{ct} + Mg/Zb} \quad \text{Equation 2-6}$$

c. Compressive Stress in Service (Top section)

$$f_{cw} \geq \frac{Pe}{Ac} - \frac{Pe * e}{Zt} + \frac{M_{tot}}{Zt} \quad \text{Equation 2-7}$$

Solving for e

$$e \geq -\frac{Zt * f_{cw}}{\eta P_i} + \frac{Zt}{Ac} + \frac{M_{tot}}{\eta P_i} \quad \text{Equation 2-8}$$

Solving for p

$$p_i \leq \frac{f_{cw} - M_{tot}/Zt}{\eta * (1/Ac - e/Zt)}$$

$$\frac{1}{P_i} \geq \frac{\eta * (1/Ac - e/Zt)}{f_{cw} - M_{tot}/Zt} \quad \text{Equation 2-9}$$

d. Tensile Stress in Service (Top section)

$$f_{tw} \leq \frac{Pe}{Ac} + \frac{Pe * e}{Zb} - \frac{M_{tot}}{Zb} \quad \text{Equation 2-10}$$

Solving for e

$$e \geq -\frac{Zb * f_{tw}}{\eta P_i} - \frac{Zb}{Ac} + \frac{M_{tot}}{\eta P_i} \quad \text{Equation 2-11}$$

Solving for p

$$p_i \geq \frac{-f_{tw} + M_{tot}/Zb}{\eta * (1/Ac + e/Zb)}$$

$$\frac{1}{P_i} \leq \frac{\eta(1/Ac + e/Zb)}{-f_{tw} + M_{tot}/Zb} \quad \text{Equation 2-12}$$

Those equations solved for e gives the limiting zone of the eccentricity.

I.e. Equation 2.2 and 2.5 gives the maximum allowable limit, whereas the Equation 2.8 and 2.11 gives the minimum range of the limiting zone.

Note: - The effect of tendon profile in deflection will be discussed in section 2.3.6

Using the equations solved for p and $1/p_i$ vs. e we get the famous Magnel Diagram (5)

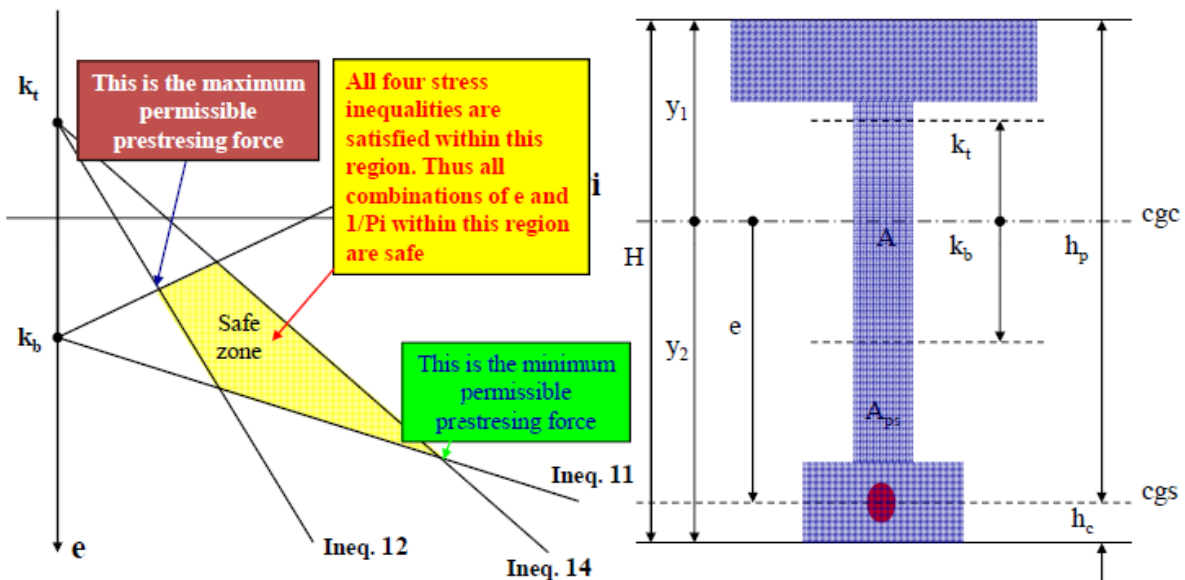


Figure 2-1 Magnel Diagram (5)

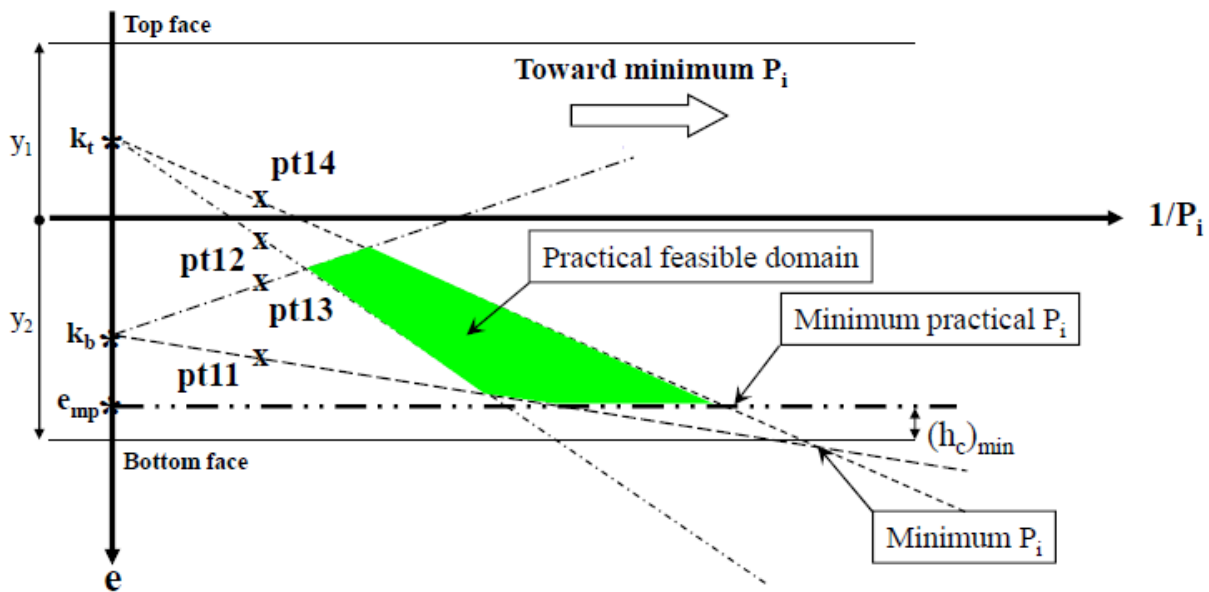


Figure 2-2 Critical Points on Magnel Diagram (5)

2.1.5 Minimum Prestressing Force and Maximum Eccentricity

As we can see from the above diagram the minimum possible prestressing ($p_{i_{min}}$) force is when $1/p_i$ is maximum in the allowable range. And at that point there will be the corresponding Maximum eccentricity (e_{max}). This condition met when the line from case A and the line from case D cross each other.

Case A Tensile stress at transfer (Top Section)

Case D Tensile stress at Service (Bottom Section)

Equating Eqn 2-3 and Eqn 2-12

$$\frac{-Zb * ftw}{\eta Pi} - \frac{Zb}{Ac} + \frac{Mtot}{\eta Pi} = \frac{Zt * ftt}{Pi} + \frac{Zt}{Ac} + \frac{Mg}{Pi} \quad \text{Equation 2-13}$$

Solving for pi

$$P_{imin} = Ac * \frac{1/\eta * (-Zb * ftw + Mtot) - (Zt * ftt + Mg)}{(Zt + Zb)} \quad \text{Equation 2-14}$$

Solving for e

$$e_{max} = \frac{Zt * Zb * (-ftw/\eta + ftt + Mtot/(\eta * Zb) + Mg/Zt)}{Ac * (-Zb * ftw + Zt * ftt + Mtot/\eta + Mg)} \quad \text{Equation 2-15}$$

Similarly Maximum Possible prestressing force and minimum eccentricity can be found using case B and C.

Case B Compressive stress at transfer (Bottom Section)

Case C Compressive Stress at Service (Top Section)

Solving for pi

$$P_{imax} = Ac * \frac{1/\eta * (Zt * fcw - Mtot) + (Zb * fct + Mg)}{(Zt + Zb)} \quad \text{Equation 2-16}$$

2.2 Deflection in Reinforced Concrete Beam

With the advancement of concrete technology, plus the use of higher strength concrete with steel reinforcement has permitted more material efficient reinforced concrete designs as prestressed members enables to produce shallower and smaller sections. Smaller sections have less stiffness that can result in larger deflections: (6)

Consequently, precise determination of short-term and long-term deflection of these structures has become more critical. In many structures, deflection rather than stress limitation is the controlling factor. Deflection computations determine the proportioning of many of the structural system elements. As prestressed concrete is hardly different from reinforced ones, understanding and analyzing of the deflection of reinforced concrete members should be the first step towards that of the analysis of deflection of prestressed concrete member. (6)

2.2.1 Material properties

The principal material parameters that influence concrete deflection are (6)

- modulus of rupture
- modulus of elasticity
- Creep, and shrinkage

2.2.1.1 Concrete modulus of rupture-

It is the flexural tensile strength of concrete. .ACI 318 (1989) recommends the following equation for computing the modulus of rupture of concrete with different density

| | |
|---|---------------|
| $f_r = 0.623 * \lambda \sqrt{f_c'} \text{ MPa}$ | Equation 2-17 |
|---|---------------|

Where λ = 1.0 for normal density concrete 2325 to 2400 kg/m³
 = 0.85 for semi low-density 1765 to 2325 kg/m³
 = 0.75 for low-density concrete 1445 to 1765 kg/m³

The above equation is to be used for low-density concrete when the tensile splitting strength, f_{ct} , is not specified. Otherwise, it should be modified by substituting $f_{ct}/6.7$ for $\sqrt{f_c'}$, but the value of $f_{ct}/6.7$ should not exceed $\sqrt{f_c'}$ (6)

ACI Committee 435 (1978) recommended the following equation for computing the modulus of rupture of concrete with densities (w_c) in the range of 1445 kg/m³ to 2325 kg/m³. This equation yields higher values of f_r (6)

| | |
|--|---------------|
| $f_r = 0.01 * \sqrt{w_c * f_c'} \text{ , MPa}$ | Equation 2-18 |
|--|---------------|

According to ACI 363 (1984), the modulus of rupture of both low-density and normal density high-strength concretes (more than 42 MPa) ranges between $0.623\sqrt{f_c'}$ and $0.997\sqrt{f_c'}$. ACI 363

(1992) recommended the following equation for the prediction of the modulus of rupture of normal density concretes having compressive strengths of 21 MPa to 83 MPa. (6)

| | |
|---------------------------|---------------|
| $f_r = 0.971 \sqrt{f_c'}$ | Equation 2-19 |
|---------------------------|---------------|

The degree of scatter in results in the above equations is indicative of the uncertainties in predicting computed deflections of concrete members. (6)

2.2.1.2 Concrete modulus of elasticity –

It is the slope of stress and strain diagram or simply the ratio of stress to strain. The modulus of elasticity of concrete is mainly influenced by the concrete materials and proportions used. As the compressive strength of concrete increases the modulus of Elasticity also increases, since the slope of the ascending branch of the stress-strain diagram becomes steeper for higher-strength concretes, but at a lower rate than the compressive strength. The value of the secant modulus of elasticity for normal-strength concretes at 28 days is usually around 28,000 MPa, whereas for higher-strength concretes, the modulus of elasticity can range between 49,000 to 56,000 MPa. These higher values of the modulus can be used to reduce short-term and long term deflection of flexural members since the compressive strength is higher, resulting in lower creep levels. (6)

Normal strength concretes are those with compressive strengths up to 42 MPa while higher strength concretes achieve strength values beyond 42 MPa. ACI 435 (1963) recommended the following expression for computing the modulus of elasticity of concretes with densities in the range of 1445 kg/m³ to 2325 kg/m³ based on the secant modulus at 0.0031fc' intercept (6)

| | |
|--|---------------|
| $E = 0.043 * w_c^{1.5} * \sqrt{f_c'} \text{ MPa}$ | Equation 2-20 |
| For normal weight concrete around (150pcf)/2400Kg/m ³ - $E_c = 57000 * \sqrt{f_c'} \text{ psi}$ Or $E_c = 4734 * \sqrt{f_c'} \text{ MPa}$ | Equation 2-21 |

However, as the strength of concrete increases, the E_c value determined by this formula will be lower than the actual value. Therefore ACI 363 (1984) recommended the following modified expression for normal weight concrete: (6)

| | |
|---|---------------|
| $E_C = 3321 * \sqrt{f_c'} + 6895, \text{Mpa}$ | Equation 2-22 |
|---|---------------|

2.2.1.3 Steel reinforcement modulus of elasticity-

ACI 318 specifies using the value $E_s = 200 \times 10^6 \text{ MPa}$ ($29 \times 10^6 \text{ psi}$) for the modulus of elasticity of non prestressed reinforcing steel. (6)

2.2.1.4 Concrete creep and shrinkage-

Deflections are also a function of the age of concrete at the time of loading due to the long-term effects of shrinkage and creep which significantly increase with time. A CI 435

(1978) suggested that the average values for C_u and $(\epsilon_{sh})_u$ can be estimated as 1.60 and 400×10^{-6} respectively. (6)

Where C_u = ultimate creep coefficient of concrete
 $(\epsilon_{sh})_u$ = ultimate shrinkage strain of concrete

These values correspond to the following conditions:

- 70 percent average relative humidity
- age of loading, 20 days for both moist and steam cured concrete
- Minimum thickness of component, 6 in. (152 mm)

Table 2.1 of ACI 435 gives creep and shrinkage ratios at different times after loading

The coefficient for creep at time t (days) after load application, is given by the following expression: (6)

| | |
|--|---------------|
| $Ct = \left(\frac{t^{0.6}}{10 + t^{0.6}} \right) * C_u$ | Equation 2-23 |
|--|---------------|

Where $C_u = 2.35 * \gamma CR$

$\gamma CR = K_{hc} * K_{dc} * K_{sc} * K_{fc} * K_{acc} * K_{toc} = 1$ for standard condition

Graphic representations and general equations for the modification factors (K -values) for non-standard conditions are given in Fig. 2.1 of ACI 435.

For moist-cured concrete, the free shrinkage strain which occurs at any time t in days, after 7 days from placing the concrete (6)

| | |
|---|---------------|
| $(\epsilon_{sh})_t = \left(\frac{t}{35 + t} \right) * (\epsilon_{sh})_u$ | Equation 2-24 |
|---|---------------|

And for steam cured concrete, the shrinkage strain at any time t in days, after 1-3 days from placing the concrete

| | |
|---|---------------|
| $(\epsilon_{sh})_t = \left(\frac{t}{55+t} \right) * (\epsilon_{sh})_u$ | Equation 2-25 |
|---|---------------|

Where $(\epsilon_{sh})_u \max = 780E - 6 * \gamma sh$

$\gamma sh = K_{hs} * K_{ds} * K_{fs} * K_{acs} * K_{bs} = 1$ For standard condition.

Graphic representations and general equations for the modification factors (K -values) for non-standard conditions are given in Fig. 2.1 of ACI 435

Except for age of concrete at load application, the standard conditions for both creep and shrinkage are (6)

- a) Age of concrete at load applications = 3 days (steam), 7 days (moist)
- b) Ambient relative humidity = 40 percent
- c) Minimum member thickness = 6 in. (150 mm)
- d) Concrete consistency = 3 in. (75 mm)
- e) Fine aggregate content = 50 percent f) Air content = 6 percent

2.2.2 Short-term Deflection

2.2.2.1 Uncracked members - Gross moment of Inertia, I_g

When the maximum flexural moment at service load in a beam or a slab causes a tensile stress less than the modulus of rupture, no flexural tension cracks develop at the tension side of the concrete element if the member is not restrained or the shrinkage and temperature tensile stresses are negligible. In such a case, the effective moment of inertia of the uncracked transformed section, (I_t) is applicable for deflection computations. However, for design purposes, the gross moment of inertia (I_g) neglecting the reinforcement contribution, can be used with negligible loss of accuracy. (6)

The elastic deflection for non-cracked members can thus be expressed in the following general form

| | |
|--|---------------|
| $\delta = K * \frac{M * l^2}{E_c * I_g}$ | Equation 2-26 |
|--|---------------|

Where: - K is a factor that depends on support fixity and loading conditions. M is the maximum flexural moment along the span. E_c is the modulus of elasticity. (6)

2.2.2.2 Cracked members-Effective moment of inertia I_e

Tension cracks occur when the imposed loads cause bending moments in excess of the cracking moment, thus resulting in tensile stresses in the concrete that are higher than its modulus of rupture. The cracking moment, M_{cr} computed as follows.

| | |
|----------------------------------|---------------|
| $M_{Cr} = \frac{f_r * I_g}{Y_t}$ | Equation 2-27 |
|----------------------------------|---------------|

Where y_t is the distance from the neutral axis to the tension face of the beam, and f_r is the modulus of rupture of the concrete. (6)

Cracks develop at several sections along the member length. While the cracked moment of inertia, I_{cr} applies to the cracked sections, the gross moment of I_g inertia, applies to the uncracked concrete between these sections. (6)

the initial deflections δ_i occurring in a beam or a slab after the maximum moment M_a has exceed the cracking moment can be evaluated using the effective moment of inertia I_e .

To find I_e according to ACI 318 – 89

a. Simply Supported beams - the effective moment of inertia I_e proposed by Branson

| | |
|---|---------------|
| $I_e = \left(\frac{M_{cr}}{M_a}\right)^3 * I_g + \left[1 - \left(\frac{M_{cr}}{M_a}\right)^3\right] * I_{cr} \leq I_g$ $I_e = I_{cr} + \left(\frac{M_{cr}}{M_a}\right)^3 * (I_g - I_{cr}) \leq I_g$ | Equation 2-28 |
|---|---------------|

The two moments of inertia I_g and I_{cr} are based on the assumption of bilinear load-deflection

behavior. I_e provides the transition between the upper bounds of I_g and lower bounds of I_e . The cracking moment of inertia, I_{cr} can be obtained from Fig. 2.3 of ACI 435R – 95 (6)

b. Continuous beams – I_e , effective moment of inertia taken as the average values obtained from the above equation for critical positive and negative moment section i.e. at mid span and the support section. Accordingly ACI 318 – 89 given the following weighted average formula. (6)

For beams continuous on one end only

| | |
|---|---------------|
| $I_e = 0.85 * (I_{em}) + 0.15 * (I_{e1})$ | Equation 2-29 |
|---|---------------|

For beams continuous on both ends

| | |
|--|---------------|
| $I_e = 0.70 * (I_{em}) + 0.15 (I_{e1} + I_{e2})$ | Equation 2-30 |
|--|---------------|

Where m refers to mid span and 1 and 2 refers to the two end span.

2.2.3 Long - Term Deflection

2.1.3.1 ACI method. Time dependent deflection of one way flexural member is due to creep and shrinkage and can be calculated by applying a multiplier, λ , to the elastic deflection ACI-318. (7)

| | |
|-------------------------------------|---------------|
| $\lambda = \frac{\xi}{1 + 50\rho'}$ | Equation 2-31 |
|-------------------------------------|---------------|

ρ' = reinforcement ratio for non-prestressed compression steel reinforcement

ξ = time dependent factor, from (ACI 318, 1989)

Therefore the total long term deflection is

| | |
|---|---------------|
| $\delta_{lt} = \delta_l + \lambda t * \delta_{sus}$ | Equation 2-32 |
|---|---------------|

δ_l = initial live load deflection

δ_{sus} = initial deflection due to sustained load

λt = time dependent multiplier for a defined duration time.

Due to lower creep strain characteristics, high strength concrete members exhibit less sustained load deflection than those of low strength concrete members.

ACI 365R – 95 Introduce a modifier μ to account for material and section property (6)

| | |
|--|---|
| $0.7 \leq \mu = 1.3 - 0.00005fc' \leq 1.0$ | Equation 2-33 |
| Accordingly | $\lambda = \frac{\mu\xi}{1 + 50\mu\rho'}$ |

2.2.4 Temperature-induced deflections

In unrestrained flexural member deflection occur when there is a temperature gradient between the opposite faces of the member. If the member is restrained from deforming under the action of temperature changes, internal stresses are developed even if the temperature is uniform on the opposite faces. Cracking that occurs when tensile stresses exceed the concrete tensile strength reduces the flexural stiffness of the member and results in increased deflections under subsequent loading. (6)

2.3 Deflection of Prestressed Concrete Beam

In the design of prestressed concrete structures, the deflections (i.e. both short term and long term) are usually the governing criteria in the determination of the required member sizes. The use of high strength materials which result in slender members leads to higher deflection. And because of this deflection in prestressed member should be carefully examined. (6)

2.3.1 Prestressing Reinforcement

Because of the creep and shrinkage which occurs in concrete, effective prestressing can only be achieved by using high strength steel. (6)

2.3.1.1 *Modulus of elasticity-*

In considering time-dependent deflections resulting from shrinkage and creep at the level of the prestressing steel, it is important to have a reasonably good estimate of the modulus of elasticity of the prestressing reinforcement. However for short term deflection, since the cross sectional area of the reinforcing tendon in a beam is insignificant the deflection is calculated based on the gross moment of inertia of concrete. (6)

since the reinforcement is rarely stressed into the inelastic range in calculating deflections under working loads, it is sufficient to use the modulus of elasticity of the prestressing reinforcement rather than to be concerned with the characteristics of the entire stress-strain curve. According to PCI Design hand book the modulus of elasticity of prestressed reinforcement $E = 28.5E6$ psi (196.5Gpa). (6)

2.3.1.2 *Steel relaxation-*

Stress relaxation in prestressing steel is the loss of prestress that occurs when the wires or strands are subjected to essentially constant strain over a period of time. As time goes the loss of prestress force increases. This decreasing of the magnitude of prestress force depends not only on the duration of the sustained prestressing force, but also on the ratio f_{pi}/f_{py} of the initial prestress to the yield strength of the reinforcement. Such a loss in stress is termed intrinsic stress relaxation. (6)

2.3.2 Loss of prestress

2.3.2.1 *Elastic shortening loss –*

A concrete element shortens when a prestressing force is applied to it due to the axial compression imposed. Simultaneously the tendons that are bonded to the adjacent concrete shorten because of this they lose part of the prestressing force that they carry. In pretensioned members, this, force results in uniform longitudinal shortening, which in turn results in a prestress loss. In posttensioned beams, elastic shortening is zero if all tendons are simultaneously

jacked and becomes half the value of that of the pretensioned case if several sequential jacking steps are applied. (6)

2.3.2.2 Loss of prestress due to creep of concrete-

The deformation or strain resulting from creep losses is a function of the

- Magnitude of the applied load and its duration
- Properties of the concrete including its mix proportions
- Curing conditions
- The size and shape of the element
- Its age at first loading and the environmental conditions. (6)

The creep stress/strain relationship is linear and one can relate the elastic strain (ϵ_{el}) to the creep strain (ϵ_{cr}).

According to ACI 435 – 95 the ultimate creep coefficient $C_u = \epsilon_{cr}/\epsilon_{el}$

As we discussed in the reinforced concrete section (6)

| | |
|--|---------------|
| $Ct = \left(\frac{t^{0.6}}{10 + t^{0.6}} \right) * C_u$ | Equation 2-35 |
|--|---------------|

The value of C, usually ranges between 2 and 4, with an average of 2.35 for ultimate creep.

The prestress loss due to creep is defined as (6)

| | |
|--|---------------|
| $\Delta f_{pcr} = C_u \frac{EPS}{EC} f_{cs}$ | Equation 2-36 |
|--|---------------|

Where f_{cs} is the stress in the concrete at the level of the prestressing tendon centroid. In post tension tendon members, the loss can be considered essentially uniform along the whole span. Therefore an average value of the concrete stress between the anchorage points can be used for calculating the creep in post-tensioned members.

Accordingly A modified ACI-ASCE expression for creep loss is

| | |
|--|----------------|
| $\Delta f_{pcr} = K_{cr} \frac{EPS}{EC} (f_{cs}' - f_{csd})$ | Equation 2-37/ |
|--|----------------|

Where $K_{cr} = 2.0$ for pretensioned member

$= 1.60$ for post tensioned

f_{cs}' = stress in concrete at the cgs level of the reinforcement immediately after transfer

f_{csd} = stress in concrete at the cgs level of the reinforcement due to all superimposed dead loads applied after prestressing is accomplished. (6)

2.3.2.3 Loss of prestress due to shrinkage of concrete –

Factors that affect the magnitude of shrinkage of concrete is pretty much the same as that of creep. In addition type of aggregate and cement also affect magnitude of shrinkage of concrete plus magnitude of the applied load has no effect on it.

According to ACI 365 Approximately 80 percent of shrinkage takes place in the first year of life of the structure. The average value of ultimate shrinkage strain in both moist-cured and stream-cured concrete is given as $780E-6$ mm/mm. This average value is affected by the duration of initial moist curing, ambient relative humidity, volume-surface ratio, temperature; and concrete composition. To take such effects into account, the average value of shrinkage strain should be multiplied by adjusting for relative humidity at volume-to-surface ratio a correction factor γ_{sh} (6)

| | |
|--|---------------|
| $\epsilon_{sh} = (780E - 6) * \gamma_{sh}$ | Equation 2-38 |
|--|---------------|

PCI handbook gives nominal ultimate shrinkage strain $\epsilon_{shu} = 820E-6$ mm/mm (8)

The loss in prestressing in pretensioned members is

| | |
|---|---------------|
| $\Delta f_{psh} = \epsilon_{sh} * E_{ps}$ | Equation 2-39 |
|---|---------------|

For post tensioned members

| | |
|--|---------------|
| $\Delta f_{psh} = (8.2E - 6) * K_{sh} * E_{ps} \left(1 - 0.06 \frac{V}{S}\right) (100 - RH)$ | Equation 2-40 |
|--|---------------|

Where $K_{sh} = 1.0$ for pretensioned members

K_{sh} value for post tensioned member is give in table 3.1 of ACI 365 – 95

V/S is the volume surface ratio.

ϵ_{sh} is the shrinkage strain after adjusting for relative humidity at volume-to-surface ratio V/S (6)

Adjustment of shrinkage losses for standard conditions as a function of time t in days (6)

➤ Moist curing, after seven days:

| | |
|--|----------------|
| $(\epsilon_{sh})_t = \frac{t}{35 + t} (\epsilon_{sh})_u$ | Equation 2-41; |
|--|----------------|

➤ Steam curing, after one to three days

| | |
|--|---------------|
| $(\epsilon_{sh})_t = \frac{t}{55 + t} (\epsilon_{sh})_u$ | Equation 2-42 |
|--|---------------|

2.3.2.4 Friction losses in post-tensioned beams -

Loss of prestressing occurs in post-tensioned members due to friction between the tendons and the surrounding concrete ducts.

The magnitude of this loss is a function of

- The curvature effect (the tendon alignment and form)
- The wobble effect (local deviation in alignment)

Section 186.2 of ACI 318-89 give the friction coefficients that apply to the friction loss in the various types of prestressing wires and tendons. (6)

2.3.2.5 Total Loss allowed for design-

It is normal practice in the design of prestressed concrete members to assume total loss of stress as a percentage of the initial stress and provide for this in the design computations.

Assuming temporary overstressing is done to reduce relaxation, to compensate for friction and anchorage losses the following table is provided as a summary of average losses in *prestressed concrete*, fourth edition by N Krishna Raju. (2)

| Types of losses | percentage of losses | |
|--|----------------------|-----------------|
| | Pre-tensioning | Post-tensioning |
| Elastic shortening and bending of concrete | 4 | 1 |
| Creep of concrete | 6 | 5 |
| Shrinkage of concrete | 7 | 6 |
| Creep in steel | 8 | 8 |
| Total | 25 | 20 |

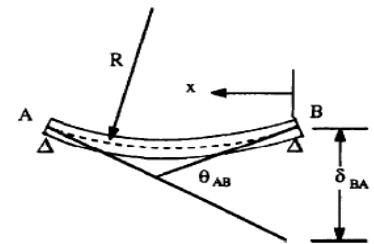
$$n(\text{reduction factor}) = \frac{f_{pi}}{f_{pe}}$$

The value of n is generally taken as 0.75 for pre-tensioning and 0.8 for post-tensioning. (2)

2.3.3 General approach to curvature and Deflection

The curvature at any section is defined as $\Phi = 1/R$ where R is the radius of the curve. And from the famous Mohr circle (moment area theorem) the two equations can be derived. (6)

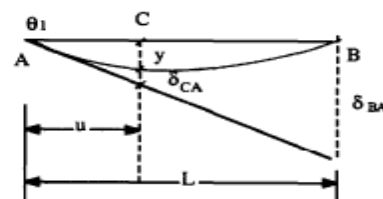
| | |
|--|---------------|
| $(\text{Rotation}) \theta_{AB} = \int_A^B \Phi dx$ | Equation 2-43 |
| $(\text{Deflection}) \delta_{BA} = \int_B^A \Phi x dx$ | Equation 2-44 |



When the material is linearly elastic Φ can be replaced by M/EI

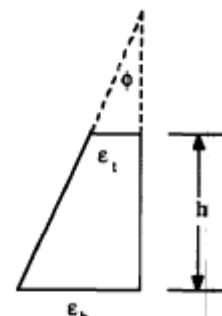
To calculate the deflection at any point

| | |
|------------------------------------|---------------|
| $\theta = \delta_{BA}/L$ | Equation 2-45 |
| $\delta_{BA} = \int_B^A \Phi x dx$ | Equation 2-46 |
| $y = \theta_1 u - \delta_{CA}$ | Equation 2-47 |



Critical variables that affect the magnitude of short term deflection of a prestressed beam are the magnitude of the strain or stress gradient or the curvature at a section and its variation along the span. Which are a function of

- the magnitude and distribution of the load
- the magnitude and eccentricity of the prestress,
- the length of the span,
- the size and configuration of the cross section,
- boundary conditions
- and the properties of the concrete. (6)

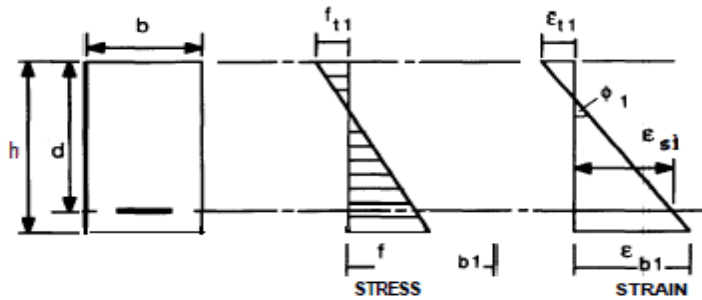


$$\text{Curvature } \Phi = (\epsilon_b - \epsilon_t)/h = M/(Ecl) \quad (2.26)$$

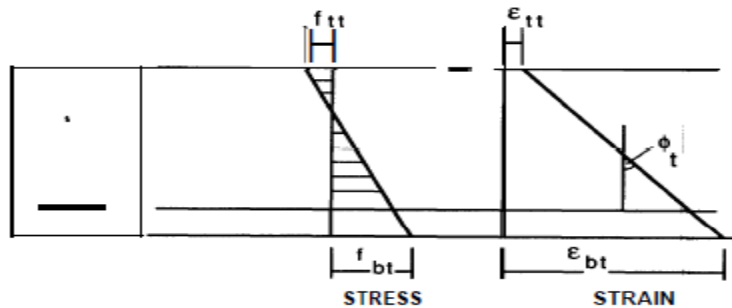
2.3.3.1 Beams subjected to prestressing only-

The stress at any level is given by (6)

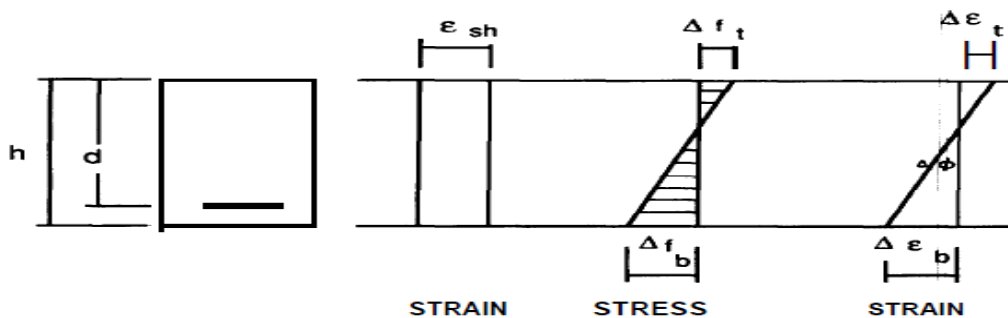
| | |
|------------------------------------|---------------|
| $f = \frac{P}{A} \pm \frac{My}{I}$ | Equation 2-48 |
| $M = P * e$ | Equation 2-49 |



1. *Stress and strain distribution immediately after application of prestress*



2. *Stress and strain distribution at a time t after initial application of prestress*



3. *Stress and strain due to shrinkage*

The distribution of shrinkage strain causes a reduction in the reinforcement strain which corresponds to a reduction in the prestress. The loss in prestress causes a change in the stress

distribution over the depth of the section. (6)

| | |
|--|---------------|
| $\Delta\Phi = \frac{\Delta\epsilon_b - \Delta\epsilon_t}{h}$ | Equation 2-50 |
|--|---------------|

The effect of the relaxation losses in the steel reinforcement is quite similar to that of shrinkage. The effects of the creep of the concrete are not as simple, since the reduction in steel stress causes changes in the rate of creep strain. The change in strain caused by creep change the strain distribution. This change involves a contraction at the level of the steel, hence, a reduction in prestress. The reduction in prestress caused by creep, shrinkage, and relaxation decreases the normal stress, which in turn reduces the rate of creep. (6)

2.3.3.2 Beams subjected to prestressing and external loads

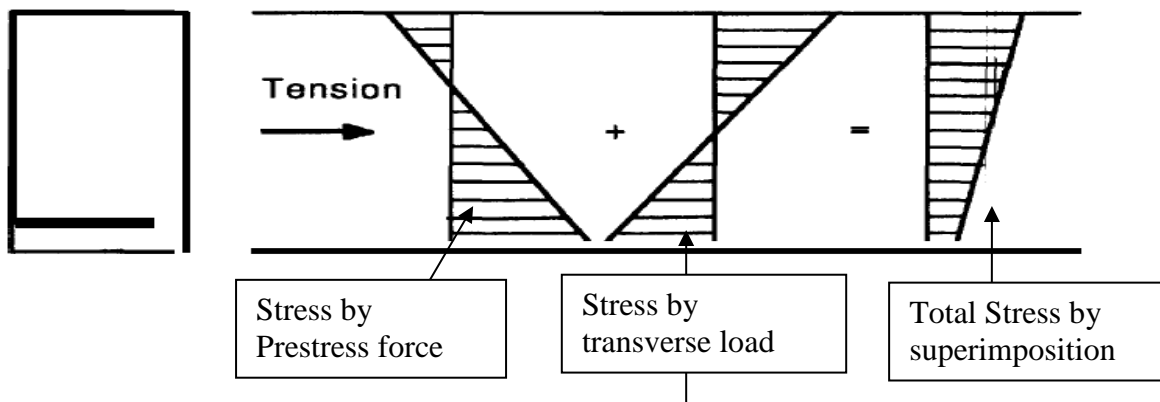


Figure 2-3 stress under the application of different loading

In the above diagram it is assumed that neither concrete nor reinforcement is strained into the inelastic range.

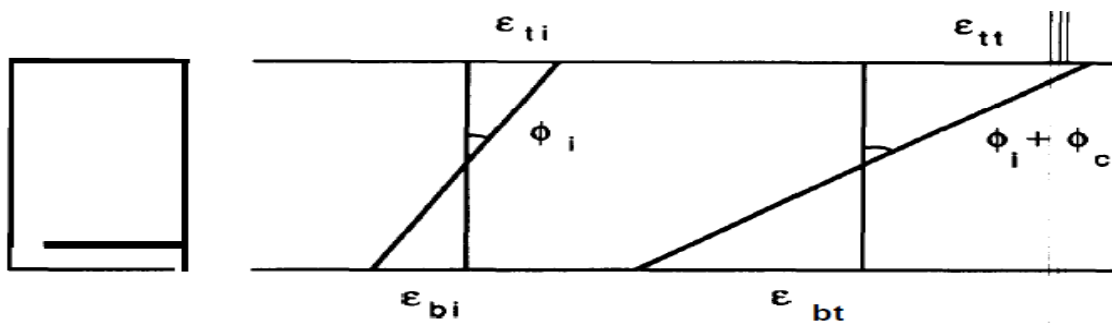


Figure 2-4 strain under the application of different loading

| | | |
|--|---------------|---|
| $\phi_i = \frac{\epsilon_{bi} - \epsilon_{ti}}{h}$ | Equation 2-51 | Strain distribution by transverse load only |
|--|---------------|---|

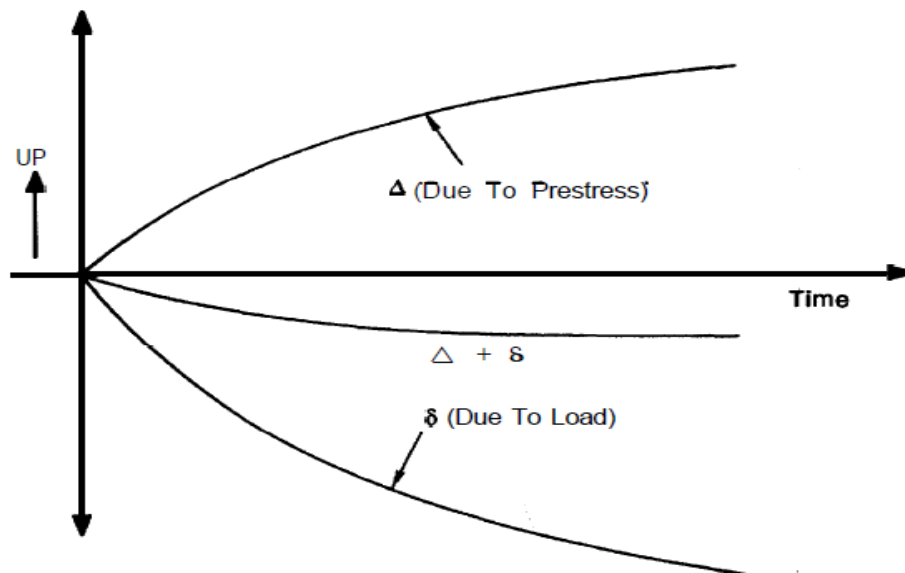


Figure 2-5 Deflection versus time due to prestress and transverse loads

The changes in the curvature or in the deflection of the beam caused by the combined prestress and the transverse load are determined by superposition.

2.3.3.3 *Moment-curvature relationship*

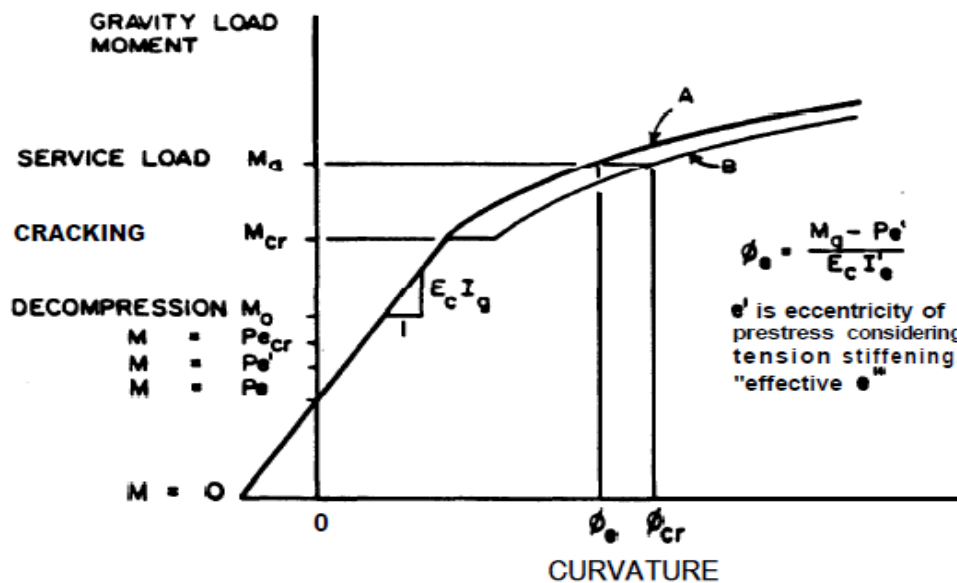


Figure 2-6 Moment curvature diagram according to ACI 435

Concrete can sustain tensile stresses and contribute to the carrying capacity of a member until cracking occurs at a moment M_{cr} . A moment M_a , larger than the cracking moment M_{cr} produces curvature that can be defined as follows (6)

| | |
|--|---------------|
| $\Phi_{cr} = \frac{M_a - P * e_{cr}}{h}$ | Equation 2-52 |
|--|---------------|

e_{cr} is the eccentricity of prestress force (p) relative to the centroid of the cracked section. The drop in rigidity due to cracking is represented by the horizontal line at the M_{cr} level. For the prestressed section, both I_{cr} and y_{cr} (and in turn e_{cr}) are dependent on the loading level, with the $M - \Phi$ becoming nonlinear after cracking. It is important to note that the shift in the centroid of the cross section upon cracking results in larger prestressing force eccentricity, e_{cr} than the uncracked member eccentricity. This fact is particularly significant in flanged members, such as double tees which are characterized by the relatively low steel area ratio (p_f) and because concrete tensile strength is not zero, cracking does not extend to the neutral axis. In addition, uncracked concrete which exists between cracks in the tension zone, contributes to the stiffness of the member (tension stiffening). Taking this into account, the $M - \Phi$ diagram becomes continuous, as indicated by line A. (6)

2.3.4 Short-term deflection and camber evaluation in prestressed beams

2.3.4.1 Uncracked Members –

When a concrete section is subjected to a flexural stress which is lower than the modulus of rupture of concrete f_r , the section is assumed to be uncracked and thus its behavior is linear. Under this condition, the deflection is calculated by the basic principles of mechanics of elastic structures. In prestressed concrete, the immediate deflection, or camber, due to the effects of initial prestressing P_i and member self-weight is generally in the elastic uncracked range. Therefore the elastic formulas presented in the previous discussion could be used to calculate the instantaneous deflection of the member. P_i is the prestress force after the initial loss due to anchorage set, elastic shortening and relation between jacking and release time. (6)

For uncracked section we use the gross moment of inertia I_g for pretensioned member and the net moment of inertia I_n for post tensioned member with unbonded tendons.

2.3.4.2 Cracked Members –

Effective I_e method--In prestressed concrete members, cracks can develop at several sections along the span under maximum load. The cracked moment of inertia I_{cr} applies at cracked sections while the gross moment of inertia applies in between cracks. Therefore we use an effective moment of inertia (I_e), which has equivalent effect for the whole section. (6)

| | |
|--|---------------|
| $I_e = I_{cr} + \left(\frac{M_{cr}}{M_a}\right)^3 * (I_g - I_{cr}) \leq I_g$ | Equation 2-53 |
|--|---------------|

Where

| | |
|--|---------------|
| $\left(\frac{M_{cr}}{M_a}\right) = \left(1 - \frac{ftl - fr}{fl}\right)$ | Equation 2-54 |
|--|---------------|

λ = reduction factor for sand light weight concrete 0.85 and 0.7 for all light weight concrete.

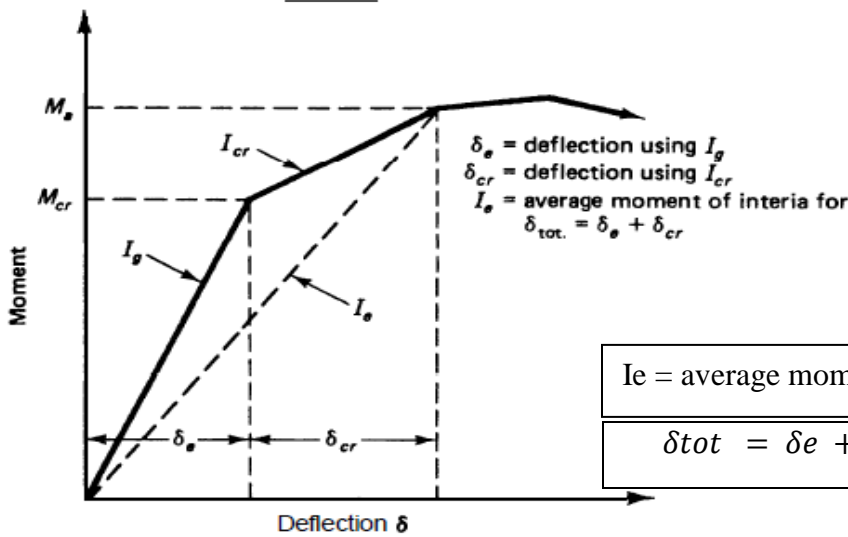
fr = modulus of rupture = $7.5\lambda\sqrt{fc}$

ftl = total calculated stress in member.

fl = calculated stress due to live load.

yt = distance from the neutral axis to tensile face

2.3.4.3 Bilinear computation method –



| | |
|---|---------------|
| $I_e =$ average moment of inertia | |
| $\delta_{tot} = \delta_e + \delta_{cr}$ | Equation 2-55 |

Bilinear moment - deflection relationship

Computation of deflection in the cracked zone in the bonded tendon beams is based on the transformed section whenever the tensile stress ft in the concrete exceeds the modulus of rupture fr , hence, δ_{cr} is evaluated using the transformed I_{cr} utilizing the contribution of the reinforcement in the bilinear method of deflection computation. The cracked moment of inertia can be calculated by the PCI approach for fully prestressed members. (8)

| | |
|--|---------------|
| $I_{cr} = np * A_{ps} * dp^2 * (1 - 1.6\sqrt{np * \rho p}) = C * b * dp^3$ | Equation 2-56 |
|--|---------------|

Where $np = E_{ps}/E_c$ and $\rho p = A_{ps}/(b * d)$

C is a coefficient can be obtained from table 3.3 of ACI 435

In partial prestressing (where non – prestressed reinforcement is used to carry the tensile stress)

| | |
|---|----------------|
| $I_{cr} = (np * A_{ps} * dp^2 + ns * A_s * d^2) * (1 - 1.6 \sqrt{np * \rho_p + ns * \rho})$ | Equation 2-57. |
|---|----------------|

Where $ns = E_s/E_c$ for non prestressed steel
 d = effective depth to the center of mild steel.

2.3.4.4 Incremental moment-curvature method –

The analysis is performed assuming two stages of behavior, namely, elastic uncracked stage and cracked stage. The cracked moment of inertia can be calculated more accurately from the moment-curvature relationship along the beam span and from the stress and, consequently, strain distribution across the depth of the critical sections. (6)

For strain ϵ_{ci} at first cracking

| | |
|--|---------------|
| $\Phi_{cr} = \frac{\epsilon_{cr}}{c} = \frac{M}{E_c * I_{cr}}$ | Equation 2-58 |
|--|---------------|

ϵ_{cr} is the strain at extreme compression fiber at first cracking

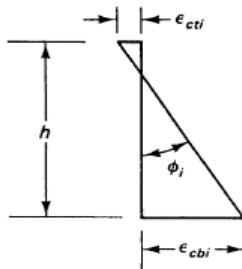
M is the net moment

f is the stress at extreme compression fiber.

Then rearranging the above equation

| | |
|---|---------------|
| $I_{cr} = \frac{M}{E_c * \Phi_{cr}} = \frac{Mc}{f}$ | Equation 2-59 |
|---|---------------|

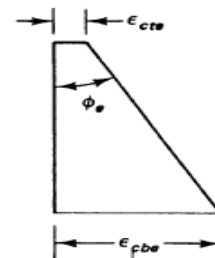
i. Initial prestress



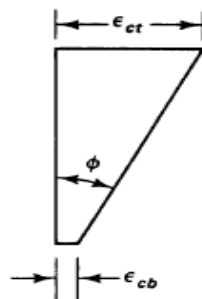
| | |
|--|---------------|
| $\Phi_i = \frac{\epsilon_{cbi} - \epsilon_{cti}}{h}$ | Equation 2-60 |
|--|---------------|

ii. effective prestress after loss

| | |
|--|---------------|
| $\Phi_e = \frac{\epsilon_{cbe} - \epsilon_{cti}}{h}$ | Equation 2-61 |
|--|---------------|



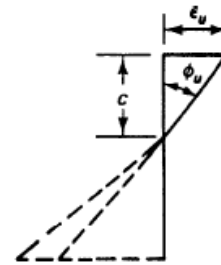
iii. service load



| | |
|--|---------------|
| $\Phi = \frac{\epsilon_{ct} - \epsilon_{cb}}{h}$ | Equation 2-62 |
|--|---------------|

iv. failure

| | |
|---------------------------------|---------------|
| $\Phi_u = \frac{\epsilon_u}{c}$ | Equation 2-63 |
|---------------------------------|---------------|



Note: - a plus sign for tensile strain and a minus sign for compressive strain

It is important to recognize that curvatures Φ at various load levels and at different locations along the span can be specifically evaluated if the beam is divided into enough small segments. (6)

2.3.5 Long-term deflection and camber evaluation in prestressed Beams.

As time goes the deflection in prestressed member increase mainly because of the effects of creep and shrinkage of concrete and relaxation of the prestressing reinforcement. The determination of long-term camber and deflection in prestressed members is more complex than for non prestressed members due to the following factors:

1. The long-term effect of the variation in prestressing force resulting from the prestress losses.
2. The increase in strength of the concrete after release of prestress and because the camber and deflection are required to be evaluated at time of erection. (6)

2.3.5.1 PCI Multipliers Method

ACI -435 recommended PCI multiplier method for calculating long term deflection. That is the most popular method for predicting time-dependent camber and deflection of precast, prestressed member is the set of multipliers given in table 8.7.1-1 of PCI Bridge manual 1997. The use of this method is fairly straight forward. First, short term deflection are calculated using conventional elastic analysis techniques. And these values are multiplied by the appropriate factor selected from table 8.7.1-1 (of PCI Bridge manual 1997) to determine the deflection that will occur as a result of time-dependent behavior. (8)

| -PCI multipliers C, for long-term camber and deflection | | |
|--|---------------------------|------------------------|
| | Without composite topping | With composite topping |
| At Erection | | |
| Deflection (downward) component-apply to the elastic deflection due to the member weight at release of prestress | 1.85 | 1.85 |
| Camber (upward) component-apply to the elastic camber due to pre- stress at the time of release of prestress | 1.8 | 1.8 |
| Final | | |
| Deflection (downward) component-apply to the elastic deflection due to the member weight at release of prestress | 2.7 | 2.4 |
| Camber (upward) component-apply to the elastic camber due to pre- stress at the time of release of prestress | 2.45 | 2.2 |
| Deflection (downward)--apply to the elastic deflection due to the superimposed dead load only | 3 | 3 |
| Deflection (downward)-apply to the elastic deflection caused by the composite topping | | 2.3 |

Table 2-3 PCI suggested multipliers to be used for calculating long term camber and deflection.

2.3.5.2 Incremental time-steps method –

The incremental time-steps method is based on combining the computations of deflections with those of prestress losses due to time-dependent creep, shrinkage, and relaxation. The design life of the structure is divided into several increasingly larger time intervals. The strain distributions, curvatures, and prestressing forces are calculated for each interval together with the incremental shrinkage, creep, and relaxation losses during the particular time interval. The procedure is repeated for all subsequent incremental intervals, and an integration or summation of the incremental curvatures is made to give the total time dependent curvature at the particular section along the span. These calculations should be made for a sufficient number of points along the span to be able to determine with reasonable accuracy the form of the moment-curvature diagram. (6)

The general expression for the total curvature at the end of a time interval (6)

| | |
|--|---------------|
| $\Phi_t = \frac{P_i * ex}{E_c i * I_c} + \sum_0^t (P(n - 1) - P_n) * \frac{ex}{E_c * I_c} - \sum_0^t (C_n - C(n - 1)) * P(n - 1) * \frac{ex}{E_c * I_c}$ | Equation 2-64 |
|--|---------------|

Where P_i = initial prestress (at transfer) before losses
 ex = eccentricity of tendon at any section along the span
 C = creep coefficient

The total deflection at a particular section and at a particular time t is

| | |
|-------------------------------|---------------|
| $\delta x = \Phi t * k * l^2$ | Equation 2-65 |
|-------------------------------|---------------|

Where k is a function of the span and geometry of the section, and the location of prestressing tendon. The total deflection (upward or downward) due to prestressing force can be obtained from

| | |
|--------------------------------|---------------|
| $\Phi T = \Phi n - 1 + \Phi n$ | Equation 2-66 |
| $\delta T = \Phi T k l^2$ | Equation 2-67 |

Where k is the aging coefficient varies from 0 to 1.0 being 0.7 -0.8 for most application (according to ACI 365). Several investigators have proposed different formats for estimating the additional time-dependent deflection. (6)

1. integrating the modified curvature along the beam span (Tadros and Dilger)
2. expressed the long-term deflection in terms of midspan and support curvatures at a time interval t (Naaman)

Naaman's expression gives, for a parabolic tendon,

| | |
|---|---------------|
| $\Delta \delta(t) = \Phi 1(t) * \frac{l^2}{8} = [\Phi 2(t) - \Phi 1(t)] * \frac{l^2}{48}$ | Equation 2-68 |
| $\Phi(t) = \frac{M}{Ece(t)Ic}$ | Equation 2-69 |
| $Ece(t) = \frac{Ec(t1)}{1 + x * Cc(t)}$ | Equation 2-70 |

Where $\Phi 1(t)$ = midspan curvature at time t

$\Phi 2(t)$ = support curvature at time t

$Ece(t)$ = time adjusted modulus

$Ec(t1)$ = modulus of elasticity of concrete at start of interval

x = aging coefficient usually assumed equal to 0.8

$Cc(t)$ = creep coefficient at end of time interval

2.3.5.3 Approximate time-steps method-

The approximate time-steps method is based on a simplified form of summation of constituent deflections due to the various time dependent factors. (6)

| | |
|--|---------------|
| $\Phi e = \frac{P1 * ex}{Ec * Ic} + (Pi - Pe) * \frac{ex}{Ec * Ic} - \left(\frac{Pi + Pe}{2} \right) * \frac{ex}{Ec * Ic} * Cu$ | Equation 2-71 |
| $\delta et = -\delta e - \left(\frac{\delta i + \delta e}{2} \right) * Cu \quad (2.49)$ | Equation 2-72 |

Where Cu = long-term creep coefficient

Φe = curvature at effective prestress Pe

δet = final deflection under Pe

The final time-dependent increase in deflection due to prestressing and sustained loads is given by

| | |
|--|---------------|
| $\Delta\delta = -\delta e - \left(\frac{\delta i + \delta e}{2}\right) * Cu + (\delta d + \delta sd) * (1 + Cu)$ | Equation 2-73 |
|--|---------------|

Then the final net deflection becomes.

| | |
|---|---------------|
| $\delta T = -\delta e - \left(\frac{\delta i + \delta e}{2}\right) * Cu + (\delta d + \delta sd) * (1 + Cu) + \delta L$ | Equation 2-74 |
|---|---------------|

Where δd and δsd are deflection due to self weight and superimposed dead load
 δL = deflection due to live load. (6)

2.3.5.4 Axial strain and curvature method (Ghali-Favre)-

This approach gives a procedure for the analysis of instantaneous and long-term stresses and strains in reinforced concrete cross-sections, with or without prestressing. The method does not require determination of prestress losses. It introduces the deflection by such effect as in the Naaman approach. In this method after cracking, the concrete in tension is ignored and only the concrete in the compression zone of depth c is included in calculating the properties of the transformed section. The transformed section is composed of the area of concrete and the area (prestressing reinforcement) A_{ps} and (non prestressed reinforcement) A_s of the reinforcement multiplied by the respective modular ratios, n_{ps} or n . (6)

2.3.5.5 Prestress loss method-

This method assumes that sustained dead load due to self weight does not produce cracking such that the effects of creep, shrinkage, and relaxation are considered only for uncracked cross sections. Additional stress in the concrete caused by live load may result in cracking when the tensile strength of concrete is exceeded. Whether cracking occurs, and the extent to which it occurs when the live load is applied depend upon the magnitude of the prestress losses. (6)

The method recommends stress loss coefficients due to creep, shrinkage and relaxation such that the change in the prestressing force ΔP_c , is given by. (6)

| | |
|--|---------------|
| $\Delta P_c = -A_t s * (\Delta f_{psh} + \Delta f_{pcr} - A_{ps} * \Delta f_{pr})$ | Equation 2-75 |
| $\delta t d = (1 + Cu) * (\delta d + \delta i) + (1 + Cu') * \delta sd + (1 + x * Cu) * \delta pl$ | Equation 2-76 |

$\delta t d$ = total deflection before live load application

δd = self-weight deflection

δi = initial prestress camber

δsd = superimposed dead load deflection, and

δpl = prestress loss deflection

Cu, Cu', x are given in table 3.5 of ACI 365

2.3.6 Effect of Tendon Profile on Deflection

In most of the cases of prestressed beam, tendons are located with eccentricities towards the soffit of a beam to counteract the sagging of bending moment due to transverse loads. Consequently, the beam deflect upwards (camber) on the application of prestress forces. Since the prestressing force and eccentricity, the tendon profile itself will represent the shape of the bending moment diagram. The method of computing deflection of beam with different cable profile is outlined as follows. (2) Note deflection (δ) = is symbolized as **a** in the figure.

2.3.6.1 Straight Tendon

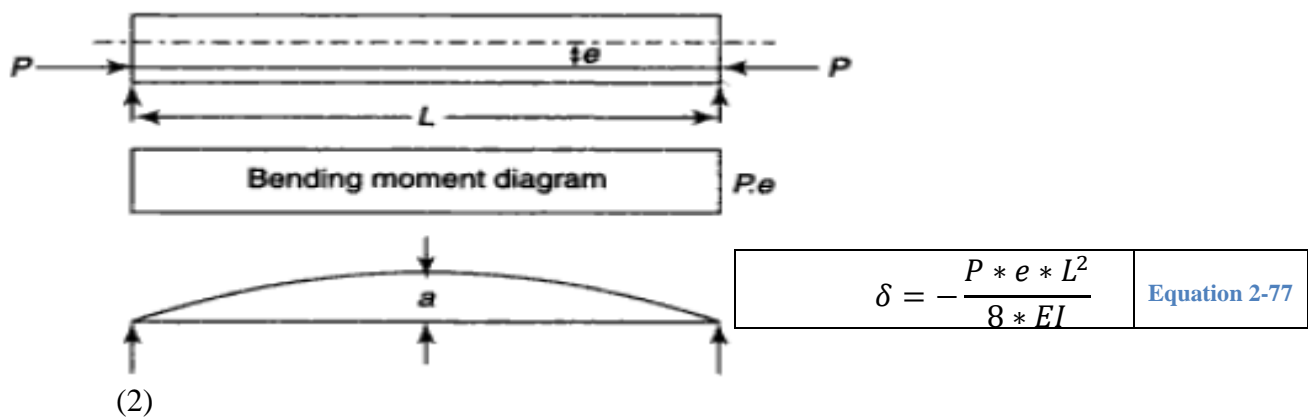


Figure 2-7 Camber of beam with straight tendon (2)

2.3.6.2 Trapezoidal Tendon

The deflection at the center of a beam is obtained by taking the moment area of the bending moment diagram over one-half of a beam.

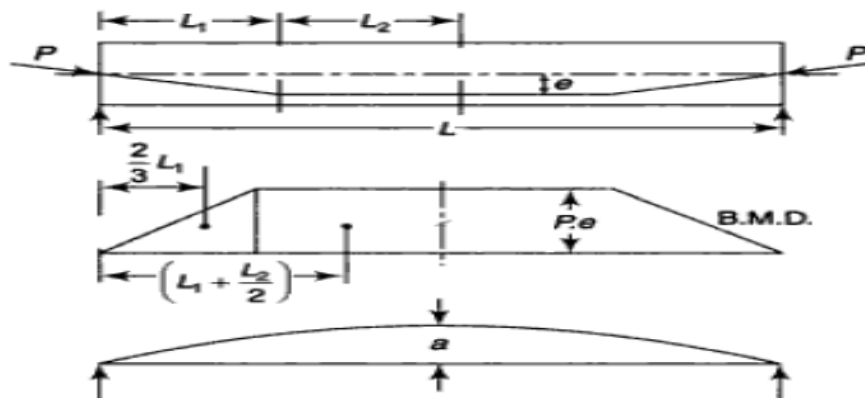


Figure 2-8 Camber of a beam Trapezoidal or Draped Tendon

| | |
|--|---------------|
| $\delta = -\frac{P * e}{6 * EI} * (2 * L1^2 + 6 * L1 * L2 + 3 * L2^2)$ | Equation 2-78 |
|--|---------------|

2.3.6.3 Parabolic tendon central anchors

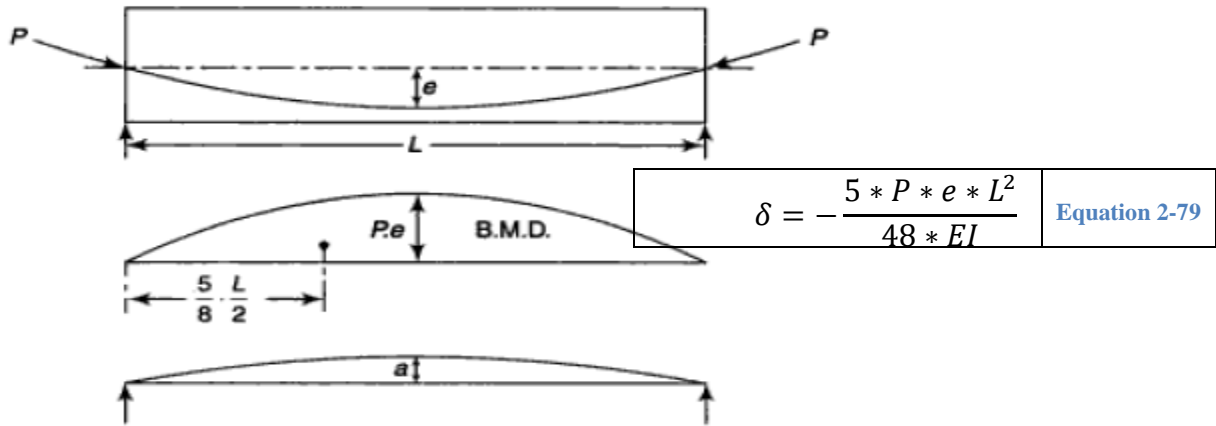


Figure 2-9 camber of parabolic tendon central anchors (2)

2.3.6.4 Parabolic tendon eccentric anchors

The resultant deflection at the center is obtained as the sum of the upward deflection of a beam with a parabolic tendon eccentricity (e_1+e_2) at the center and zero at the supports and the downward deflection of a beam subjected to uniform sagging bending moment of $Pe * e_2$ throughout the length.

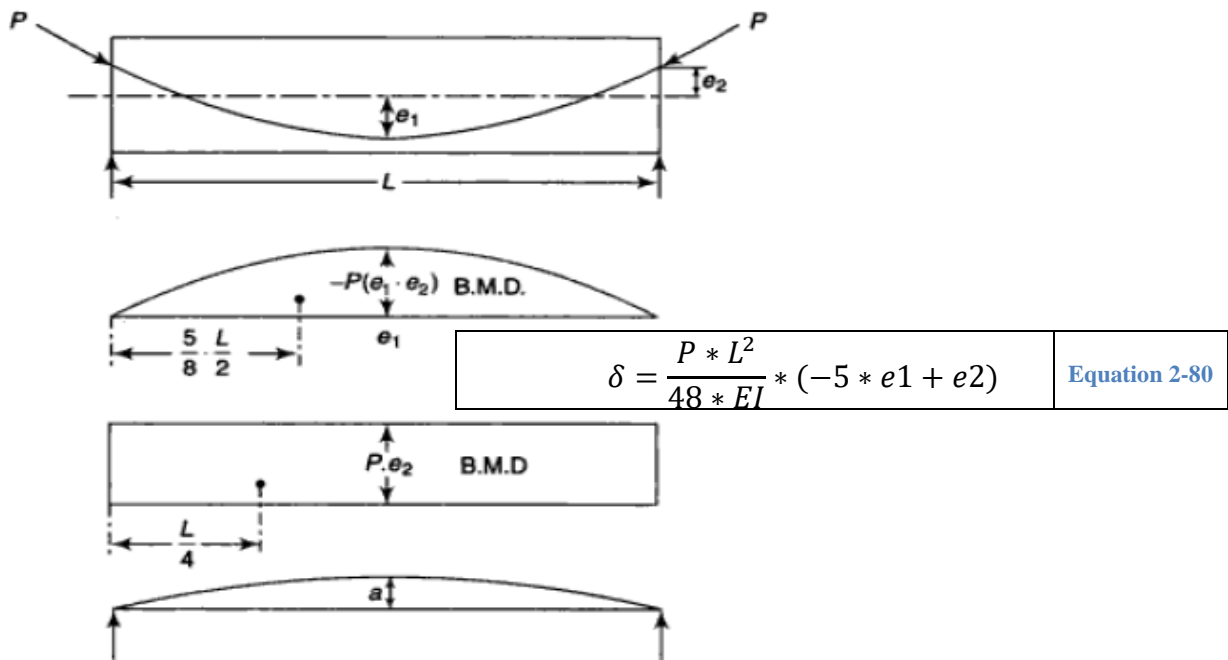


Figure 2-10 Camber of parabolic tendon eccentric anchors (2)

2.3.6.5 Sloping tendon eccentric anchor

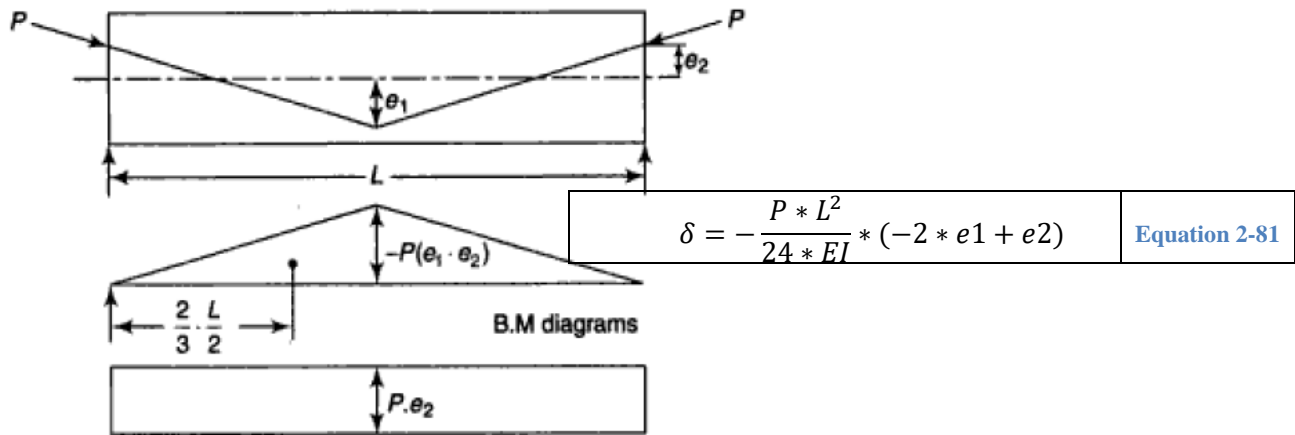


Figure 2-11 camber of sloping tendon eccentric anchor (2)

2.3.6.6 Parabolic and straight tendon central anchor

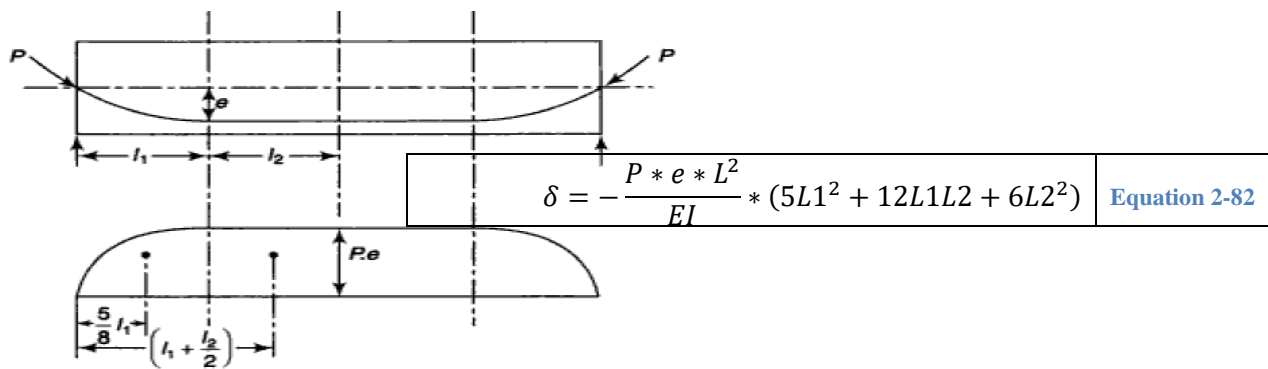


Figure 2-12 camber of parabolic and straight tendon central anchor (2)

2.3.6.7 Parabolic and straight tendon eccentric anchor

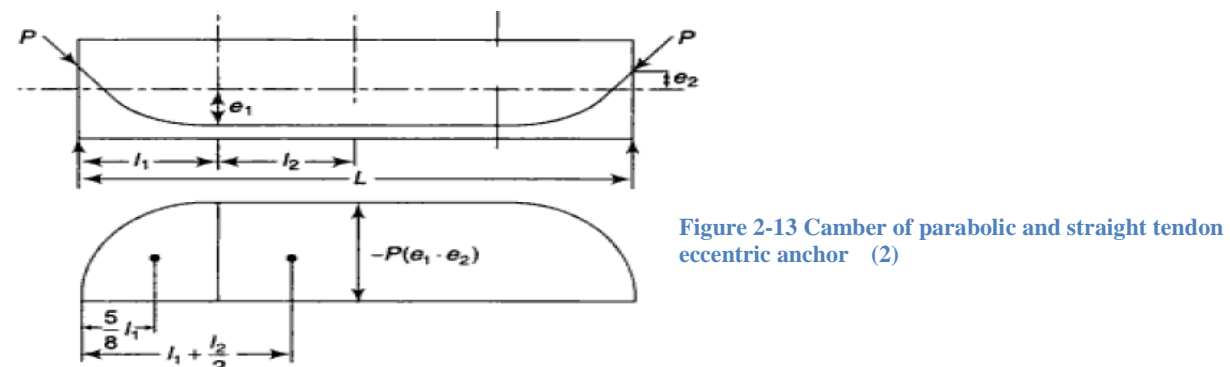


Figure 2-13 Camber of parabolic and straight tendon eccentric anchor (2)

$$\delta = -\frac{P * (e1 + e2) * L^2}{12 * EI} * (5L1^2 + 12L1L2 + 6L2^2) + \left(\frac{P * e2 * L^2}{8 * EI}\right) \quad \text{Equation 2-83}$$

2.4 Allowable Limit According to AREMA MRE volume 2

2.4.1 Deflection and Camber

According to section 17.13 of AREMA MRE volume 2

Flexural members of bridge structures shall be designed to have adequate stiffness to limit deflections or any deformations that may adversely affect strength and serviceability of the structure at service load. Members having simple or continuous spans shall be designed so that the deflection due to service live load plus impact does not exceed $l/640$ of the span. (9)

2.4.2 Minimum Concrete Cover

- a. For Precast Concrete the following minimum concrete cover shall be provided for prestressing tendons and non-prestressed reinforcement, and ducts:

| | Minimum Cover |
|------------------------------------|--|
| Pre-tensioning tendons | 1½ in. (40 mm) |
| Post-tensioning ducts | 1½ in. (40 mm), but not less than $dd/2$ |
| Non-prestressed reinforcement..... | 1½ in. (40 mm) |
| Stirrups, ties and spirals..... | 1 in. (25 mm) |

- b. For Cast-in-Place Concrete, the following minimum concrete cover shall be provided for prestressing tendons and non-prestressed reinforcement, and ducts:

| | Minimum Cover |
|------------------------------------|---|
| Post-tensioning ducts | 3 in. (75 mm), but not less than $dd/2$ |
| Non-prestressed reinforcement..... | 2 in. (50 mm) |
| Stirrups, ties and spirals | 2 in. (50 mm) |
| Concrete cast against earth | 3 in. (75 mm) |

- c. In corrosive or marine environments or other severe exposure conditions, the amount of tendon and reinforcement protection shall be increased by use of more dense and impervious concrete, by increasing the minimum cover or other suitable means. (9)

Where dd is outside diameter of post-tensioning duct, in. (mm)

3 Methodology

3.1 Camber due to prestressing Tendon

In this paper the short term and long term deflection of a simply supported prestressed railway girder with parabolic tendon eccentric anchor is computed according to the recommendation of ACI – 435 R 95.

Camber due to prestressing tendon is calculated using Equation 2-78 in which

$$\delta = -\frac{P * e * L^2}{48 * EI} * (-5 * e1 + e2)$$

3.2 Short Term Deflection

From equation 2-25 the general deflection formula for simply supported beam is.

| | |
|----------------------------------|--------------|
| $\delta_s = \frac{5wL^4}{384EI}$ | Equation 3-1 |
|----------------------------------|--------------|

Before crack occurs in a member the whole section is effective and deflection in this stage is computed by using the second moment of area of the gross concrete section. Therefore short term deflection is calculated using elastic method (i.e. using gross moment of inertia I_g)

After crack a prestressed concrete behaves in a manner similar to that of a reinforced concrete beam and the computation of deflection in this stage is made by considering a moment curvature relationship, which the section properties of cracked beam. Therefore if the section is cracked, deflection is computed using effective moment of inertia.

Uncracked Section: - When a concrete section is subjected to a flexural stress which is lower than the modulus of rupture of concrete f_r , the section is assumed to be uncracked and thus its behavior is linear. Under this condition, the deflection is calculated by the basic principles of mechanics of elastic structures. In prestressed concrete, the immediate deflection, or camber, due to the effects of initial prestressing P_i and member self-weight is generally in the elastic uncracked range. Therefore the elastic formulas presented in the previous discussion could be used to calculate the instantaneous deflection of the member. P_i is the prestress force after the initial loss due to anchorage set, elastic shortening and relation between jacking and release time. For uncracked section we use the gross moment of inertia I_g for pretensioned member and the net moment of inertia I_n for post tensioned member with unbonded tendons.

Cracked Section: - Effective I_e method-In prestressed concrete members, cracks can develop at several sections along the span under maximum load. The cracked moment of inertia I_{cr} applies at cracked sections while the gross moment of inertia applies in between cracks. Therefore we use an effective moment of inertia (I_e), which has equivalent effect for the whole section.

| | |
|--|---|
| $I_e = I_{cr} + \left(\frac{M_{cr}}{M_a}\right)^3 * (I_g - I_{cr}) \leq I_g$ | $\left(\frac{M_{cr}}{M_a}\right) = \left(1 - \frac{f_{tl} - f_r}{f_l}\right)$ |
|--|---|

| | |
|---|---|
| Where | |
| $f_t =$ modulus of rupture $= 7.5\lambda\sqrt{f_c}$ | $f_l =$ calculated stress due to live load |
| $f_t l =$ total calculated stress in member. | $y_t =$ distance from the neutral axis to tensile face. |

3.3 Long Term Deflection

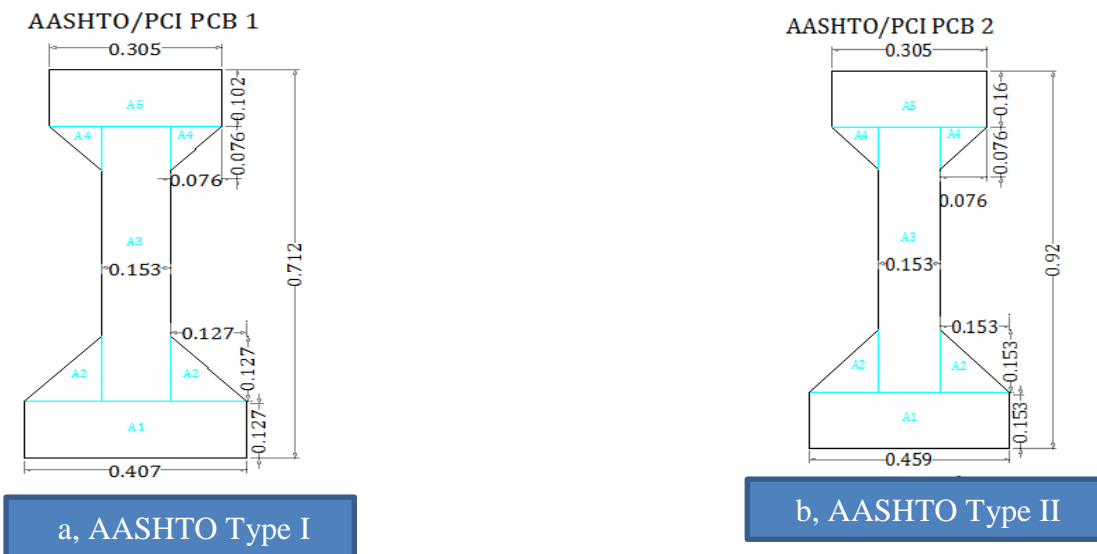
For long term deflection PCI multipliers method is used as recommended by ACI -435.

In this method the long term deflection is obtained by multiplying the initial deflection by the constant values as provided in table 2-3

3.4 Geometry

Initially it was assumed it would be enough to do the analysis for all AASHTO I beams as presented in Appendix B of PCI Bridge Design Manual, i.e. from type I to type VI. In which the units are converted to SI unit and presented as follows. But during the process I found out that largest AASHTO I beam (type 6) works without failure about up to 22 m for this loading. As a result I decided to include another custom made I beam in which its important dimensions are inputted by the user. In this case the number of dimensions that the users are going to feed is kept to the minimum to simplify the usage of the program.

Note: - I beams are chosen since they have a high second moment of area (Moment of inertia). That is because since the two flanges (or the mass of the area) is on the two other end of the centroidal axis. This in turn increases the moment arm of those flange area. As moment of inertia is the square product of this moment arm, I beam has largest moment of inertia with equivalent area of other section. As a result they are exceptionally strong in bending and shear and this makes them a good choice for the construction of I beam.



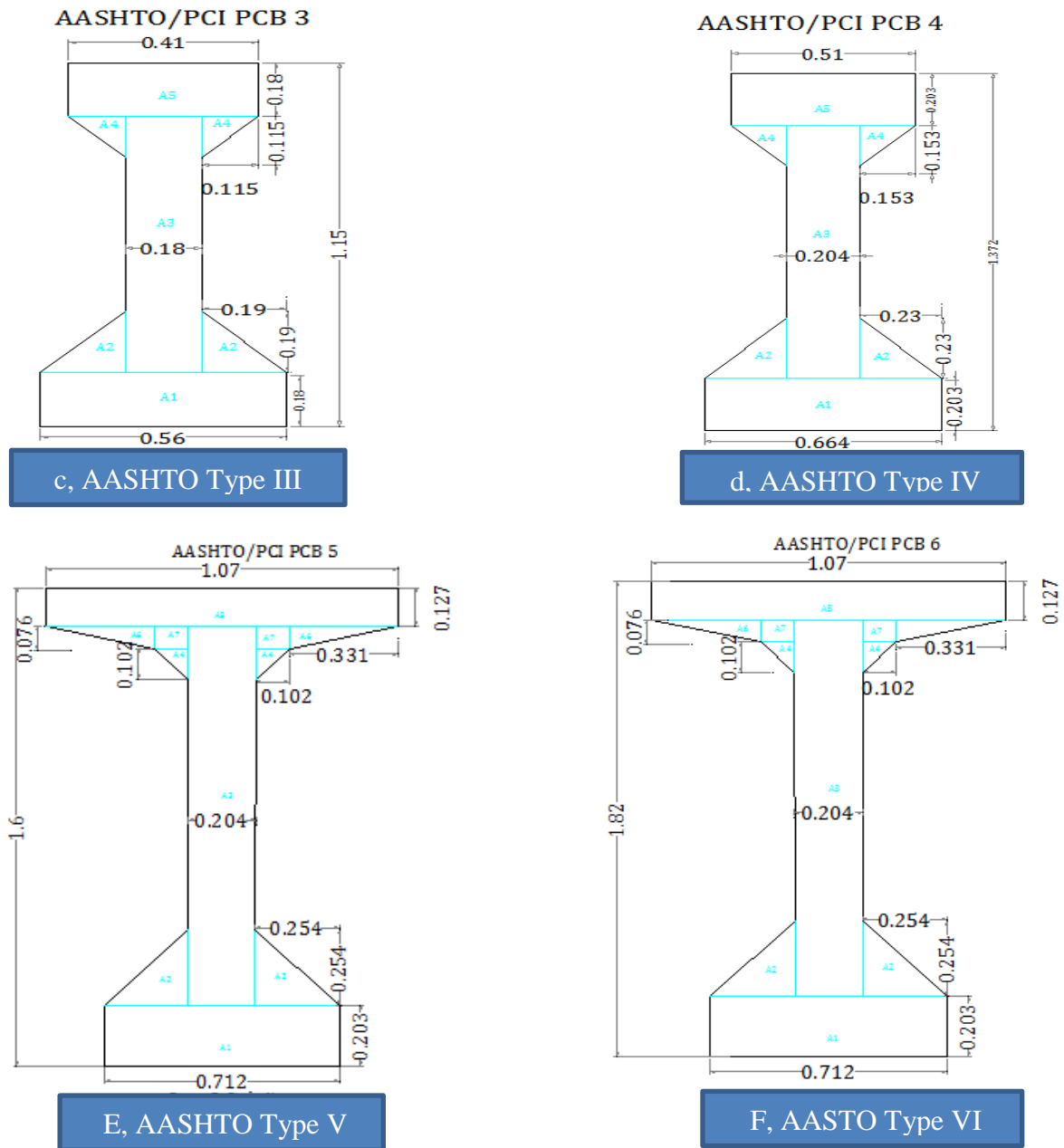


Figure 3-1 AASHTO/PCI I Beams

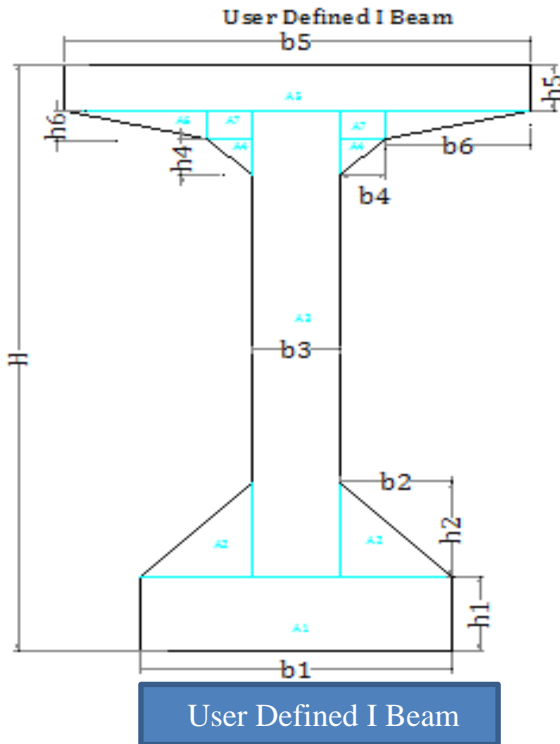


Figure 3-2 User Defined I beam based AASHTO I beam.

3.5 Loading

Super imposed dead load- the values given in AREMA MRE volume 2 will be used

Live load- Cooper loading E80 and E60 will be used for live rail loading as provided in AREMA manual for railway engineering volume 2.

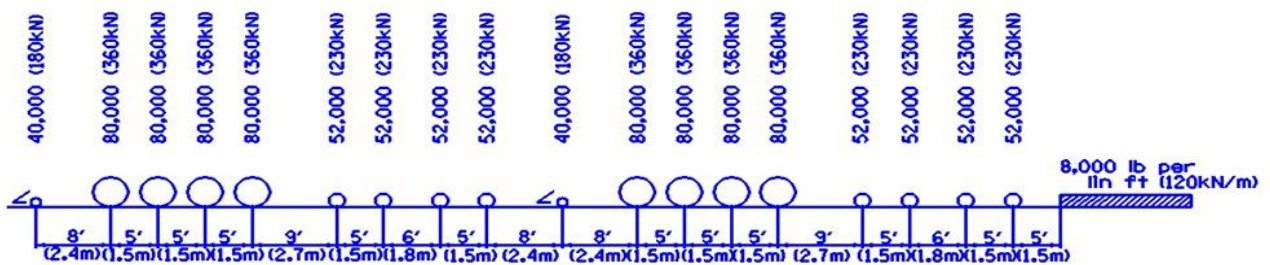


Figure 3-3 Cooper E-80 (EM 360) Axle load Diagram (9)

Finally is the calculation will be coded in MATLAB programing language and presented

Sample charts will be generated and provided in this paper.

4 Analysis

4.1 Factors affecting Deflection

The deflections of prestressed concrete members are influenced by the following factors.

1. Self-weight and Imposed load
2. Span Length of a member
3. Second moment of area of cross section
4. Modulus of elasticity of concrete
5. Shrinkage, creep and relaxation of steel stress.
6. Magnitude of the prestressing force
7. Cable (Tendon) Profile
8. Fixity condition.

4.2 Loading

According to AREMA Manual for Railway Engineering the following loads and forces shall be considered in the design of railway concrete structures supporting tracks:

- Dead Load
- Live Load
- Impact
- Centrifugal Force
- Longitudinal Force from Live Load
- Longitudinal Force due to Friction or Shear Resistance at Expansion Bearings
- Earth pressure
- Buoyancy
- Wind Load on Structure
- Wind Load on Live Load
- Earthquake (Seismic)
- Stream Flow Pressure
- Ice Pressure

Of all these loads we will only choose the dead load (self-weight plus superimposed dead load), the live load and the impact load. Which directly affect the deflection of the beam.

4.2.1 Self-weight (Wdl)

Self weight per unit meter length is the cross sectional area of a beam times unit weight of concrete which is equal to 25KN/m³

$$Wdl = A_c * \gamma_c$$

Equation 4-1

4.2.2 Super imposed Dead Load

The unit weight of materials comprising the dead load, except in special cases involving unusual conditions or materials, shall be assumed as follows

- Track rails, inside guardrails and fastenings – 200 lb. per linear foot of track. (3kN/m)
- Ballast, including track ties – 120 lb. per cubic foot. (1900 kg/m³)
- Reinforced concrete – 150 lb. per cubic foot. (2400 kg/m³)
- Earth filling materials – 120 lb. per cubic foot. (1900 kg/m³)
- Waterproofing and protective covering – estimated weight

Table 4-1 Summary of Super Imposed Dead Load

Assuming Double Track and Two Girder as The LRT case

| <i>Super Imposed Dead Load KN/m</i> | | |
|---|----------------------------------|---------------------------------|
| Item | Total | For one Girder |
| Track rail, inside guardrails and fastenings | 3 | 1.5 |
| Ballast | $19 \cdot 0.3 \cdot ccb \cdot 2$ | Wb |
| Sleeper: The numbers of sleepers per rail length can be known by taking the design standard from LRT. Sleeper spacing = 0.6m | 3.0307 | 1.51536 |
| Deck slab | $25 \cdot ts \cdot le$ | Ws |
| Concrete curb | 15 | 7.5 |
| Waterproofing and protective covering | 0.15 | 0.075 |
| Catenary system | 0.02 | 0.01 |
| Future utilities | 0.05 | 0.025 |
| Girder cross tie (diaphragm) is a transverse girder that is used to stiffen the main load bearing girders. According to AREMA, Art. 8.17.12 c, diaphragm for I-beam section is not required. | 0 | 0 |
| Total | $57.16 + Ws + Wb$ | 10.625 + Ws Wb |

Where Ws is weight of the Deck slab per unit meter length of beam

4.2.3 Live Load

The recommended live load for each track of main line structure is Cooper E 80 (EM 360) loading with axle loads and axle spacing as shown in Fig 3.2 On branch lines and in other locations where the loading is limited to the use of light equipment, or cars only, the live load may be reduced, as directed by the engineer. For structures wherein the material in the primary load-carrying members is not concrete, the E loading used for the concrete design shall be that used for the primary members. (9)

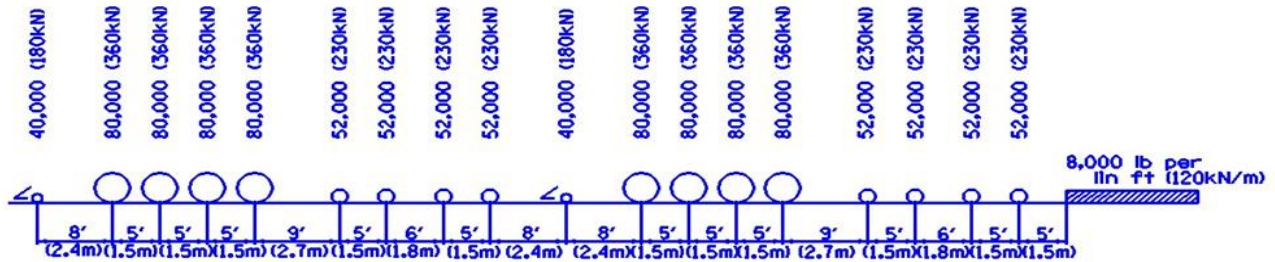


Figure 4-1 Cooper E-80 (EM 360) Axle load Diagram (9)

Fortunately for simple span this load is tabulated in table 15-1-15 of AREMA manual for railway engineering volume 2 as follows.

Table 4-2 Calculation of moments on short, simple span from Table 15-1-6 of AREMA MRE

| Span, L | Location of M _{max} | Maximum Moment (Cooper E-80) |
|---|------------------------------|---|
| 0.00 ft. < L £ 8.54 ft. | L/2 | M _{max} = 10L |
| 8.54 ft. < L £ 11.12 ft. | L/2 +/-1.25 ft | M _{max} = 20L - 100 + 125/L |
| 11.12 ft. < L £ 18.66 ft. | L/2 | M _{max} = 30L - 200 |
| 18.66 ft. < L £ 27.61 ft. | L/2 +/-1.25 ft L/2 +/- | M _{max} = 40L - 400 + 250/L |
| 27.61 ft. < L £ 34.97 ft. | 0.389 ft L/2 +/-0.961 ft | M _{max} = 45L - 530 + 27.2/L |
| 34.97 ft. < L £ 38.72 ft. | L/2 +/-0.211 ft L/2 +/- | M _{max} = 51.5L - 762 + 190/L |
| 38.72 ft. < L £ 49.56 ft. | 1.45 ft L/2 +/-0.127 ft | M _{max} = 58L - 1009 + 10.35/L |
| 48.31 ft. < L £ 53.54 ft. | L/2 +/-1.374 ft L/2 +/- | M _{max} = 64.5L - 1334 + 542.2/L |
| 53.54 ft. < L £ 58.47 ft. | 0.068 ft L/2 +/-0.088 ft | M _{max} = 71L - 1672 + 4.6/L |
| 58.47 ft. < L £ 63.42 ft. | | M _{max} = 77.5L - 2062 + 585.4/L |
| 63.42 ft. < L £ 75.15 ft. | | M _{max} = 84L - 2465 + 1.6/L |
| 75.15 ft. < L £ 79.83ft | | M _{max} = 97L - 3442 + 3/L |
| 1At L = 80 ft., the last formula will give a value which is 99.98% of the value given in Table 15-1-15. | | |
| Span, L | Location of M _{max} | Max Moment (Alt LL: 4 - 100k Axles) |
| 0.00 ft. < L £ 8.54 ft. | L/2 | M _{max} = 12.5L |
| 8.54 ft. < L £ 12.94 ft. | L/2 +/-1.25 ft L/2 +/- | M _{max} = 25L - 125 + 156.25/L |
| 12.94 ft. < L £ 20.24 ft. | 0.167 ft L/2 +/-1.5 ft | M _{max} = 37.5L - 275 + 4.17/L |
| L > 20.24 ft. | | M _{max} = 50L - 550 + 450/L |

Table 4-3 Maximum moments, shears and pier Reaction for Cooper E 80 Live load or alternate load (9)

Note all values are for one rail (one half-track load)

| Span Length Ft | Maximum Moment Ft-Kips | | Maximum Moment Quarter Point Ft-Kips | | Maximum Shears Kips | | | | | | Maximum Pier Reaction Kips (2) | |
|----------------|------------------------|---------|--------------------------------------|---------|---------------------|--------|------------------|--------|-----------|-------|--------------------------------|--------|
| | | | | | At End | | At Quarter Point | | At Center | | | |
| | E-80 | Alt. | E-80 | Alt. | E-80 | Alt. | E-80 | Alt. | E-80 | Alt. | E-80 | Alt. |
| 5 | 50 | 62.5 | 37.5 | 46.88 | 40 | 50 | | | 20 | 25 | 40 | 50 |
| 6 | 60 | 75 | 45 | 56.25 | 46.67 | 58.33 | 30 | 37.5 | 20 | 25 | 53.33 | 58.33 |
| 7 | 70 | 87.5 | 55 | 68.75 | 51.43 | 64.29 | 31.43 | 39.29 | 20 | 25 | 62.86 | 71.43 |
| 8 | 80 | 100 | 70 | 87.5 | 55 | 68.75 | 35 | 43.75 | 20 | 25 | 70 | 81.25 |
| 9 | 93.89 | 117.36 | 85 | 106.25 | 57.58 | 72.22 | 37.78 | 47.23 | 20 | 25 | 75.76 | 88.89 |
| 10 | 112.5 | 140.63 | 100 | 125 | 60 | 75 | 40 | 50 | 20 | 25 | 80 | 95 |
| 11 | 131.36 | 164.2 | 115 | 143.75 | 65.45 | 77.27 | 41.82 | 52.28 | 21.82 | 27.28 | 87.28 | 100 |
| 12 | 160 | 188.02 | 130 | 162.5 | 70 | 83.33 | 43.33 | 54.17 | 23.33 | 29.17 | 93.33 | 108.33 |
| 13 | 190 | 212.83 | 145 | 181.25 | 73.84 | 88.46 | 44.61 | 55.76 | 24.61 | 30.76 | 98.46 | 115.39 |
| 14 | 220 | 250.3 | 165 | 200 | 77.14 | 92.86 | 47.14 | 57.14 | 25.71 | 32.14 | 104.29 | 121.43 |
| 16 | 280 | 325.27 | 210 | 250 | 85 | 100 | 52.5 | 62.5 | 27.5 | 34.38 | 113.74 | 131.25 |
| 18 | 340 | 400.24 | 255 | 318.79 | 93.33 | 111.11 | 56.67 | 68.05 | 28.89 | 36.11 | 121.33 | 138.89 |
| 20 | 412.5 | 475 | 300 | 362.5 | 100 | 120 | 60 | 72.5 | 28.7 | 37.5 | 131.1 | 145 |
| 24 | 570.42 | 668.75 | 420 | 500 | 110.83 | 133.33 | 70 | 83.33 | 31.75 | 41.67 | 147.92 | 154.17 |
| 28 | 730.98 | 866.07 | 555 | 650 | 120.86 | 142.86 | 77.14 | 92.86 | 34.29 | 46.43 | 164.58 | |
| 32 | 910.85 | 1064.06 | 692.5 | 800 | 131.44 | 150 | 83.12 | 100 | 37.5 | 50 | 181.94 | |
| 36 | 1097.3 | 1262.5 | 851.5 | 950 | 141.12 | 155.56 | 88.9 | 105.56 | 41.1 | 55.56 | 199.06 | |
| 40 | 1311.3 | 1461.25 | 1010.5 | 1100 | 150.8 | 160 | 93.55 | 110 | 44 | 60 | 215.9 | |
| 45 | 1601.2 | 1710 | 1233.6 | 1287.48 | 163.38 | 164.44 | 100.27 | 114.45 | 45.9 | 64.45 | 237.25 | |
| 50 | 1901.8 | 1959 | 1473 | 1481.05 | 174.4 | | 106.94 | 118.42 | 49.73 | 68 | 257.52 | |
| 55 | 2233.1 | | 1732.3 | | 185.31 | | 113.58 | 120.91 | 52.74 | 70.91 | 280.67 | |
| 60 | 2597.8 | | 2010 | | 196 | | 120.21 | 123.33 | 55.69 | 73.33 | 306.42 | |
| 70 | 3415 | | 2608.2 | | 221.04 | | 131.89 | | 61.45 | 77.14 | 354.08 | |
| 80 | 4318.9 | | 3298 | | 248.4 | | 143.41 | | 67.41 | 80 | 397.7 | |
| 90 | 5339.1 | | 4158 | | 274.46 | | 157.47 | | 73.48 | 82.22 | 437.15 | |
| 100 | 6446.3 | | 5060.5 | | 300 | | 173.12 | | 78.72 | 84 | 474.24 | |
| 120 | 9225.4 | | 7098 | | 347.35 | | 202.19 | | 88.92 | | 544.14 | |
| 140 | 12406 | | 9400 | | 392.59 | | 230.23 | | 101.64 | | 614.91 | |

| Span Length Ft | Maximum Moment Ft–Kips | | Maximum Moment Quarter Point Ft–Kips | | Maximum Shears Kips | | | | | | Maximum Pier Reaction Kips (2) | |
|----------------|------------------------|------|--------------------------------------|------|---------------------|------|------------------|------|-----------|------|--------------------------------|------|
| | | | | | At End | | At Quarter Point | | At Center | | | |
| | E-80 | Alt. | E-80 | Alt. | E-80 | Alt. | E-80 | Alt. | E-80 | Alt. | E-80 | Alt. |
| 160 | 15908.00 (1) | | 11932 | | 436.51 | | 265.51 | | 115.2 | | 687.5 | |
| 180 | 19672.00 (1) | | 14820 | | 479.57 | | 281.96 | | 128.12 | | 762.22 | |
| 200 | 23712.00 (1) | | 17990 | | 522.01 | | 306.81 | | 140.8 | | 838 | |
| 250 | 35118.00 (1) | | 27154 | | 626.41 | | 367.3 | | 170.05 | | 1030.4 | |
| 300 | 48800.00 (1) | | 38246 | | 729.34 | | 426.37 | | 197.93 | | 1225.3 | |
| 350 | 65050.00 (1) | | 51114 | | 831.43 | | 484.64 | | 225.51 | | 1421.7 | |
| 400 | 83800.00 (1) | | 65588 | | 933 | | 542.4 | | 252.44 | | 1619 | |

Note (1) - Values for Cooper E-80 Live Load. Moment values taken at center span. Note (2) - Maximum pier reactions are for equal span lengths.

The values are converted to SI unit and also adjusted to copper E60 live load as follows

Table 4-4 Maximum Live load moments for cooper E80 and cooper E 60 live load

| Span Length (m) | Maximum Moments at Mid span (KNm) | |
|-----------------|------------------------------------|----------------|
| | E - 80 Loading | E - 60 Loading |
| 1.52 | 67.79 | 50.84 |
| 1.83 | 81.35 | 61.01 |
| 2.13 | 94.91 | 71.18 |
| 2.44 | 108.46 | 81.35 |
| 2.74 | 127.30 | 95.47 |
| 3.05 | 152.53 | 114.40 |
| 3.35 | 178.10 | 133.57 |
| 3.66 | 216.93 | 162.70 |
| 3.96 | 257.60 | 193.20 |
| 4.27 | 298.28 | 223.71 |
| 4.88 | 379.62 | 284.72 |
| 5.49 | 460.97 | 345.73 |
| 6.10 | 559.27 | 419.45 |
| 7.32 | 773.38 | 580.03 |
| 8.53 | 991.06 | 743.30 |
| 9.75 | 1234.93 | 926.20 |
| 10.97 | 1487.72 | 1115.79 |

| Span Length (m) | Maximum Moments at Mid span (KNm) | |
|-----------------|------------------------------------|----------------|
| | E - 80 Loading | E - 60 Loading |
| 12.19 | 1777.86 | 1333.40 |
| 13.72 | 2170.91 | 1628.18 |
| 15.24 | 2578.46 | 1933.85 |
| 16.76 | 3027.64 | 2270.73 |
| 18.29 | 3522.10 | 2641.57 |
| 21.34 | 4630.06 | 3472.54 |
| 24.38 | 5855.56 | 4391.67 |
| 27.43 | 7238.75 | 5429.06 |
| 30.48 | 8739.89 | 6554.92 |
| 36.58 | 12507.80 | 9380.85 |
| 42.67 | 16820.05 | 12615.04 |
| 48.77 | 21568.07 | 16176.05 |
| 54.86 | 26671.30 | 20003.47 |
| 60.96 | 32148.73 | 24111.55 |
| 76.20 | 47612.98 | 35709.74 |
| 91.44 | 66163.04 | 49622.28 |
| 106.68 | 88194.79 | 66146.09 |
| 121.92 | 113616.04 | 85212.03 |

4.2.4 Impact Load

Impact forces, applied at the top of rail, shall be added to the axle loads specified. For rolling equipment without hammer blow (diesels, electric locomotives, tenders alone, etc.), the impact shall be equal to the following percentages of the live load: (9)

$$\begin{aligned} \text{For } L < 4\text{m} & \quad I = 60 \\ \text{For } 4\text{ m} < L < 39\text{ m} & \quad I = 125/\sqrt{L} \\ \text{For } L > 39\text{ m} & \quad I = 20 \end{aligned}$$

Where L is the span length in feet (meters).

This formula is intended for ballasted-deck spans and substructure elements as required.

4.3 Geometry

4.3.1 Precast Section

As described on the above section, I have selected AASHTO I beams for the calculation of deflection. The analysis will be done for all AASHTO I beams as presented in Appendix B of

PCI Bridge Design Manual, i.e. from type I to type VI. Section property for each of AASHTO I beam is calculated and tabulated as follows.

| Precast Girder only | | | | | PCB 1 | | | | |
|---------------------|-------|-------|---------------|--------|-----------------|----------------------------|----------------|------------------------------|---|
| No | b | h | A | y | Ay _i | I = (b*h ³)/12 | d _i | Ad _i ² | I = I _o + Ad _i ² |
| A1 | 0.407 | 0.127 | 0.0517 | 0.0635 | 0.00328 | 6.95E-05 | 0.2567 | 0.00341 | 0.00348 |
| A2 | 0.127 | 0.127 | 0.0161 | 0.1693 | 0.00273 | 1.45E-05 | 0.1509 | 0.00037 | 0.00038 |
| A3 | 0.153 | 0.483 | 0.0739 | 0.3685 | 0.02723 | 1.44E-03 | 0.0483 | 0.00017 | 0.00161 |
| A4 | 0.076 | 0.076 | 0.0058 | 0.5847 | 0.00338 | 1.85E-06 | 0.2645 | 0.00040 | 0.00041 |
| A5 | 0.305 | 0.102 | 0.0311 | 0.6610 | 0.02056 | 2.70E-05 | 0.3408 | 0.00361 | 0.00364 |
| TOTAL | | | 0.1786 | | 0.05719 | | | | 0.00951 |

| Precast Girder Only | | | |
|--------------------------|------------------|------------------|------------------------|
| Area | Ac = | ∑A | 0.17860 m ² |
| Centroid | Y = | ∑AY/∑A | 0.32018 m |
| Second Moment of Inertia | I = | ∑I | 0.00951 m ⁴ |
| Centroid | y _b = | Y | 0.32018 m |
| | Y _t = | H-Y _b | 0.39182 m |
| Section Modulus | Z _t = | I/Y _t | 0.02428 m ³ |
| | Z _b = | I/y _b | 0.02971 m ³ |

Table 4-5 section properties of AASHTO I beam type I

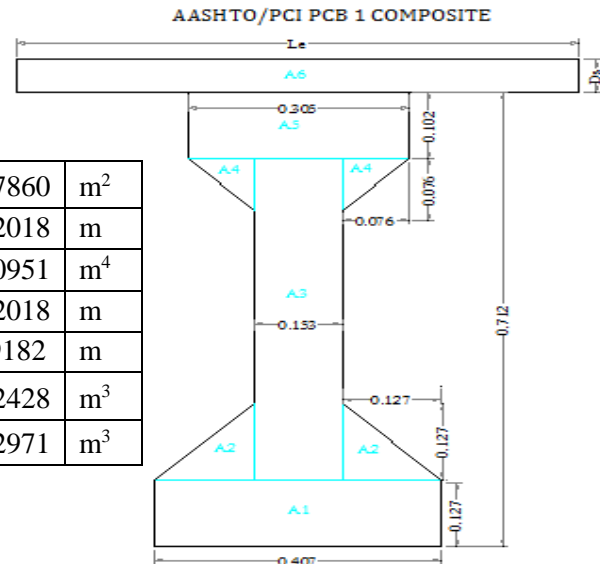


Figure 4-2 AASHTO I beam Type II composite section

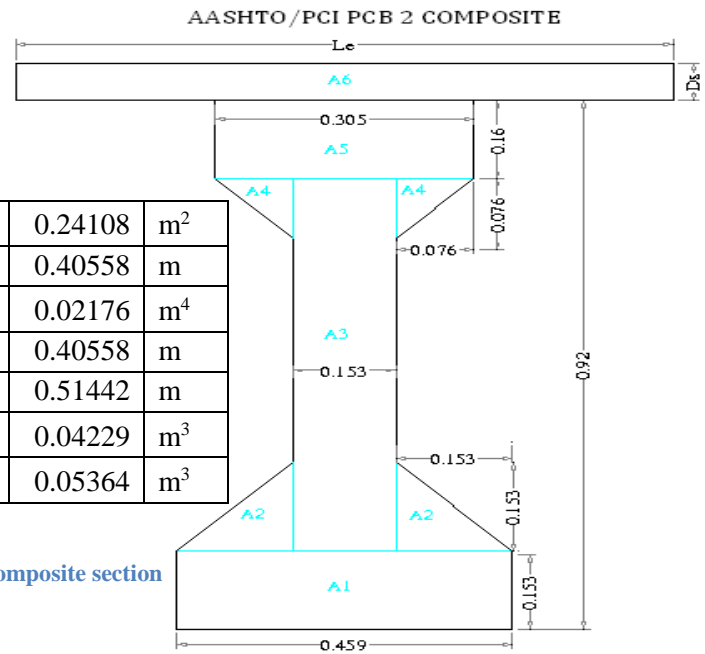
Drawn By Fiseha N.

| Precast Girder only | | | | | PCB 2 | | | | |
|---------------------|------|-------|---------------|--------|-----------------|---------------------------|----------------|------------------------------|---|
| No | b | h | A | y | Ay _i | I = (b*h ³)/x | d _i | Ad _i ² | I = I _o + Ad _i ² |
| A1 | 0.46 | 0.153 | 0.0702 | 0.0765 | 0.0054 | 1.37E-04 | 0.3291 | 0.00761 | 0.00774 |
| A2 | 0.15 | 0.153 | 0.0234 | 0.2040 | 0.0048 | 3.04E-05 | 0.2016 | 0.00095 | 0.00098 |
| A3 | 0.15 | 0.607 | 0.0929 | 0.4565 | 0.0424 | 2.85E-03 | 0.0509 | 0.00024 | 0.00309 |
| A4 | 0.08 | 0.076 | 0.0058 | 0.7347 | 0.0042 | 1.85E-06 | 0.3291 | 0.00063 | 0.00063 |
| A5 | 0.31 | 0.16 | 0.0488 | 0.8400 | 0.0410 | 1.04E-04 | 0.4344 | 0.00921 | 0.00931 |
| TOTAL | | | 0.2411 | | 0.0978 | | | | 0.02176 |

| Precast Girder Only | | | | |
|--------------------------|---------|--------------------------|---------|-------|
| Area | A_c | $\sum A$ | 0.24108 | m^2 |
| Centroid | $Y =$ | $\frac{\sum AY}{\sum A}$ | 0.40558 | m |
| Second Moment of Inertia | I | $\sum I$ | 0.02176 | m^4 |
| Centroid | $y_b =$ | Y | 0.40558 | m |
| | $Y_t =$ | $H - Y$ | 0.51442 | m |
| Section Modulus | $Z_t =$ | I/Y_t | 0.04229 | m^3 |
| | $Z_b =$ | I/y_b | 0.05364 | m^3 |

Table 4-6 section properties of AASHTO I beam type II

Figure 4-3 AASHTO I beam Type II composite section

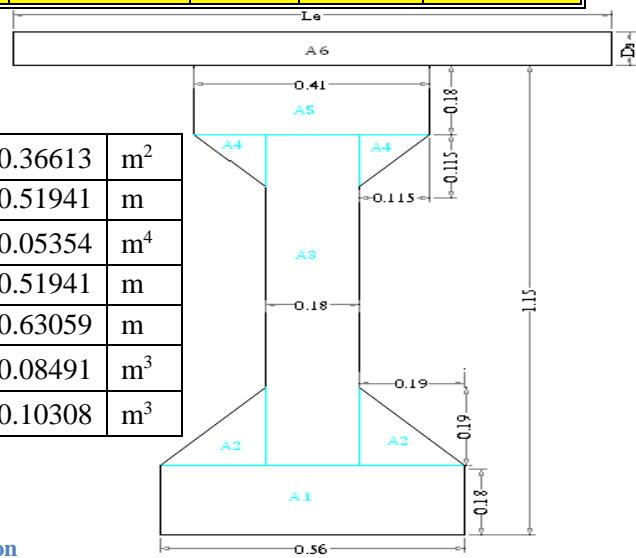


| Precast Girder only | | | | PCB 3 | | | | | |
|---------------------|-------|-------|---------------|--------|----------------|------------------------|--------|----------|--------------------|
| No | b | h | A | y | Ay_i | $I = (b \cdot h^3)/12$ | d_i | Ad_i^2 | $I = I_o + Ad_i^2$ |
| A1 | 0.560 | 0.180 | 0.1008 | 0.0900 | 0.00907 | 2.72E-04 | 0.4294 | 0.01859 | 0.01886 |
| A2 | 0.190 | 0.190 | 0.0361 | 0.2433 | 0.00878 | 7.24E-05 | 0.2761 | 0.00275 | 0.00282 |
| A3 | 0.180 | 0.790 | 0.1422 | 0.5750 | 0.08177 | 7.40E-03 | 0.0556 | 0.00044 | 0.00783 |
| A4 | 0.115 | 0.115 | 0.0132 | 0.9317 | 0.01232 | 9.72E-06 | 0.4123 | 0.00225 | 0.00226 |
| A5 | 0.410 | 0.180 | 0.0738 | 1.0600 | 0.07823 | 1.99E-04 | 0.5406 | 0.02157 | 0.02177 |
| TOTAL | | | 0.3661 | | 0.19017 | | | | 0.05354 |

| Precast Girder Only | | | | |
|--------------------------|---------|--------------------------|---------|-------|
| Area | $A_c =$ | $\sum A$ | 0.36613 | m^2 |
| Centroid | $Y =$ | $\frac{\sum AY}{\sum A}$ | 0.51941 | m |
| Second Moment of Inertia | I | $\sum I$ | 0.05354 | m^4 |
| Centroid | $y_b =$ | Y | 0.51941 | m |
| | $Y_t =$ | $H - Y$ | 0.63059 | m |
| Section Modulus | $Z_t =$ | I/Y_t | 0.08491 | m^3 |
| | $Z_b =$ | I/y_b | 0.10308 | m^3 |

Table 4-7 section properties of AASHTO I beam type III

Figure 4-4 AASHTO I beam Type III composite section



PCB3, Drawn By Fiseha N.

| Precast Girder only | | | | PCB 4 | | | | | |
|---------------------|-------|-------|---------------|--------|-----------------|----------------------------|----------------|------------------------------|---|
| No | b | h | A | y | Ay _i | I = (b*h ³)/12 | d _i | Ad _i ² | I = I _o + Ad _i ² |
| A1 | 0.664 | 0.203 | 0.1348 | 0.1015 | 0.01368 | 4.63E-04 | 0.5265 | 0.03737 | 0.03783 |
| A2 | 0.230 | 0.230 | 0.0529 | 0.2797 | 0.01479 | 1.55E-04 | 0.3484 | 0.00642 | 0.00658 |
| A3 | 0.204 | 0.966 | 0.1971 | 0.6860 | 0.13519 | 1.53E-02 | 0.0580 | 0.00066 | 0.01599 |
| A4 | 0.153 | 0.153 | 0.0234 | 1.1180 | 0.02617 | 3.04E-05 | 0.4900 | 0.00562 | 0.00565 |
| A5 | 0.510 | 0.203 | 0.1035 | 1.2705 | 0.13153 | 3.56E-04 | 0.6425 | 0.04273 | 0.04309 |
| TOTAL | | | 0.5117 | | 0.32137 | | | | 0.10913 |

| Precast Girder Only | | | |
|--------------------------|------------------|------------------|------------------------|
| Area | Ac | ∑A | 0.51170 m ² |
| Centroid | Y = | ∑AY/∑A | 0.62805 m |
| Second Moment of Inertia | I | ∑I | 0.10913 m ⁴ |
| Centroid | y _b = | Y | 0.62805 m |
| | Y _t = | H - Y | 0.74395 m |
| Section Modulus | Z _t = | I/Y _t | 0.14669 m ³ |
| | Z _b = | I/y _b | 0.17377 m ³ |

Table 4-8 section properties of AASHTO I beam type IV

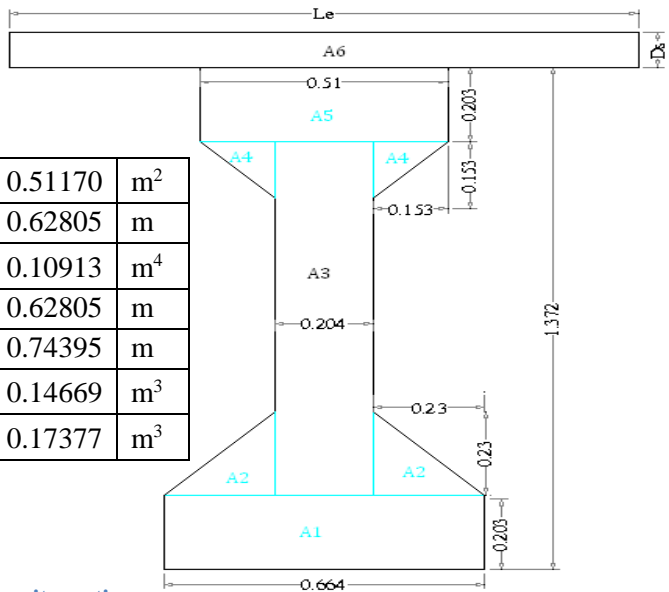
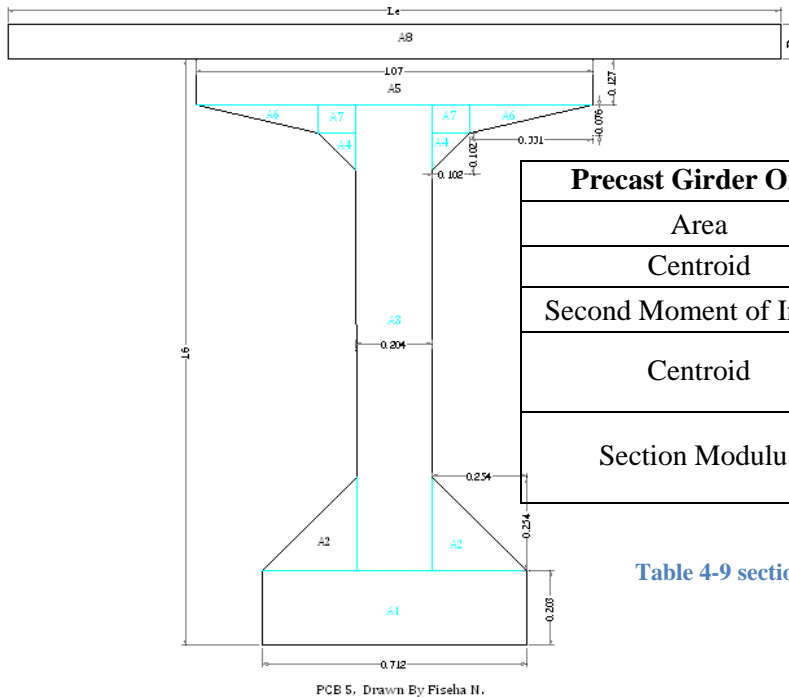


Figure 4-5 AASHTO I beam Type IV composite section

PCB4, Drawn By Fiseha N.

| Precast Girder only | | | | PCB 5 | | | | | |
|---------------------|-------|-------|---------------|--------|-----------------|----------------------------|----------------|------------------------------|---|
| No | b | h | A | y | Ay _i | I = (b*h ³)/12 | d _i | Ad _i ² | I = I _o + Ad _i ² |
| A1 | 0.712 | 0.203 | 0.1445 | 0.1015 | 0.0147 | 4.96E-04 | 0.7106 | 0.0730 | 0.0735 |
| A2 | 0.254 | 0.254 | 0.0645 | 0.2877 | 0.0186 | 2.31E-04 | 0.5244 | 0.0177 | 0.0180 |
| A3 | 0.204 | 1.27 | 0.2591 | 0.8380 | 0.2171 | 3.48E-02 | 0.0259 | 0.0002 | 0.0350 |
| A4 | 0.102 | 0.102 | 0.0104 | 1.3630 | 0.0142 | 6.01E-06 | 0.5509 | 0.0032 | 0.0032 |
| A6 | 0.331 | 0.076 | 0.0252 | 1.4477 | 0.0364 | 2.64E-05 | -0.6356 | 0.0102 | 0.0102 |
| A7 | 0.102 | 0.076 | 0.0155 | 1.4350 | 0.0222 | 2.49E-06 | 0.6229 | 0.0060 | 0.0060 |
| A5 | 1.07 | 0.127 | 0.1359 | 1.5365 | 0.2088 | 1.83E-04 | 0.7244 | 0.0713 | 0.0715 |
| TOTAL | | | 0.6551 | | 0.5320 | 3.58E-02 | | 0.1815 | 0.2173 |

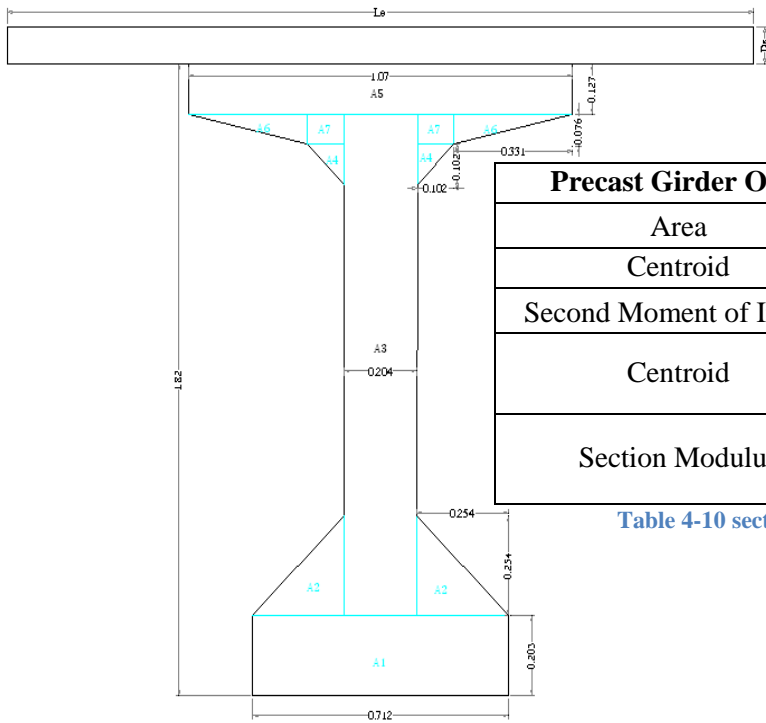


| Precast Girder Only | | | | |
|--------------------------|------|--------------------------|---------|----------------|
| Area | Ac = | $\sum A$ | 0.65509 | m ² |
| Centroid | Y = | $\frac{\sum AY}{\sum A}$ | 0.81210 | m |
| Second Moment of Inertia | I = | $\sum I$ | 0.21731 | m ⁴ |
| Centroid | yb = | Y | 0.81210 | m |
| | Yt = | H - Y | 0.78790 | m |
| Section Modulus | Zt = | I/Yt | 0.27580 | m ³ |
| | Zb = | I/yb | 0.26760 | m ³ |

Table 4-9 section properties of AASHTO I beam Type V

Figure 4-6 AASHTO I beam Type V composite section

| Girder only | | | | PCB 6 | | | | | |
|--------------|-------|-------|---------------|--------|-----------------|----------------------------|----------------|------------------------------|---|
| No | b | h | A | y | Ay _i | I = (b*h ³)/12 | d _i | Ad _i ² | I = I _o + Ad _i ² |
| A1 | 0.712 | 0.203 | 0.1445 | 0.1015 | 0.01467 | 4.96E-04 | 0.8188 | 0.09689 | 0.09739 |
| A2 | 0.254 | 0.254 | 0.0645 | 0.2877 | 0.01856 | 2.31E-04 | 0.6326 | 0.02582 | 0.02605 |
| A3 | 0.204 | 1.49 | 0.3040 | 0.9480 | 0.28815 | 5.62E-02 | 0.0277 | 0.00023 | 0.05647 |
| A4 | 0.102 | 0.102 | 0.0104 | 1.5830 | 0.01647 | 6.01E-06 | 0.6627 | 0.00457 | 0.00458 |
| A6 | 0.331 | 0.076 | 0.0252 | 1.6677 | 0.04195 | 2.64E-05 | -0.7474 | 0.01405 | 0.01408 |
| A7 | 0.102 | 0.076 | 0.0155 | 1.6550 | 0.02566 | 2.49E-06 | 0.7347 | 0.00837 | 0.00837 |
| A5 | 1.07 | 0.127 | 0.1359 | 1.7565 | 0.23869 | 1.83E-04 | 0.8362 | 0.09503 | 0.09521 |
| TOTAL | | | 0.7000 | | 0.64415 | | | | 0.30214 |



PCB 6. Drawn By: Fiseha N.

| Prest Girder Only | | | | |
|--------------------------|---------|--------------------------|---------|-------|
| Area | $A_c =$ | $\sum A$ | 0.69997 | m^2 |
| Centroid | $Y =$ | $\frac{\sum AY}{\sum A}$ | 0.92027 | m |
| Second Moment of Inertia | $I =$ | $\sum I$ | 0.30214 | m^4 |
| Centroid | $y_b =$ | Y | 0.92027 | m |
| | $Y_t =$ | H- Y | 0.89973 | m |
| Section Modulus | $Z_t =$ | I/Y_t | 0.33581 | m^3 |
| | $Z_b =$ | I/y_b | 0.32832 | m^3 |

Table 4-10 section properties of AASHTO I beam type VI

Figure 4-7 AAHSTO I beam Type VI composite section

4.3.1.1 Effective Length (L_e)

According to AASHTO -2005 section 4.6.2.6

For edge beam

| | |
|---|--------------|
| $L_e \leq \frac{CCG}{2} + \text{minimum of } \left[\begin{array}{c} L/8 \\ 6 * ts + fwe \\ Wg \end{array} \right]$ | Equation 4-2 |
| $fwe = \text{maximum of } \left(\begin{array}{c} fwi/4 \\ bwi/2 \end{array} \right)$ | Equation 4-3 |

➤ **Effective Length (L_e)**

For interior beam

| | |
|---|--------------|
| $L_e \leq \text{minimum of } \left[\begin{array}{c} L/4 \\ 12 * ts + fwm \\ CCG \end{array} \right]$ | Equation 4-4 |
| $fwm = \text{maximum of } \left(\begin{array}{c} fwi/2 \\ bwi \end{array} \right)$ | Equation 4-5 |

Where

Le: - is effective length

CCG: - center to center distance between adjacent girders

L: - Span of a girder

ts: - thickness of cast insitu slab

fwi: - top flange width of precast section

bwi:- web thickness of precast section

Wg:- overhang length of edge girder

4.4 Material Property

4.4.1 Concrete

Unit weight of concrete (γ_c) taken as 25KN/m³

In the program one Can choose the cubic strength (C) of concrete for which the deflection is about to be calculated and presented in the chart.

Once the cubic strength is known the rest of the important parameter of the concrete is calculated as follows. (10)

It is assumed that the quality of concrete is to be used for the cast insitu slab and the precast prestressed beam may differ. Therefore the modulus of elasticity of cast insitu concrete (Ecs) and precast concrete is equal to Ecp, gives modular ratio between the two concrete (η_m) is equal to Ecp/Ecs.

- The characteristic strength of concrete (Fck)

| | |
|-----------------|--------------|
| $Fck = 0.8 * C$ | Equation 4-6 |
|-----------------|--------------|

- Modulus of Elasticity of concrete (Ec)

| | |
|------------------------|--------------|
| $Ec = 4700 * \sqrt{C}$ | Equation 4-7 |
|------------------------|--------------|

- Modulus of Rupture of Concrete (fr)

| | |
|-------------------------|--------------|
| $fr = 0.623 * \sqrt{C}$ | Equation 4-8 |
|-------------------------|--------------|

- Permissible stress

- At transfer

| | |
|--|--------------|
| $Allowable\ compressive\ strenght\ Fct \leq 0.6 * Fck$ | Equation 4-9 |
|--|--------------|

| | |
|--|---------------|
| $Allowable\ tensile\ strenght\ Ftt = 0.21 * (Fck)^{2/3}$ | Equation 4-10 |
|--|---------------|

- Underworking

| | |
|--|---------------|
| $Allowable\ compressive\ strenght\ Fcw \leq 0.5 * Fck$ | Equation 4-11 |
|--|---------------|

| | |
|--|---------------|
| $Allowable\ tensile\ strenght\ Ftw = 0.75 * Ftt$ | Equation 4-12 |
|--|---------------|

- Permissible stress limit under service

| | |
|---|---------------|
| $Stress\ limit\ at\ the\ top\ Ftr = Fcw + \eta * Ftt$ | Equation 4-13 |
|---|---------------|

| | |
|---|---------------|
| $Stress\ limit\ at\ the\ botom\ Fbr = Fct + \eta * Ftw$ | Equation 4-14 |
|---|---------------|

η is the ratio of effective stress to initial stress see the next section

4.4.2 Prestressing Tendon

Though the default value of 1860 Mpa is to be used in the computation tensile strength of the tendon (Fpk) is to be imputed by the user.

Stress loss (η) the expected stress loss is again to be provided by the user. The default value is 18%

Modulus of elasticity of tendon (Ep)

$$Ep = 196.5E3\ Mpa$$

- The characteristic tensile strength of prestressing tendon (F_{py})

| | |
|-------------------------|---------------|
| $F_{py} = 0.9 * F_{pk}$ | Equation 4-15 |
|-------------------------|---------------|

- Stress limit

- *Initial Tensioning*

| | |
|--------------------------|---------------|
| $F_{pit} = 0.8 * F_{pk}$ | Equation 4-16 |
|--------------------------|---------------|

- *At transfer*

| | |
|--------------------------|---------------|
| $F_{pi} = 0.75 * F_{pk}$ | Equation 4-17 |
|--------------------------|---------------|

- *Under working*

| | |
|-------------------------|---------------|
| $F_{pw} = 0.8 * F_{pi}$ | Equation 4-18 |
|-------------------------|---------------|

- Effective stress (F_{pe})

| | |
|----------------------------|---------------|
| $F_{pe} \geq 0.6 * F_{pk}$ | Equation 4-19 |
|----------------------------|---------------|

- Modular ratio between tendon and concrete (η_p)

| | |
|---|---------------|
| $\eta_p = \frac{E_p}{E_c} = \frac{196.5 * 10^3}{E_c}$ | Equation 4-20 |
|---|---------------|

4.5 Eccentricity and Minimum prestressing reinforcement

4.5.1 Eccentricity

Eccentricity refers to the offset of prestressing tendon from the neutral axis of the precast girder section. The tendon eccentricity both at the support and at mid span will be imputed by the user. The possible range of those eccentricities for a given section will be calculated and provide to guide the user. The possible range of the eccentricities (maximum and minimum eccentricities at a section) will be calculated using Magnel diagram

Limiting Zone of prestressing

- A. At support where moment is zero

$$1. \quad e \leq \frac{Z_t * F_{tt}}{P_i} + \frac{Z_t}{A_c} \quad \text{Equation 4-21}$$

$$2. \quad e \leq \frac{Z_b * F_{ct}}{P_i} - \frac{Z_b}{A_c} \quad \text{Equation 4-22}$$

$$3. \quad e \geq -\frac{Z_t * F_{cw}}{\eta * P_i} + \frac{Z_t}{A_c} \quad \text{Equation 4-23}$$

$$4. \quad e \geq -\frac{Z_b * F_{tw}}{\eta * P_i} - \frac{Z_b}{A_c} \quad \text{Equation 4-24}$$

B. At Mid Span

$$1. \quad e \leq \frac{Z_t * F_{tt}}{P_i} + \frac{Z_t}{A_c} + \frac{M_{gl}}{P_i} \quad \text{Equation 4-25}$$

$$2. \quad e \leq \frac{Z_b * F_{ct}}{P_i} - \frac{Z_b}{A_c} + \frac{M_{gl}}{P_i} \quad \text{Equation 4-26}$$

$$3. \quad e \geq -\frac{Z_t * F_{cw}}{\eta * P_i} + \frac{Z_t}{A_c} + \frac{M_{tot}}{\eta * P_i} \quad \text{Equation 4-27}$$

$$4. \quad e \geq -\frac{Z_b * F_{tw}}{\eta * P_i} - \frac{Z_b}{A_c} + \frac{M_{tot}}{\eta * P_i} \quad \text{Equation 4-28}$$

4.5.2 Minimum Prestressing reinforcement

If we introduce two parameters F_{inf} and F_{sup} defined as

$$F_{inf} = -\frac{f_{tw}}{n} + \frac{(M_{dl} + M_{sl} + M_{ll})}{n * Z_b} \quad \text{Equation 4-29}$$

$$F_{sup} = -f_{tt} - M_{dl}/Z_t \quad \text{Equation 4-30}$$

Then 2-14 of minimum prestressing forces simplified as

$$P_{imin} = A_c * \left(\frac{F_{inf} * Z_b + F_{sup} * Z_t}{Z_t + Z_b} \right) \quad \text{Equation 4-31}$$

and 2-15 of the corresponding maximum eccentricity simplified as

$$e_{max} = \frac{(F_{inf} - F_{sup}) * Z_t * Z_b}{A_c * (F_{sup} * Z_t + F_{inf} * Z_b)} \quad \text{Equation 4-32}$$

Accordingly the minimum prestressing reinforcement area is defined as

$$A_{smin} = \frac{P_{imin}}{f_{pi}} \quad \text{Equation 4-33}$$

4.6 Deflection of Prestressed Beam

4.6.1 Section Stress

4.6.1.1 At transfer

| | |
|---|---------------|
| a. Mid Span | |
| Top: $f_{tim} = \frac{P_i}{A_c} - \frac{P_i \cdot e_c}{Z_t} + \frac{Mdl}{Z_t}$ | Equation 4-34 |
| Bottom: $f_{bim} = \frac{P_i}{A_c} + \frac{P_i \cdot e_c}{Z_b} - \frac{Mdl}{Z_b}$ | Equation 4-35 |
| b. Support | |
| Top: $f_{tis} = \frac{P_i}{A_c} - \frac{P_i \cdot e_e}{Z_t}$ | Equation 4-36 |
| Bottom: $f_{bis} = \frac{P_i}{A_c} + \frac{P_i \cdot e_e}{Z_b}$ | Equation 4-37 |

- If all stresses (f_{tim} , f_{bim} , f_{tis} , f_{bis}) is in the range between ($-f_r$, f_{ct}) i.e. greater than $-f_r$ and less than f_{ct} the section is neither cracked nor crushed so elastic method of analysis will be used in the section.
- If one of them is less than $-f_r$ the section is cracked then effective I_e method of deflection calculation will be used in this section and in the following section.
- If one of them is greater than $> f_{ct}$ the section is cracked and deflection calculation will be stopped and the program return a value of zero in this and the following section.

4.6.1.2 After un-shored slab is cast

| | |
|---|---------------|
| a. Mid Span | |
| Top: $f_{tSM} = \frac{P_e}{A_c} - \frac{P_e \cdot e_c}{Z_t} + \frac{(Mdl + Msd)}{Z_t}$ | Equation 4-38 |
| Bottom: $f_{bSM} = \frac{P_e}{A_c} + \frac{P_e \cdot e_c}{Z_b} - \frac{(Mdl + Msd)}{Z_b}$ | Equation 4-39 |
| b. Support | |
| Top: $f_{tSS} = \frac{P_i}{A_c} - \frac{P_i \cdot e_c}{Z_t}$ | Equation 4-40 |
| Bottom: $f_{bSS} = \frac{P_i}{A_c} + \frac{P_i \cdot e_c}{Z_b}$ | Equation 4-41 |

- If all stresses ($f_{tsm}, f_{bsm}, f_{tss}, f_{bss}$) is in the range between ($-f_r, f_{ct}$) i.e. greater than $-f_r$ and less than f_{ct} the section is neither cracked nor crushed so elastic method of analysis will be used in the section.
- If one of them is less than $-f_r$ the section is cracked then effective I_e method of deflection calculation will be used in this section and in the following section.
- If one of them is greater than $> f_{ct}$ the section is cracked and deflection calculation will be stopped and the program return a value of zero in this and the following section.

4.6.1.3 At service load for precast section

| | |
|--|---------------|
| a. Mid Span | |
| Top: $f_{tem} = \frac{Pe}{Ac} - \frac{Pe.ec}{Z_t} + \frac{(Mdl + Msd)}{Z_t} + \frac{Mld}{Z_{tp}}$ | Equation 4-42 |
| bottom: $f_{bem} = \frac{Pe}{Ac} + \frac{Pe.ec}{Z_b} - \frac{(Mdl + Msd)}{Z_b} - \frac{Mld}{Z_{bp}}$ | Equation 4-43 |

a. At support.

Since the moment is zero at support the stresses are the same as the previous section.

- If all stresses (f_{tem}, f_{bem}) is in the range between ($-f_r, f_{ct}$) i.e. greater than $-f_r$ and less than f_{ct} the section is neither cracked nor crushed so elastic method of analysis will be used in the section.
- If one of them is less than $-f_r$ the section is cracked then effective I_e method of deflection calculation will be used in this section and in the following section.
- If one of them is greater than $> f_{ct}$ the section is cracked and deflection calculation will be stopped and the program return a value of zero in this and the following section.

4.6.2 Deflection Calculation

4.6.2.1 At Transfer

1. Due to initial prestressing

| | |
|--|---------------|
| $\delta_{pi} = -\frac{P_i * L^2}{48 * E_c * I_g} * (-5 * ec + ee)$ | Equation 4-44 |
|--|---------------|

2. Due to Self weight

a. If the section is un-cracked

| | |
|---|---------------|
| $\delta_{dl} = \frac{5w_{dl} * L^4}{384 * E_c * I_g}$ | Equation 4-45 |
|---|---------------|

b. If the section is cracked

| | |
|---|---------------|
| $\delta_{dl} = \frac{5w_{dl} * L^4}{384 * E_c * I_e}$ | Equation 4-46 |
|---|---------------|

| | |
|---|---------------|
| From Equation 2-52, 2-53 and 2-55 | |
| $I_e = I_{cr} + \left(\frac{M_{cr}}{M_a}\right)^3 * (I_g - I_{cr}) \leq I_g$ | |
| $\left(\frac{M_{cr}}{M_a}\right) = \left(1 - \frac{f_{tl} - f_r}{f_l}\right)$ | |
| $f_{tl} = \text{total calculated stress in member} = f_{bim}$ | |
| f_l = calculated stress due to self weight load only = M_{dl}/Z_b | |
| Where $n_p = E_{ps}/E_c$ and $\rho_p = A_{ps}/(b * d_p)$ | |
| $d_p = e_c + y_t + d_s$ | |
| Therefore net deflection at transefr is | |
| $\delta_{nett} = \delta_i + \delta_{dl}$ | Equation 4-47 |

4.6.2.2 After un-shored slab is cast

3. Due to Super imposed dead load.

a. If the section is un-cracked

| | |
|---|---------------|
| $\delta_{sl} = \frac{5w_{sl} * L^4}{384 * E_c * I_g}$ | Equation 4-48 |
|---|---------------|

b. If the section is cracked

| | |
|--|---------------|
| $\delta_{sl} = \frac{5w_{sl} * L^4}{384 * E_c * I_e}$ | Equation 4-49 |
| From Equation 2-52, 2-53 and 2-55 | |
| $I_e = I_{cr} + \left(\frac{M_{cr}}{M_a}\right)^3 * (I_g - I_{cr}) \leq I_g$ | |
| $\left(\frac{M_{cr}}{M_a}\right) = \left(1 - \frac{f_{tl} - f_r}{f_l}\right)$ | |
| $f_{tl} = \text{total calculated stress in member} = f_{bsm}$ | |
| $f_l = M_{sl}/Z_b$ if the section cracks in this stage $f_l = (M_{dl} + M_{sd})$ if the section cracked in the transfer stage | |
| Where $n_p = E_{ps}/E_c$ and $\rho_p = A_{ps}/(b * d_p)$ | |
| $d_p = e_c + y_t + d_s$ | |
| Therefore net deflection after un - shored is cast is | |
| $\delta_{nets} = \delta_{nett} + \delta_{sl}$ | |

4.6.2.3 Immediate service load deflection.

4. Due to live load
 - a. If the section is un-cracked

| | |
|---|---------------|
| $\delta ll = \frac{5wll * L^4}{384 * Ec * Igc}$ | Equation 4-50 |
|---|---------------|

- a. If the section is cracked

| | |
|--|---------------|
| $\delta ll = \frac{5wll * L^4}{384 * Ec * Ie}$ | Equation 4-51 |
| From Equation 2-52, 2-53 and 2-55 | |
| $Ie = Icr + \left(\frac{Mcr}{Ma}\right)^3 * (Igc - Icrc) \leq Ig$ | |
| $\left(\frac{Mcr}{Ma}\right) = \left(1 - \frac{ftl - fr}{fl}\right)$ | |
| $ftl = \text{total calculated stress in member} = fbem$ | |
| $fl = Mll/Zb \text{ if the section cracks in this stage}$ $fl = (Msl + Mll)/Zb \text{ if the section cracks after the slab is cast}$ $fl = (Mdl + Msl + Mll) \text{ if the section cracked in the transfer stage}$ | |
| Where $np = Eps/Ec$ and $pp = Aps/(b * dp)$ | |
| $dp = ec + yt + ds$ | |
| Therefore net immediate deflection at service is | |
| $\delta netl = \delta nets + \delta ll$ | |

4.6.2.4 Long term deflection

Using table 2-3 of PCI multipliers

- Net deflection at transfer (δnet) = $\delta nett$
- Net erection deflection before superimposed dead load (δne)

| | |
|--|---------------|
| $\delta ne = \delta pi * 1.8 + \delta dl * 1.85$ | Equation 4-52 |
|--|---------------|

- Net erection deflection immediately after superimposed dead load (δnes)

| | |
|--------------------------------------|---------------|
| $\delta nes = \delta ne + \delta sl$ | Equation 4-53 |
|--------------------------------------|---------------|

- Net erection deflection immediately after service load (δnel)

| | |
|---------------------------------------|---------------|
| $\delta nel = \delta nes + \delta ll$ | Equation 4-54 |
|---------------------------------------|---------------|

- Net final deflection before superimposed dead load ($\delta nelf$)

| | |
|---|---------------|
| $\delta nelf = \delta pi * 2.2 + \delta dl * 2.4$ | Equation 4-55 |
|---|---------------|

- Net final deflection immediately after superimposed dead load (δ_{nfs})

| | |
|--|---------------|
| $\delta_{nef} = \delta_{nf} + \delta_{sl} * 3$ | Equation 4-56 |
|--|---------------|

- Net final deflection immediately after service load (δ_{nfl})

| | |
|---|---------------|
| $\delta_{nfl} = \delta_{nfs} + \delta_{ll}$ | Equation 4-57 |
|---|---------------|

Note: - The upward deflection (camber) is assigned as negative value and the downward deflection is assigned as positive value.

4.6.3 Example 4.1

I. DATA

Input

| | |
|---|-------------|
| The cubic strength of concrete for precast beam (fc) | 50.00 Mpa |
| The tensile strength of tendon (Fpk) | 1862.00 Mpa |
| Expected prestress loss | 18.00% |
| The cubic strength of concrete for cast insitu slab (fcs) | 30.00 Mpa |
| Span Length L | 18.29 m |
| Beam type | 6 |
| Depth of cast insitu slab (ds) | 250.00 mm |
| center to center distance between girder (ccb) | 2200.00 mm |
| Cantilever distance if it is edge girder (W) | 1500.00 mm |
| Area of prestressing tendon (Aps) = Aps Minimum | 4698.85 mm |
| eccentricity at support | 115.00 mm |
| eccentricity at midspan | 100.0 m |

II. Material Properties

| Concrete | | Prestressing Reinf |
|-----------------------------------|-----------------|-----------------------------------|
| fc' = | 50 Mpa | fpk = 1862.00 Mpa |
| fck = 0.8*fc' | 40 Mpa | fpy = 0.9*fpk = 1675.80 Mpa |
| fc' (toping) = | 30 Mpa | fpi = 0.75*fpk = 1396.50 Mpa |
| fr = 0.623*√fc' = | 4.405275247 Mpa | Eps = 196500.00 Mpa |
| Ecp = 4730*√fc' | 33234.01872 Mpa | |
| Ecc = 4730*√fc's | 25742.9602 Mpa | Prestress loss 18% |
| fct = 0.6*fck | 24 Mpa | n = 82% |
| ftt = 0.21*(fck) ^(2/3) | 2.4561749 Mpa | Aps min = 4698.85 mm ² |
| fcw = 0.5*fct | 20 Mpa | Aps = 4698.85 mm ² |
| ftw = 0.75*ftt | 1.842131175 Mpa | Pi = 6561938.50 N |
| ns = Ecp/Ecc = | 0.774596669 | |

III. Geometric Properties

| Type of Beam | PCB 6 | | |
|--------------|-------------|-----------|-----------------|
| ds = | 250.00 mm | | |
| ccb= | 2200.00 mm | | |
| W = | 1500.00 mm | | |
| | Precast | Composite | |
| Ac = | 699966 | 1.349966 | mm ² |
| Ic= | 3.02E+11 | 6.59E+11 | mm ⁴ |
| Cb = | 920.2659077 | 1413.6688 | mm |
| Ct= | 899.7340923 | 406.33118 | mm |
| Zb = | 3.28E+08 | 4.66E+08 | mm ³ |
| Zt = | 3.36E+08 | 1.62E+09 | mm ³ |
| Zts = | | 9.61E+08 | mm ³ |
| Zbs= | | 1.55E+09 | mm ³ |
| Span = | 18.29 m | | |

Depth of Slab $D_s = 0.25$ m
 Effective Length $L_e = 2.6$ m
 Transformed effective length
 $l_{et} = L_e \cdot E_{cp} / E_{cs} = 2.01395$ m

(Impact Factor) IF =
 $1 + 1.2 / \sqrt{L} = 1.28$

IV. Load

$M_I =$ From Table 15.15 of AREMA MRE Manual 3522.82 KNm

| | |
|-----------------------|--|
| $W_{dl} = 17.50$ KN/m | $M_{dl} = 731.74$ KNm |
| $W_{sl} = 41.70$ KN/m | $M_{sl} = 1743.51$ KNm |
| $W_{ll} = 84.25$ KN/m | $M_{ll} = IF \cdot M_I = 4511.29852$ KNm |
| | $M_{tot} = 6986.55$ KNm |

V. Other

$$\begin{aligned}
 ec &= 115.00 \text{ mm} && \text{Out of a range} \\
 ee &= 100.00 \text{ mm} && \text{Ok} \\
 f_{inf} &= M_{tot}/(n \cdot Z_b) - f_{tw}/n = 23.70 \text{ Mpa} \\
 f_{sup} &= -M_{dl}/z_t - f_{tt} = -4.64 \text{ Mpa}
 \end{aligned}$$

Minimum prestressing force

$$\begin{aligned}
 P_{imin} &= A_c \cdot (z_b \cdot f_{inf} + z_t \cdot f_{sup}) / (z_b + z_t) && 6561938.50 \text{ N} \\
 a_{psmin} &= P_{imin} / f_{pi} && 4698.85 \text{ mm}^2 \\
 e_{maxp} &= 716.97 \text{ mm} \\
 \text{Allowable eccentricity} &&& \\
 \text{At support} &&& \text{At mid span} \\
 e_{max} &= 605.45 \text{ mm} && 716.96 \text{ mm} \\
 e_{min} &= -581.45 \text{ mm} && 716.96 \text{ mm}
 \end{aligned}$$

VI. Deflection Calculation

Effective I_e method for short term and PCI Method for long term deflection

Allowable Stress

$$\begin{aligned}
 f_c &= 24.00 \text{ Mpa} \\
 f_{cw} &= 20.00 \text{ Mpa} \\
 f_r &= 4.41 \text{ Mpa} \\
 \eta_p &= E_p / E_{cp} = 5.84
 \end{aligned}$$

1.00 Mid Span Section Stress

$$\begin{aligned}
 f_{pi} &= 1583.63 \text{ Mpa} \\
 ec &= 115.00 \text{ mm} \\
 P_i &= A_s \cdot f_{pi} = 6561938.50 \text{ N} \\
 M_d &= W_d \cdot L^2 / 8 = 731.74 \text{ KNm}
 \end{aligned}$$

a At transfer

$$f_t = \frac{P_i}{A_c} - \frac{P_i \cdot e_c}{Z_t} + \frac{M_d}{Z_t}$$

9.36 Mpa Ok

$$f_b = \frac{P_i}{A_c} + \frac{P_i \cdot e_c}{Z_b} - \frac{M_d}{Z_b}$$

9.44 Mpa OK

After unshored slab**b is cast**

At this load level

$$f_{pe} = 1145.13 \text{ Mpa}$$

$$P_e = A_s \cdot f_{pe} = 5380789.57 \text{ N}$$

$$W_{sd} = 41.70 \text{ Kn/m}$$

$$M_{sd} = W_{sd} \cdot L \cdot L / 8 = 1743.51 \text{ KNm}$$

$$f_t = \frac{P_e}{A_c} - \frac{P_e \cdot e_c}{Z_t} + \frac{M_d}{Z_t} + \frac{M_{sd}}{Z_t}$$

13.22 Mpa Ok

$$f_b = \frac{P_e}{A_c} + \frac{P_e \cdot e_c}{Z_b} - \frac{M_d}{Z_b} - \frac{M_{sd}}{Z_b}$$

2.03 Mpa OK

At service load for precast section**c**

$$M_l = W_l \cdot L \cdot L / 8$$

4511.30 KNm

$$f_t = \frac{P_e}{A_c} - \frac{P_e \cdot e_c}{Z_t} + \frac{M_d}{Z_t} + \frac{M_{sd}}{Z_t} + \frac{M_l}{Z_t}$$

16.00 Mpa OK

$$f_b = \frac{P_e}{A_c} + \frac{P_e \cdot e_c}{Z_b} - \frac{M_d}{Z_b} - \frac{M_{sd}}{Z_b} - \frac{M_l}{Z_b}$$

-7.64 Mpa Cracked

c Composite Slab stress**Precast =**

$$E_{cp} = 4734 \cdot (f_c')^{1/2}$$

33474.44 Mpa

$$E_{ci} = 25929.19 \text{ Mpa}$$

$$\eta = E_{ci}/E_{cp} \quad 0.77$$

$$f_{cst} = \eta * M_l / Z_{ct} = 3.64 \text{ Mpa}$$

$$f_{csb} = \eta * M_l / Z_{cb} = 2.26 \text{ Mpa}$$

2.00 support Section Stress

$$ee = 100.00 \text{ mm}$$

a At transfer

$$f_t = p_i / A_c - P_i * ee / Z_t$$

$$7.42 \text{ Mpa} > f_{tt} \quad \text{Ok}$$

$$f_b = p_i / A_c + P_i * ee / Z_b$$

$$11.37 \text{ Mpa} < f_{ct} \quad \text{OK}$$

b After unshored slab is cast

At this load level

$$P_e = A_s * f_{pe} = 5,380,789.57$$

$$f_t = p_e / A_c - P_e * ee / Z_t$$

$$7.36 \text{ Mpa} \quad \text{Ok}$$

$$f_b = p_e / A_c + P_e * ee / Z_b$$

$$9.33 \text{ Mpa} \quad \text{OK}$$

c At service load for precast section

$$f_t = p_e / A_c - P_e * ee / Z_t$$

$$7.36 \text{ Mpa} \quad \text{OK}$$

$$f_b = p_e / A_c - P_e * ee / Z_b$$

$$9.33 \text{ Mpa} \quad \text{Ok}$$

| summary of stress (Mpa) | | Mid Span | | Support | |
|-------------------------|--------|----------|---------|---------|----|
| At Transfer | Top | 9.36 | OK | 7.42 | OK |
| | Bottom | 9.44 | OK | 11.37 | OK |
| After unshored slab | Top | 13.22 | OK | 7.36 | OK |
| | Bottom | 2.03 | OK | 9.33 | OK |
| At Service | Top | 16.00 | OK | 7.36 | OK |
| | Bottom | -7.64 | Cracked | 9.33 | OK |

3.00 Camber and Deflection calculation at transfer

$$E_{ci} = 29,937.92$$

$$E_c = 33,474.44$$

due to initial prestress only

$$\delta_i = \frac{p_i * L^2}{48 * E_{ci} * I_g} * (-5 * e_c + e_e)$$

-2.40 mm Upward

due to self-weight

$$\delta_d = \frac{5 * W_d * l^4}{384 * E_{ci} * I_g}$$

2.82 mm Downward

$$\delta_{net} = \delta_i - \delta_d =$$

0.42 mm Downward

3.00 Immediate Service Load Deflection

Effective Ie Method

$$f_r = 4.41 \text{ Mpa}$$

$$d_p = e_c + y_t + d_s$$

1149.73 mm

$$\rho_p = \frac{A_{ps}}{b d_p} = 1.86E-03$$

$$I_{cr} = \eta_p * A_{ps} * (d_p^2) * (1 - 1.6 * (\eta_p * \rho_p)^{1/2})$$

3.02E+10 mm⁴

$$\frac{M_{cr}}{M_a} = 1 - \frac{(f_t - f_r)}{f_l} = 0.67$$

$$\left(\frac{M_{cr}}{M_a}\right)^3 = 0.30$$

$$I_e = \left(\frac{M_{cr}}{M_a}\right)^3 (I_g - I_{cr}) + I_{cr} \leq I_g = 1.10E+11 \text{ mm}^4$$

$$I_e = 1.10E+11 \text{ mm}^4$$

Before Service load and
crack δ_{sd} due to the cast
insitu slab

$$\delta_{sd} = (5 * w_{sd} * l^4) / (384 * E_{cp} * I_g)$$

6.01 mm

After Service load and
crack δ_l due to the
service load

$$\delta_l = (5 * w_{ld} * l^4) / (384 * E_{cp} * I_e)$$

33.20 mm

5.00 Long Term Deflection (Camber) By PCI multiplier

| -PCI multipliers C, for long-term camber and deflection | | |
|--|---------------------------|------------------------|
| | Without composite topping | With composite topping |
| At Erection | | |
| Deflection (downward) component-apply to the elastic deflection due to the member weight at release of prestress | 1.85 | 1.85 |
| Camber (upward) component-apply to the elastic camber due to prestress at the time of release of prestress | 1.8 | 1.8 |
| Final | | |
| Deflection (downward) component-apply to the elastic deflection due to the member weight at release of prestress | 2.7 | 2.4 |
| Camber (upward) component-apply to the elastic camber due to prestress at the time of release of prestress | 2.45 | 2.2 |
| Deflection (downward)--apply to the elastic deflection due to the superimposed dead load only | 3 | 3 |
| Deflection (downward)-apply to the elastic deflection caused by the composite topping | | 2.3 |

| Deflection/Camber (mm) | | | | | | |
|-------------------------------|----------------------|-----------------|-----------------------|-----------------|------------------------|-----------------|
| Load | At Transfer | PCI Multiplier | Erection | PCI Multiplier | δ Final | |
| Prestressing Load Only (P) | $\delta_i = -2.40$ | 1.80 | -4.32 | 2.20 | -9.51 | |
| Self Weight (Wd) | 2.82 | 1.85 | 5.21 | 2.40 | 12.52 | |
| δ_{net} | $\delta_{nt} = 0.42$ | Downward | 0.89 | Downward | 3.01 | Downward |
| Super Imposed Dead Load (Wsd) | | | 6.01 | 3.00 | 18.02 | |
| $\delta_{net} =$ | | | $\delta_{nes} = 6.90$ | Downward | 21.03 | Downward |
| Service Load (Wl) | | | 33.20 | | 33.20 | |
| δ_{net} | 0.42 | Downward | 40.10 | Downward | $\delta_{nfl} = 54.23$ | Downward |

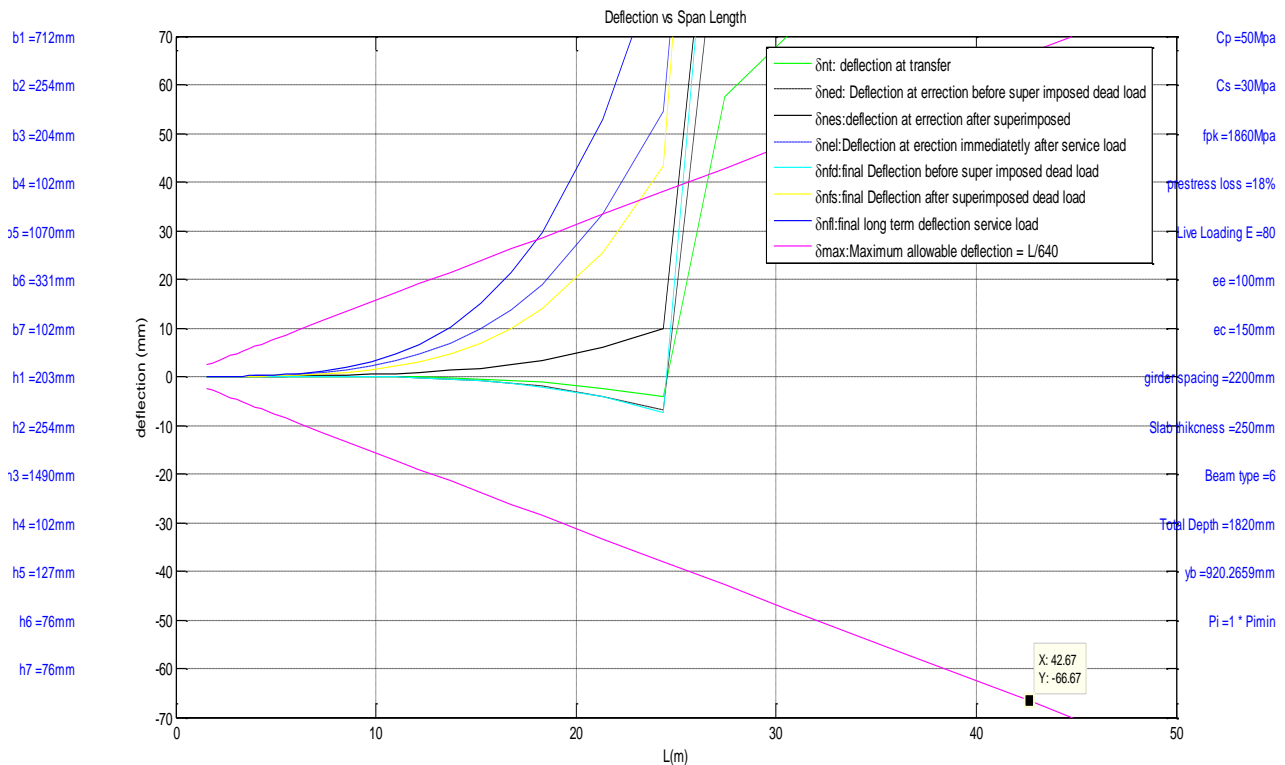


Figure 4-8 Deflection Chart for AASHTO Type 6 I beam.

5 Result and Discussion

As I was developing the chart for different beams something strange happened. That is the deflection vs. span length chart will show some unexpected behavior after a certain span length. It suddenly changes its dimension and direction in an unanticipated manner. I was curious what makes this sudden shift, so I try to change the eccentricity of the tendon profile. And for that I have to know the maximum and the minimum allowable range both at the support and mid span. I write the code for those parameters and draw a chart. Amazingly the maximum and minimum limits of the eccentricity will cross each other at some point both for mid span and Support section that means there is a span length for which the maximum limit become less than the minimum, which is practically impossible.

In this stage I doubt my code and start to calculate manually and using Microsoft excel template which I developed it for checking purpose. But the result was still the same. That means the section has a span length limit for a given load beyond which it will no longer work. Or it will fail if we chose to build it with some eccentricity.

The reason behind the maximum span length limit is to avoid tensile failure of concrete at mid span. In which for a given prestressing force and given self-weight the maximum eccentricity is limited to avoid the tensile failure at the top and the compressive failure at the bottom during transfer. But in this case the tensile strength of concrete always dictate the maximum possible eccentricity. In other words the maximum eccentricity is set to avoid tensile failure at the top during transfer. On the other hand for a given prestressing force and a given service load the minimum eccentricity is set to avoid the tensile failure at the bottom and compressive failure at the top during service. Yet again the tensile strength of concrete comes to dictate the minimum possible eccentricity, which means the minimum possible eccentricity is set to avoid the tensile failure at the bottom during service. However after a certain span length it become impossible to avoid tensile failure at the one surface while maintaining the safety of the other surface. It means after a certain span length the eccentricity needed to avoid the tensile failure at the top during transfer will be less than the minimum allowable eccentricity required to avoid the tensile failure at the bottom during service and vice versa. In addition to that the maximum allowable prestressing force becomes less than the minimum allowable span length after

Note the whole same thing happen for the support section too. Since it happens after the mid-span section it does not govern the maximum span length.

What I found interesting in this chart was this shift of the maximum and minimum eccentricity will happen also prior to some span length that is the maximum allowable eccentricity will be less than the minimum up to a certain span length. This means unlike in reinforced concrete

which has no minimum span length limit structurally speaking prestressed member has a minimum limit of span length due to the applied axial compression force.

The reason for the minimum span length limit is to avoid the crushing of concrete. As discussed in the above paragraph, for a given prestressing force and given self-weight the maximum eccentricity is limited to avoid the tensile failure at the top and the compressive failure at the bottom during transfer. And in this case the maximum eccentricity is set to avoid compressive failure at the bottom during transfer (The tensile failure at the will also occur juts right before the minimum span length). And for a given prestressing force and a given service load the minimum eccentricity is set to avoid the tensile failure at the bottom and compressive failure at the top during service. In this case the minimum possible eccentricity is set to avoid the compressive failure at the top during service. However before a certain span length the eccentricity needed to avoid the compressive failure at the bottom during transfer will be less than the minimum allowable eccentricity required to avoid the compressive failure at the top during service and vice versa.

If one use the minimum prestressing force as an applied force the maximum allowable mid span eccentricity (*emaxm*), the minimum allowable mid-span eccentricity (*eminm*) and the maximum mid-span eccentricity corresponding to the minimum prestressing force (*emaxc*) will be the same for a working range. Before or beyond that range the maximum allowable mi-span eccentricity (*emaxm*) will be less than the maximum mid-span eccentricity corresponding to the minimum prestressing force (*emaxc*) which in turn less than the minimum allowable mid-span eccentricity (*eminm*).

That is $emaxm = eminm = emaxc$ for the possible working range and

$$emaxm < emaxc < eminm \text{ before and beyond the possible working range.}$$

Which means if one has to choose the minimum prestressing force as an applied prestressing force in prestressing design there is only one specific point that can use as the eccentricity of tendon at the mid span section.

By range I mean span length.

However If one chooses to use the applied prestressing force higher than the minimum value the maximum allowable mid span eccentricity (*emaxm*) will be higher than the minimum allowable mid-span eccentricity (*eminm*) for the working range and the maximum allowable mid span eccentricity (*emaxm*) will be lower than the minimum allowable mid-span eccentricity (*eminm*) outside of the working range.

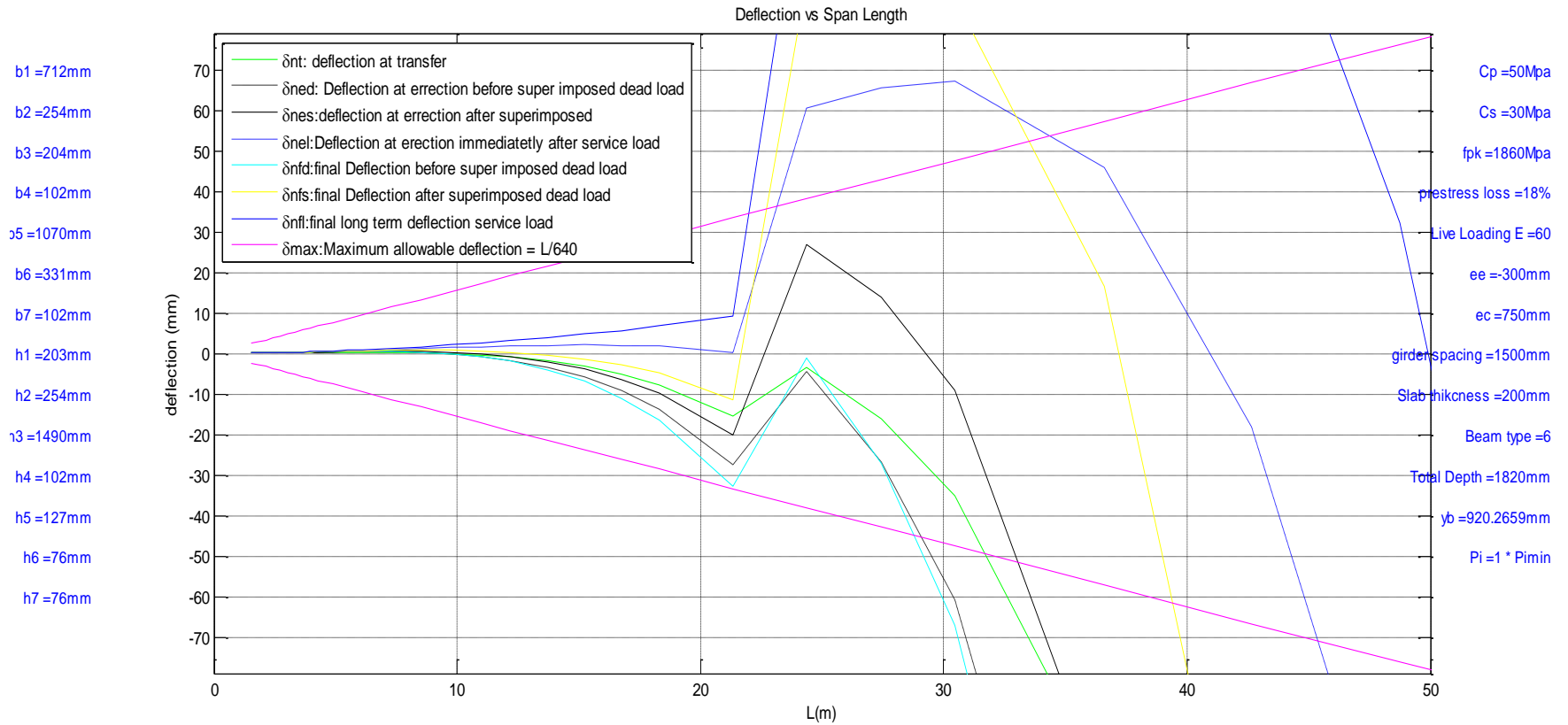


Figure 5-1 Typical deflection vs. Span Length Chart.

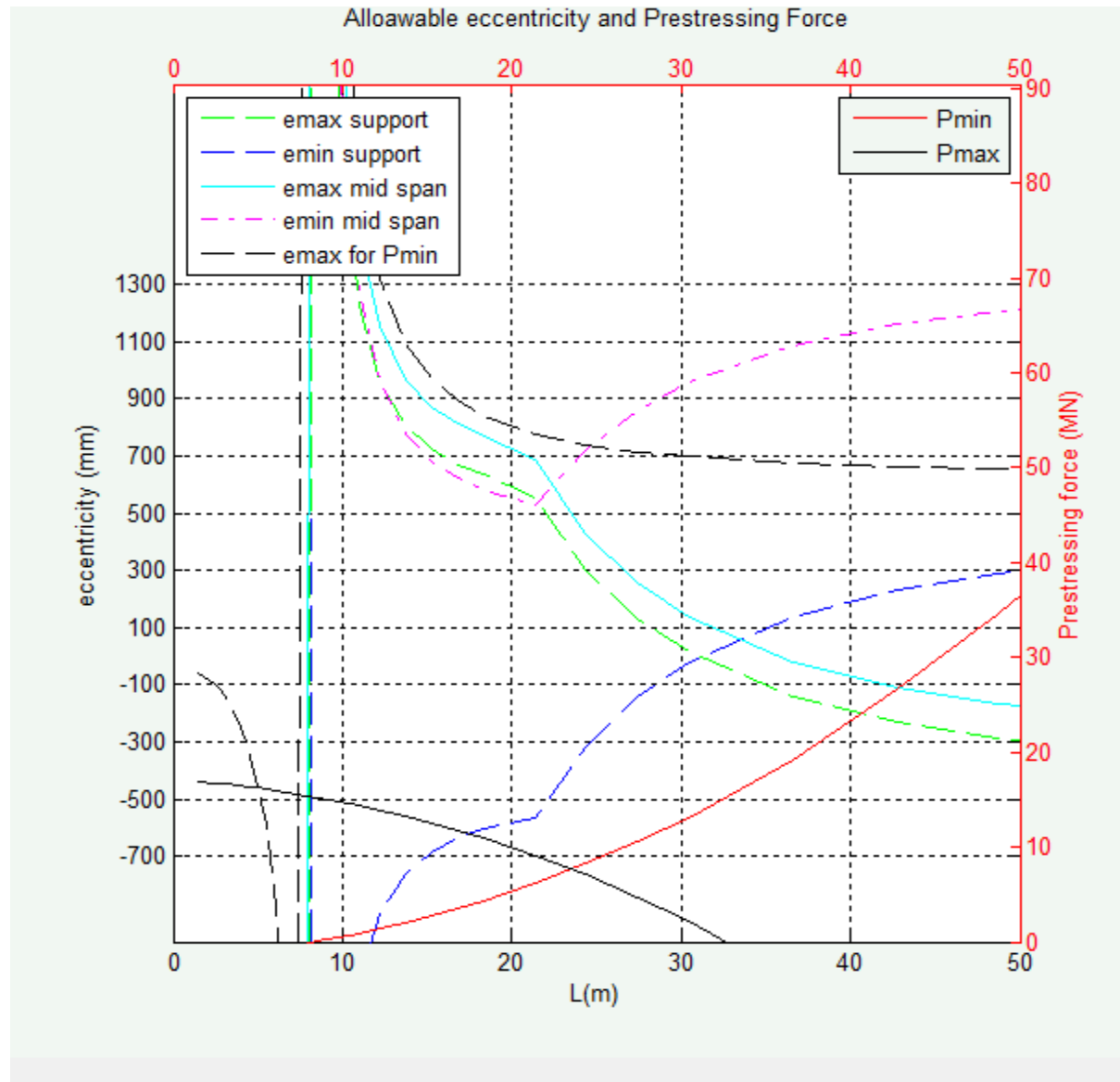


Figure 5-2 Allowable eccentricity and minimum prestressing force vs. span length for type 6 AASHTO I beam for $P_i = 1.25 \cdot P_{imin}$

As you can see in the above chart the maximum allowable mid-span eccentricity/ e_{max} mid-span (cyan color solid line) is higher than the minimum allowable mid-span eccentricity/ e_{min} mid-span (magenta broken line) in the range from 7.m – 19m. This means with this type of loading and material property AASHTO type 6 I beam works in the range of 7.0m to 19.0m.

When it comes to support eccentricity, the maximum allowable support eccentricity/ e_{max} support (the green dashed line) is again higher than the minimum allowable support

eccentricity/ e_{min} support (the blue dashed line) in the range about from 7m to 28m. Based on the support eccentricity allowable working range from 7m to 28m, however since the minimum range govern the working range of this beam is about form 7m to 19m. The above chart was developed for the ratio of applied prestressing force to the minimum prestressing force equal to 1.25 that is for $P_i = 1.25 * P_{imin}$. Now let us see for $P_i = P_{imin}$

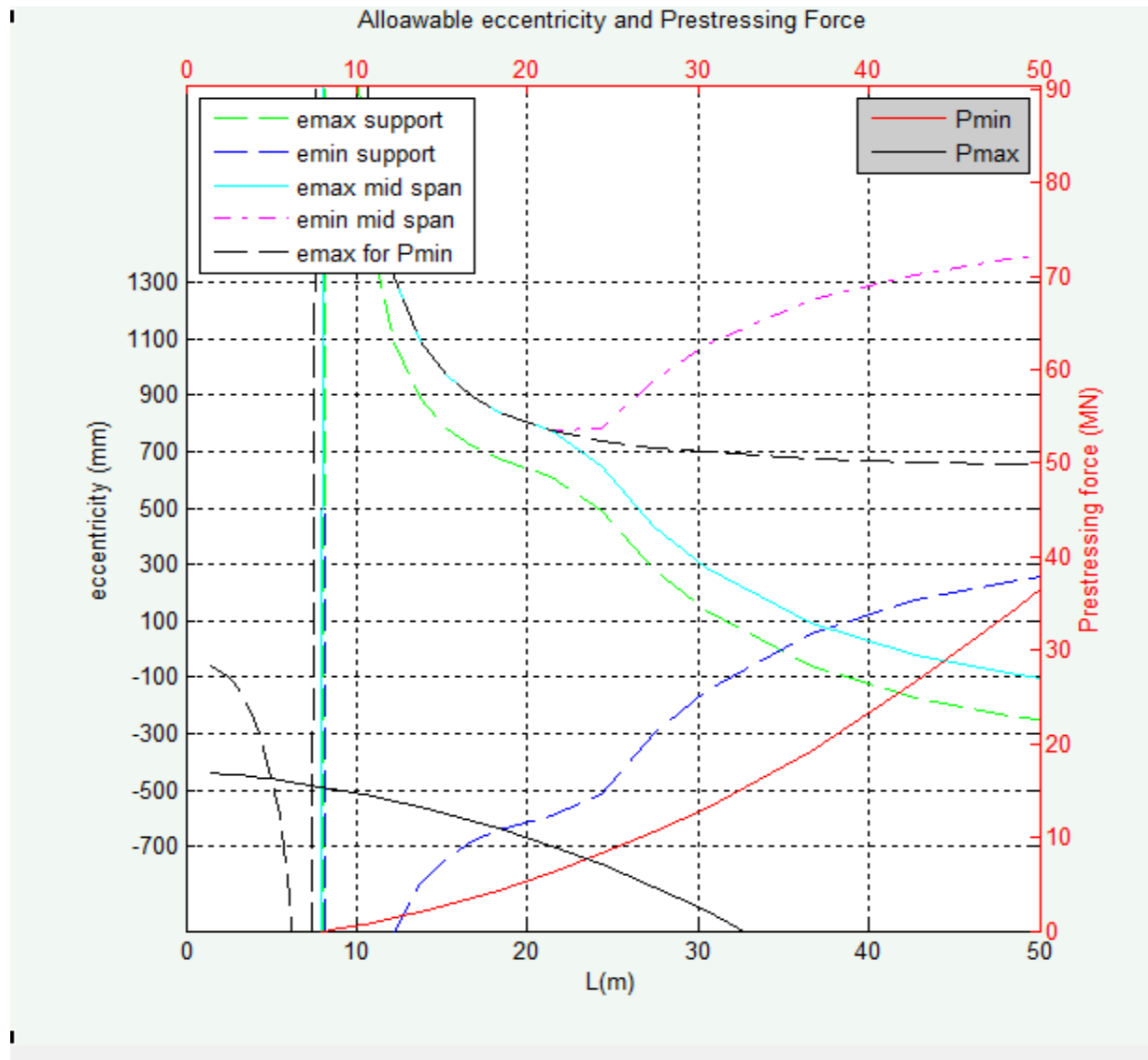


Figure 5-3 Allowable eccentricity and minimum prestressing force vs. span length for type 6 AASHTO I beam for $P_i = P_{imin}$

As you can see in the above graph the three eccentricities, maximum allowable mid span eccentricity (e_{maxm}), the minimum allowable mid-span eccentricity (e_{minm}) and the maximum

mid-span eccentricity corresponding to the minimum prestressing force (*emaxc*) is the same for a working range. That means there is one possible tendon profile at mid span if we are going to use the minimum possible prestressing force as the applied one.

As applied prestressing force increases the upward deflection (camber) increases proportionally and the overall downward deflection decreases; and vice versa.

When the mid-span eccentricity increases to the positive value the upward deflection (camber) increases proportionally and the overall downward deflection decreases, and vice versa.

When the support eccentricity increases to the positive value positive value the upward deflection (camber) decreases proportionally and the overall downward deflection increases; and vice versa.

When the support eccentricity increases in magnitude to the negative value the upward deflection (camber) increases proportionally and the overall downward deflection decreases; and vice versa.

6 Conclusion

The objective of the thesis is achieved in which a simple user friendly and versatile program is developed that plot a deflection chart for simply supported prestressed railway girder.

One can control the deflection or camber of the prestressed member with the magnitude of the applied load and varying the eccentricity of the tendon profile both at the support and at the mid-span. Especially at the support where we have a large range where we can fix the centroid of our tendon.

$$\delta = \frac{P * L^2}{48 * EI} * (-5 * e1 + e2)$$

And from the charts I developed the following points concluded as follows.

- As applied prestressing force increases the upward deflection (camber) increases proportionally and the overall downward deflection decreases; and vice versa.
- When the mid-span eccentricity increases to the positive value the upward deflection increases proportionally and the overall downward deflection decreases, and vice versa.
- When the support eccentricity increases to the positive value positive value the upward deflection decreases proportionally and the overall downward deflection increases; and vice versa.
- When the support eccentricity increases in magnitude to the negative value the upward deflection increases proportionally and the overall downward deflection decreases; and vice versa.

For a given load and a given cross-sectional geometry a prestressed member has not only a maximum span length limit but also a minimum span length limit in order to serve the intended function without failure. This minimum limit is due to the applied axial compression force and upward deflection. The applied prestressing axial force is counteracted by the self-weight of the member at transfer and the super imposed dead and the live (service) load at service. However below certain length the total weight of the member which increases with the span length may not be high enough to counteract the applied axial prestressing force and limit the stresses at the section of a beam to allowable stress limits. In which compression failure will occur either on the top or bottom surface of the member. This intern limits the minimum workable span length.

On the other hand, the maximum span length limit is governed by the applied service load and the downward deflection imposed by service load. After a certain span length the concrete will face tensile failure either on the top or bottom surface of a member.

7 Topics for Further Study

The following points could be interesting topic for further study.

- i. Questioning ACI method of deflection calculation. One can use simulation or other method of deflection calculation and compare the results with the values developed on the chart. Especially on the long term method of deflection calculation ACI recommends using PCI method of computation. However PCI bridge manual itself question the accuracy of the method for composite member.
- ii. Analyzing the effect of partial prestressing in deflection and overall design of prestressed member. That is the effect of adding non prestressing reinforcement in a prestressed member on the deflection calculation and overall design of a member.
- iii. Providing a deflection chart for continues I beam. As this thesis is for simply supported it would be interesting what happens to those results when the beam is continuous.

8 Reference

1. **Benaim, Robert.** *The Design of Prestressed Concrete Bridges, Concepts and Principles* . London and New York : Tylor and Francis Group , 2008.
2. **Raju, N Krishna.** *Prestrssed Concrete, fourth edition.* New Delhi : Tata McGraw-Hill Publishing Company Limited, 2007.
3. *An Intoduction to Prestressed Concrete.* **A J Threlfall BEng, DIC.** s.l. : British Cement Association , 2002.
4. *Civil Engineering Design, Prestressed Concrete.* **Caprani, Dr. Colin.** 2006/07.
5. *Prestressed Concrete Design, (SAB 4323)* . **Ahmad, Assoc. Prof. Baderul Hisham.** s.l. : University Technolgy Malaysia.
6. *Control of Deflection in Concrete Structure ACI 435R-95.* 2000.
7. *Building Code Requiremnts for Structural Concrete (ACI 318-08) and Commentary.* s.l. : American Concrete Institute, 2008.
8. *PCI Bridge Manual* . s.l. : Precast/Prestressed Concrete Institute, 1997.
9. *AREMA Manual for Railway Enigneering.* s.l. : American Railway Engineering and Maintainance of way Association. , 2010.
10. *Prestressed Concrete Railway Bridges, Lecture Note.* Asnake, Dr.
11. *AASHTO LRFD BRIDGE DESIGN SPECIFCATION* . s.l. : American Association of State Highway and Transportation Officials, 2012.
12. *AASHTO LRFD Bridge Design Specification Third Edition* . s.l. : American Asscoiation of State Highway and Transport Officials, 2005.
13. **F K Kong and R H Evans.** *Reinforced and Prestrssed Concrete, 3rd edition* . London : Chapman and HAll, 1993.
14. **Brian H.Hahn and Daniel T.Valentine.** *Essential Matlab for Engineers and Scientists, 5th edition.* s.l. : Elsevier, 2013.
15. <http://www.mathworks.com>. <http://www.mathworks.com>. [Online]

Appendix A: code for MATLAB Program Language

```

% Material
disp('insert the cubic strength of the prestressed concrete:in
Mpa' )
c=input('c=');
disp('insert the cubic strength of the cast insitu slab
concrete: in Mpa' )
cs = input('cs =');
disp('insert the the tensile strength of ptesstress tendon: in
Mpa ' );
fpk=input('fpk=');
Ep=196500;
disp('insert the expected prestress loss percentage:' );
prl=input('prl=');
disp('insert the ratio of applied force to the minimum
prestressing force (Pi/Pimn):' );
pff=input('pff=');
disp('choose the type of live loading: enter 80 for E-80 loading
and 60 for E-60 loading' );
cooperl = input('cooperE-');
eta=1-prl/100;
%concrete
gammac=25;
fck=0.8*c;
Ecp=4700*sqrt(c);
Ecs = 4700*sqrt(cs);
mrs = Ecp/Ecs;
mrp = Ep/Ecp;
fct=0.6*fck;
ftt=0.21*fck^(2/3);
fcw=0.5*fck;
ftw=0.75*ftt;
ftr=fcw+eta*ftt;
fbr=fct+eta*ftw;
fr=0.623*sqrt(c);

% prestressing Tendon
fpy=0.9*fpk;
fpit=0.8*fpk;
fpi=0.75*fpk;

```

```
fpew=0.8*fpi;
fpe=0.6*fpk;

% GEOMETRY
disp('insert the type of the beam enter value 1 - 6 for AASHTO I
beams and 7 for custom I beam:');
beamType=input('beamType=');

switch(beamType)
    case 1
        H = 712.00;
        b1=407.00; b2=127.00; b3=153.00; b4=076.00; b5=305.00; b6 =0.0;
        b7 =0.0;

        h1=127.00; h2=127.00; h3=483.00; h4=076.00; h5=102.00; h6=0.0;
        h7 =0.0;

    case 2
        H = 920.00;
        b1=459; b2=153; b3=153; b4=076; b5=305; b6 =0.0; b7 =0.0;

        h1=153; h2=153; h3=607; h4=76; h5=160; h6=0.0; h7 =0.0;

    case 3
        H = 1150.00;
        b1=560; b2=190; b3=180; b4=115; b5=410; b6 =0.0; b7 =0.0;

        h1=180; h2=190; h3=790; h4=115; h5=180; h6=0.0; h7 =0.0;

    case 4
        H = 1372.00;
        b1=664; b2=230; b3=204; b4=153; b5=510; b6 =0.0; b7 =0.0;

        h1=203; h2=230; h3=966; h4=153; h5=203; h6=0.0; h7 =0.0;

    case 5
        H = 1600.00;
        b1=712; b2=254; b3=204; b4=102; b5=1070; b6=331; b7=102;

        h1=203; h2=254; h3=1270; h4=102; h5=127; h6=076; h7=076;

    case 6
```

```

H = 1820.00;
b1=712; b2=254; b3=204; b4=102; b5=1070; b6=331; b7=102;

h1=203; h2=254; h3=1490; h4=102; h5=127; h6=076; h7=076;
otherwise
    bx=[4 12.7088 12.7088 9.6020 9.6020 10.8594 14.8983
14.8983 1.8106 1.8106 5.8494 7.0970 7.0970 4.0000 4];
    by=[4 4 6.483 9.5898 19.8938 21.0874 22.0170 23.5704
23.5704 22.0170 21.0874 19.8374 9.5898 6.4830 4];
    plot(bx,by);
    axis ([0 30 0 30])
    title ('I Beam')
    set(gca, 'Xtick', 0:40:40)
    set(gca, 'Ytick', 0:40:40)
    text(8.335,3, '-----b1-----
', 'fontsize', 9, 'HorizontalAlignment', 'center', 'color', 'blue')

text(13.0,5.22, 'h1', 'fontsize', 9, 'HorizontalAlignment', 'left', 'c
olor', 'blue')
    text(13.5,4, '----
', 'fontsize', 9, 'HorizontalAlignment', 'right', 'color', 'blue')
    text(13.5,6.483, '----
', 'fontsize', 9, 'HorizontalAlignment', 'right', 'color', 'blue')
    text(11.15,6.483, '--b2--
', 'fontsize', 9, 'HorizontalAlignment', 'right', 'color', 'blue')

text(13.0,8.037, 'h2', 'fontsize', 9, 'HorizontalAlignment', 'left', '
color', 'blue')
    text(13.5,6.483, '----
', 'fontsize', 9, 'HorizontalAlignment', 'right', 'color', 'blue')
    text(13.5,9.6, '----
', 'fontsize', 9, 'HorizontalAlignment', 'right', 'color', 'blue')
    text(8.35,14.74, '--b3--
', 'fontsize', 9, 'HorizontalAlignment', 'center', 'color', 'blue')

text(10.75,14.74, 'h3', 'fontsize', 9, 'HorizontalAlignment', 'center
', 'color', 'blue')
    text(11.2,19.89, '----
', 'fontsize', 9, 'HorizontalAlignment', 'right', 'color', 'blue')
    text(11,9.6, '----
', 'fontsize', 9, 'HorizontalAlignment', 'right', 'color', 'blue')
    text(10.23,21.09, '--b4--
', 'fontsize', 9, 'HorizontalAlignment', 'center', 'color', 'blue')

```

```
text(11,20.5,'h4','fontsize',9,'HorizontalAlignment','center','color','blue')
    text(12.88,21.09,'--b6--
','fontsize',9,'HorizontalAlignment','center','color','blue')

text(14.9,21.55,'h6','fontsize',9,'HorizontalAlignment','center',
,'color','blue')
    text(15.8,22.02,'-----
','fontsize',9,'HorizontalAlignment','right','color','blue')
    text(15.8,23.57,'-----
','fontsize',9,'HorizontalAlignment','right','color','blue')

text(15.6,22.80,'h5','fontsize',9,'HorizontalAlignment','right',
,'color','blue')
    text(8.36,24.22,'--b5--
','fontsize',9,'HorizontalAlignment','center','color','blue')
    text(15.1,21.09,'-----
','fontsize',9,'HorizontalAlignment','right','color','blue')

hold off
```



```

disp('enter h6')
h6 = input('h6=');
b2=h2;
b3 = b1-2*b2;
h3 = H - h1 -h5;
b4 =h4;
b6 = (b5 -b3-2*b4)/2;
h7 =h6;
b7 = b4;
end

% calculation
a1 = b1*h1;
a2=b2*h2;
a3=b3*h3;
a4=b4*h4;
a5=b5*h5;
a6 = b6*h6;
a7 = 2*b7*h7;

ac =(a1+a2+a3+a4+a5+a6+a7);

y1=h1/2;
y2=h1+h2/3;
y3=h1+h3/2;
y4=H-h5-h7-h4/3;
y5=H-h5/2;
y6 =H -h5-h6/3;
y7= H - h5 -h7/2;

AY = a1*y1+a2*y2+a3*y3+a4*y4+a5*y5+a6*y6+a7*y7;
Y = AY/ac;
yb = Y;
yt = H-yb;
Io =
(b1*h1^3/12+b2*h2^3/18+b3*h3^3/12+b4*h4^3/18+b5*h5^3/12+b6*h6^3/
18+b7*h7^3/6);
Ig = Io + (a1*(y1-Y)^2+a2*(y2-Y)^2+a3*(y3-Y)^2+a4*(y4-
Y)^2+a5*(y5-Y)^2+a6*(y6-Y)^2+a7*(y7-Y)^2);
zt = Ig/yt;

```

```

zb = Ig/yb;

epaxis = roundn((yb+500),2);
enaxis = roundn((-yt+200),2);

% Tendon profile input
str=['practical limit of eccentricity from the neutral axis in
mm',num2str(-yt), 'and' ,num2str(yb)];
disp(str)
disp('enter the ecentricity at support in mm');
ee = input ('ee =');
disp('enter the ecentricity at midspan in mm');
ec = input ('ec =');
disp('insert the center to center disatnce between girder:mm'
);
ccb=input('ccb=');
disp('insert the depth of cast in-situ slab in mm:' );
ts=input('ts=');
disp('insert 1 if the beam is edge beam and 0 if it is inetrior
beam:' );
edgeGirder=input('edgeGirder=');

if(edgeGirder==1)
    disp('insert the cantilever edge section in mm:' );
    edg=input('edg=');
else
    edg=0;
end
wg=edg;
if (wg~=0)
wsd=10.625+25*(ts/1000)*((ccb/2000)+edg/1000)+19*0.3*(edg/1000+c
cb/2000);
else
    wsd=10.625+25*(ts/1000)*(ccb/1000)+19*0.3*ccb/1000;
end
wsl = wsd;
wdl=25*ac/(1e6);

%hold on
grid on

p=0

```

```

% length array for copper e-80 loading
% L =[1.52 1.83 2.13 2.44 2.74 3.05 3.35 3.66 3.96 4.27 4.88
5.49 6.10 7.32 8.53 9.75 10.97 12.19 13.72 15.24 16.76 18.29
21.34 24.38 27.43 30.48 36.58 42.67 48.77 54.86 60.96 76.20
91.44 106.68 121.92];
% m1 =[67.79 81.35 94.91 108.46 127.30 152.53 178.10 216.93
257.60 298.28 379.62 460.97 559.27 773.38 991.06 1234.93 1487.72
1777.86 2170.91 2578.46 3027.64 3522.10 4630.06 5855.56 7238.75
8739.89 12507.80 16820.05 21568.07 26671.30 32148.73 47612.98
66163.04 88194.79 113616.04];
for i=1:1:35
    % Gemoetry for composite section
    t = 1*L(1,i)
    if (wg~=0)
        fw = max(b5/4,b3/2);
        le = ccb/2+min(L(1,i)*(1/8),min(6*ts+fw,wg));
    else

        fw = max(b5/2,b3);
        le = min(L(1,i)*(1/4), min(12*ts+fw,ccb));
    end
    lef = mrs*le;
    % MMaximum allowable defelection
    dmax(1,i)= L(1,i)/640*1000;
    cmax(1,i)= L(1,i)/640*-1000;

    % Gemoetry for composite section

    b8 = lef; h8 = ts;
    a8 = b8*h8;
    y8 = H + h8/2;
    acc = ac+a8;
    Yc = (AY+a8*y8)/acc;
    ybg = Yc;
    ytg = H - ybg;
    yts = H+ts-ybg;

    Ioc = Io + (b8*h8^3)/12;
    Igc = Ioc + (a1*(y1-Yc)^2+a2*(y2-Yc)^2+a3*(y3-
Yc)^2+a4*(y4-Yc)^2+a5*(y5-Yc)^2+a6*(y6-Yc)^2+a7*(y7-
Yc)^2+a8*(y8-Yc)^2);

    ztp = Igc/ytg;

```

```

zts = Igc/yts;
zbp = Igc/ybg;
zbs = ztp;

% Moment
%Impact factor for live load
if (L(1,i)<=4)
    k=1.6;
elseif (L(1,i)<=39)
    k=1+(120/sqrt(L(1,i)))/100;
else
    k=1.2;
end;

% Momnet
mdl= (wdl*L(1,i)^2/8)*1e6;
msl= (wsd*L(1,i)^2/8)*1e6;
mlt= k*ml(1,i) ;
wl = 8*mlt/(L(1,i)^2);
if (cooper1 == 80);
    lf = 1;
else
    lf =3/4;
end;
wll =wl*lf;
mll = wll*L(1,i)^2/8*1e6 ;
mtot=mdl+msl+mll;

%Minmum prestressing force and the corresponding maximum
%eccentricity.

finf = mtot/(eta*zb)-ftw/eta;
fsup = -mdl/zt - ftt;

Pimin = ac*(zb*finf+zt*fsup)/(zb+zt);
asmin = Pimin/fpi;
emaxp = zb*zt*(finf -fsup)/(ac*(finf*zb+fsup*zt));
Pmin(1,i) = Pimin/(1e6);
emaxc(1,i) =emaxp;
pi = pff*Pimin;
Aps =pi/fpi;
pe = eta*pi;

```

```

Pimax = ac*(zb*fct+mdl+(1/eta*(zt*fcw-mtot)))/(zb+zt);
Pmax(1,i) = Pimax/(1e6);
Paxis(1,i) =0.45*Pimin/(1e6);
    %TENDON ECCENTRCITY AT THE END
emaxs(1,i)=min(zt*ftt./pi+zt./ac,zb*fct./pi-zb./ac);
emins(1,i)=max(-zt*fcw./(eta*pi)+zt./ac,-zb*ftw./(eta*pi)-
zb./ac);

    %TENDON ECCENTRCITY AT THE CENTER
emaxm(1,i)=min(zt*ftt./pi+zt./ac+mdl./pi,zb*fct./pi-
zb./ac+mdl./pi);
eminm(1,i)=max(-zt*fcw./(eta*pi)+zt./ac+mtot/(eta*pi),-
zb*ftw./(eta*pi)-zb./ac+mtot./(eta*pi));

%A. AT TRANSFER
    % Mid Span
ftim=pi/ac-pi*ec/zt+mdl/zt;
fbim=pi/ac+pi*ec/zb-mdl/zb ;
    % At Support
ftis=pi/ac-pi*ee/zt;
fbis=pi/ac+pi*ee/zb;

if((ftim>fct)|| (fbim>fct)|| (ftis>fct)|| (fbis>fct))
    % concrete has crushed return 0
    caa=2;
elseif((ftim<-fr)|| (fbim<-fr)|| (ftis<-fr)|| (fbis<-fr))
    % concrete has cracked ..EFFECTIVE Ie METHOD
    caa=1;

else
    %((-fr<=ftim<=fct) && (-fr<=fbim<=fct) && (-
fr<=ftis<=fct) &&
    %(-fr<=ftis<=fct))
    %ELASTIC METHOD
    caa=0;
end

%B. AFTER UN-SHORED SLAB IS CAST
    % Mid Span
ftsm=pe/ac-pe*ec/zt+(mdl+mssl)/zt;
fbsm=pe/ac+pe*ec/zb-(mdl+mssl)/zb ;
    % At Support

```

```

ftss=pe/ac-pe*ee/zl;
fbss=pe/ac+pe*ee/zb;

if((ftsm>fct) || (fbsm>fct) || (ftss>fct) || (fbss>fct))
    % concrete has crushed return 0
    cab=2;
elseif((ftsm<-fr) || (fbsm<-fr) || (ftss<-fr) || (fbss<-fr))
    % concrete has cracked ..EFFECTIVE Ie METHOD
    cab=1;

else
    %((-fr<=ftsm<=fct) && (-fr<=fbsm<=fct) && (-
fr<=ftss<=fct) &&
    %(-fr<=ftss<=fct))
    %ELASTIC METHOD
    cab=0;
end

%c. AT SERVICE LOAD
ftem=pe/ac-pe*ec/zl+(mdl+mll)/zl+mll/ztp;
fbem=pe/ac+pe*ec/zb-(mdl+mll)/zb-mll/zbp ;

if((ftem>fct) || (fbem>fct))
    % concrete has crushed return 0
    cac=2;
elseif((ftem<-fr) || (fbem<-fr))
    % concrete has cracked ..EFFECTIVE Ie METHOD
    cac=1;

else
    %((-fr<=ftem<=fct) && (-fr<=fbem<=fct))
    %ELASTIC METHOD
    cac=0;
end

%DEFLECTION AND CAMBER CALCULATION.
di(1,i)=(pi*1e6*L(1,i)^2*(-5*ec-ee))/(48*Ecp*Ig);
Idi(1,i) = -1*di(1,i);
    b=ccb;
    dpp = ec+yt;
    dpc=ec+yt+ts;
    gamapp=Aps/(b*dpp);
    gamapc=Aps/(b*dpc);

```

```

Icrp=mrp*Apr*dpp^2*(max(1-1.6*sqrt(mrp*gamapp),0));
Icrc=mrp*Apr*dpc^2*(max(1-1.6*sqrt(mrp*gamapc),0));

%DECISION A
if(caa==0)
    ddl(1,i)=(5*wdl*L(1,i)^4)/(384*Ecp*Ig)*1e12;

    if(cab==0)
        dsl(1,i) = (5*wsd*L(1,i)^4)/(384*Ecp*Ig)*1e12;

        if(cac==0)
            dll(1,i) =
(5*wll*L(1,i)^4)/(384*Ecp*Igc)*1e12;
        else(cac==1)
            fll = mll/zbp;
            mr =max(1-(fbem-fr)/fll,0);
            Ie = min(mr^3*(Igc -Icrc)+Icrc,Igc);
            dll(1,i) =
(5*wll*L(1,i)^4)/(384*Ecp*Ie)*1e12;
        %else
        %dll = 0;
        end
    else
        %(cab==1)
        fsl = msl/zb;
        mr =max(1-(fbsm-fr)/fsl,0);
        Ie = min(mr^3*(Ig -Icrp)+Icrp,Ig);
        dsl(1,i) =
(5*wsl*L(1,i)^4)/(384*Ecp*Ie)*1e12;
        %if(cac==2)
        %dll = 0;
        %else
        fll = mll/zbp;
        mr =max(1-(fbem-fr)/fll,0);
        Ie = min(mr^3*(Igc -Icrc)+Icrc,Igc);
        dll(1,i) =
(5*wll*L(1,i)^4)/(384*Ecp*Ie)*1e12;
        end %end
        %else
        %dsl=0;
        % dll =0;
        %end

```

```

else
    %(caa==1)
    fdl = mdl/zb;
    mr =max(1-(fbim-fr)/fdl,0);
    Ie = min(mr^3*(Ig -Icrp)+Icrp,Ig);
    ddl(1,i) =
(5*wdl*L(1,i)^4)/(384*Ecp*Ie)*1e12;
    %if(cab==2)
    %    dsl =0;
    %    dll =0;
    %else
    fsl = msl/zb;
    mr =max(1-(fbsm-fr)/fsl,0);
    Ie = min(mr^3*(Ig -Icrp)+Icrp,Ig);
    dsl(1,i) =
(5*wdl*L(1,i)^4)/(384*Ecp*Ie)*1e12;

    % if(cac==2)
    %    dll =0;
    % else
    fll = mll/zbp;
    mr =max(1-(fbem-fr)/fll,0);
    Ie = min(mr^3*(Igc -Icrc)+Icrc,Igc);
    dll(1,i) =
(5*wll*L(1,i)^4)/(384*Ecp*Ie)*1e12;
    %end
    % end

    %else
    %if caa ==2
    %    ddl = 0;
    %    dsl =0;
    %    dll =0;
end

% if((caa==2)||(cab==2)||(cac==2))
%    dnt= 0;
%    dned =0;
%    dnes =0;
%    dnel =0;
%    dnfd=0;
%    dnfs=0,
%    dnfl=0;

```

```

% else
% Net Deflection at transfer
dnt(1,i) = di(1,i)+ddl(1,i);
% Net Deflection at erection before super imposed dead load
dned(1,i) = 1.8*di(1,i)+1.85*ddl(1,i);
% Net Deflection at erection immediately after superimposed
dead load
dnes(1,i) =(1.8*di(1,i)+1.85*ddl(1,i)) + dsl(1,i);
% Net Deflection at erection immediately after service load
dnel(1,i) = dnes(1,i) + dll(1,i);
% Net final Deflection before super imposed dead load
dnfd(1,i) = 2.2*di(1,i) + 2.4*ddl(1,i);
% Net final Deflection after superimposed dead load
dnfs(1,i) = dnfd(1,i) + 3*dsl(1,i);
% Net final deflection at service load
dnfl(1,i) = 2.2*di(1,i) + 2.4*ddl(1,i) + 3*dsl(1,i)+
dll(1,i);

%end

demin(1,i) =
min(dnt(1,i),min(dned(1,i),min(dnes(1,i),min(dnel(1,i),min(dnfd(
1,i),min(dnfs(1,i),dnfl(1,i)))))));
demax(1,i) =
max(dnt(1,i),max(dned(1,i),max(dnes(1,i),max(dnel(1,i),max(dnfd(
1,i),max(dnfs(1,i),dnfl(1,i)))))));

%plot(L(1,i),di)

p=p+1
end

figure(1);
plot(L,dnt,'-g',L,dned,'--k',L,dnes,'-K',L,dnel,'--b',L,dnfd,'-
c',L,dnfs,'-y',L,dnfl,'-b',L,dmax,'-m',L,cmax,'-m')
%plot(L,ddl,'-bs'),plot(1,2,1),plot(L,dnt,'-
g^'),plot(1,2,1),plot(L,dnes,'-Kx'),plot(1,2,1),plot(L,dnfl,'-
mh')

axis ([0 50 -69 69])
xlabel('L(m)')
ylabel('deflection (mm)')
title ('Deflection vs Span Length')

```

```

set(gca,'Xtick',0:10:50)
set(gca,'Ytick',-70:10:70)

legend('\deltant: deflection at transfer','\deltaned: Deflection
at erection before super imposed dead
load','\deltanes:deflection at erection after
superimposed','\deltanel:Deflection at erection immediatety
after service load','\deltanfd:final Deflection before super
imposed dead load','\deltanfs:final Deflection after
superimposed dead load','\deltanfl:final long term deflection
service load','\deltamax:Maximum allowable deflection =
L/640',2)
%str1(1)= {'center each line in the Uicontrol'};
%str1(2)= {'Also check out the text wrap function'};
%str2 = {'Cp =',num2str(c),'Mpa'};
%str3 = {'\deltadl:- deflection due to dead load
only',num2str(c),'Mpa'};
%str4= {'\deltant:- net deflection at
transfer',num2str(c),'Mpa'};
%str5 = {'\deltanes:-deflection at erection with super-imposed
dead load',num2str(c),'Mpa'};
%str6 = {'\deltanfl = final long term deflection at service
load',num2str(c),'Mpa'};
%uicontrol('style','text','position',[80 80 250
65],'string',str1);
%text(150,0
, str2,'fontsize',9,'HorizontalAlignment','right','color','black'
);
text(55,70,['Cp
=',num2str(c),'Mpa'],'fontsize',9,'HorizontalAlignment','right',
'color','blue')
text(55,60,['Cs
=',num2str(cs),'Mpa'],'fontsize',9,'HorizontalAlignment','right'
,'color','blue')
text(55,50,['fpk
=',num2str(fpk),'Mpa'],'fontsize',9,'HorizontalAlignment','right'
,'color','blue')
text(55,40,['prestress loss
=',num2str(prl),'%'],'fontsize',9,'HorizontalAlignment','right',
'color','blue')
text(55,30,['Live Loading E
=',num2str(cooper1)],'fontsize',9,'HorizontalAlignment','right',
'color','blue')

```

```
text(55,20,['ee
=',num2str(ee),'mm'],'fontsize',9,'HorizontalAlignment','right',
'color','blue')
text(55,10,['ec
=',num2str(ec),'mm'],'fontsize',9,'HorizontalAlignment','right',
'color','blue')
text(55,0,['girder spacing
=',num2str(ccb),'mm'],'fontsize',9,'HorizontalAlignment','right',
'color','blue')
text(55,-10,['Slab thikcnss
=',num2str(ts),'mm'],'fontsize',9,'HorizontalAlignment','right',
'color','blue')
text(55,-20,['Beam type
=',num2str(beamType)],'fontsize',9,'HorizontalAlignment','right',
'color','blue')
text(55,-30,['Total Depth
=',num2str(H),'mm'],'fontsize',9,'HorizontalAlignment','right',
'color','blue')
text(55,-40,['yb
=',num2str(yb),'mm'],'fontsize',9,'HorizontalAlignment','right',
'color','blue')
text(55,-50,['Pi =',num2str(pff),' *
Pimin'],'fontsize',9,'HorizontalAlignment','right','color','blue
')
text(-5,70,['b1
=',num2str(b1),'mm'],'fontsize',9,'HorizontalAlignment','right',
'color','blue')
text(-5,60,['b2
=',num2str(b2),'mm'],'fontsize',9,'HorizontalAlignment','right',
'color','blue')
text(-5,50,['b3
=',num2str(b3),'mm'],'fontsize',9,'HorizontalAlignment','right',
'color','blue')
text(-5,40,['b4
=',num2str(b4),'mm'],'fontsize',9,'HorizontalAlignment','right',
'color','blue')
text(-5,30,['b5
=',num2str(b5),'mm'],'fontsize',9,'HorizontalAlignment','right',
'color','blue')
text(-5,20,['b6
=',num2str(b6),'mm'],'fontsize',9,'HorizontalAlignment','right',
'color','blue')
```

```

text(-5,10,['b7
=',num2str(b7),'mm'],'fontsize',9,'HorizontalAlignment','right',
'color','blue')
text(-5,0,['h1
=',num2str(h1),'mm'],'fontsize',9,'HorizontalAlignment','right',
'color','blue')
text(-5,-10,['h2
=',num2str(h2),'mm'],'fontsize',9,'HorizontalAlignment','right',
'color','blue')
text(-5,-20,['h3
=',num2str(h3),'mm'],'fontsize',9,'HorizontalAlignment','right',
'color','blue')
text(-5,-30,['h4
=',num2str(h4),'mm'],'fontsize',9,'HorizontalAlignment','right',
'color','blue')
text(-5,-40,['h5
=',num2str(h5),'mm'],'fontsize',9,'HorizontalAlignment','right',
'color','blue')
text(-5,-50,['h6
=',num2str(h6),'mm'],'fontsize',9,'HorizontalAlignment','right',
'color','blue')
text(-5,-60,['h7
=',num2str(h7),'mm'],'fontsize',9,'HorizontalAlignment','right',
'color','blue')
grid on
hold off

figure(2);
subplot(1,2,1),plot(L,demin,'r',L,demax,'b',L,dmax,'-
m',L,cmax,'-m')
%plot(L,ddl,'-bs'),plot(1,2,1),plot(L,dnt,'-
g^'),plot(1,2,1),plot(L,dnes,'-Kx'),plot(1,2,1),plot(L,dnfl,'-
mh')
axis ([0 50 -78 78])
xlabel('L(m)')
ylabel('deflection (mm)')
title ('Deflection Envelope vs Span Length')
set(gca,'Xtick',0:10:50)
set(gca,'Ytick',-70:10:70)

legend('delta emax: maximum camber envelope ','delta emax:
maximum deflection envelope ','\deltamax:Maximum allowable
deflection = L/640');

```

```
grid on
```

```
text(58,70,['Cp
=',num2str(c),'Mpa'],'fontsize',9,'HorizontalAlignment','right',
'color','blue')
text(58,60,['Cs
=',num2str(cs),'Mpa'],'fontsize',9,'HorizontalAlignment','right',
'color','blue')
text(58,50,['fpk
=',num2str(fpk),'Mpa'],'fontsize',9,'HorizontalAlignment','right',
'color','blue')
text(58,40,['prestress loss
=',num2str(prl),'%'],'fontsize',9,'HorizontalAlignment','right',
'color','blue')
text(58,30,['Live Loading E
=',num2str(cooperl)],'fontsize',9,'HorizontalAlignment','right',
'color','blue')
text(58,20,['ee
=',num2str(ee),'mm'],'fontsize',9,'HorizontalAlignment','right',
'color','blue')
text(58,10,['ec
=',num2str(ec),'mm'],'fontsize',9,'HorizontalAlignment','right',
'color','blue')
text(58,0,['girder spacing
=',num2str(ccb),'mm'],'fontsize',9,'HorizontalAlignment','right',
'color','blue')
text(58,-10,['Slab thikcness
=',num2str(ts),'mm'],'fontsize',9,'HorizontalAlignment','right',
'color','blue')
text(58,-20,['Beam type
=',num2str(beamType)],'fontsize',9,'HorizontalAlignment','right',
'color','blue')
text(58,-30,['Total Depth
=',num2str(H),'mm'],'fontsize',9,'HorizontalAlignment','right',
'color','blue')
text(58,-40,['yb
=',num2str(yb),'mm'],'fontsize',9,'HorizontalAlignment','right',
'color','blue')
text(58,-50,['Pi =',num2str(pff),' *
Pimin'],'fontsize',9,'HorizontalAlignment','right','color','blue
')
```

```
text(-5,70,['b1
=',num2str(b1),'mm'],'fontsize',9,'HorizontalAlignment','right',
'color','blue')
text(-5,60,['b2
=',num2str(b2),'mm'],'fontsize',9,'HorizontalAlignment','right',
'color','blue')
text(-5,50,['b3
=',num2str(b3),'mm'],'fontsize',9,'HorizontalAlignment','right',
'color','blue')
text(-5,40,['b4
=',num2str(b4),'mm'],'fontsize',9,'HorizontalAlignment','right',
'color','blue')
text(-5,30,['b5
=',num2str(b5),'mm'],'fontsize',9,'HorizontalAlignment','right',
'color','blue')
text(-5,20,['b6
=',num2str(b6),'mm'],'fontsize',9,'HorizontalAlignment','right',
'color','blue')
text(-5,10,['b7
=',num2str(b7),'mm'],'fontsize',9,'HorizontalAlignment','right',
'color','blue')
text(-5,0,['h1
=',num2str(h1),'mm'],'fontsize',9,'HorizontalAlignment','right',
'color','blue')
text(-5,-10,['h2
=',num2str(h2),'mm'],'fontsize',9,'HorizontalAlignment','right',
'color','blue')
text(-5,-20,['h3
=',num2str(h3),'mm'],'fontsize',9,'HorizontalAlignment','right',
'color','blue')
text(-5,-30,['h4
=',num2str(h4),'mm'],'fontsize',9,'HorizontalAlignment','right',
'color','blue')
text(-5,-40,['h5
=',num2str(h5),'mm'],'fontsize',9,'HorizontalAlignment','right',
'color','blue')
text(-5,-50,['h6
=',num2str(h6),'mm'],'fontsize',9,'HorizontalAlignment','right',
'color','blue')
text(-5,-60,['h7
=',num2str(h7),'mm'],'fontsize',9,'HorizontalAlignment','right',
'color','blue')
```

```

    %plotyy(L,emaxc,L,Pmin,'-rp','bs')
    subplot(1,2,2),plot(L, emaxs, '--g',L, emins, '--b',L, emaxm,
'-c',L, eminm, '-.m',L,emaxc, '--k')
    axis ([0 50 enaxis epaxis])
    ax1 = gca;
    set(ax1,'XColor','k','YColor','K')
        xlabel('L(m)')
        ylabel('eccentricity (mm)')
        %y=ylabel('eccentricity (mm)')
        %set(y,'position',get(y,'position')-[-2,0,0]);

    title('Alloawable eccentricity and Prestressing Force')
    set(gca,'Xtick',0:10:50)
    set(gca,'Ytick',enaxis:200:epaxis)
    legend('emax support','emin support','emax mid span','emin
mid span','emax for Pmin',2)
        %text(100,950,'s: for
support','fontsize',9,'HorizontalAlignment','right','color','red'
)
        %text(100,850,'m: for mid-
span','fontsize',9,'HorizontalAlignment','right','color','red')
        %text(100,750,'c: coresponding to
pmin','fontsize',9,'HorizontalAlignment','right','color','red')
    grid on

ax2 = axes('Position',get(ax1,'Position'),...
'XAxisLocation','top',...
'YAxisLocation','right',...
'Color','none',...
'XColor','r','YColor','r');
imax = find(max(Paxis)==Paxis);
axis ([0 50 0 Paxis(imax)])
set(gca,'Xtick',0:50:50)
set(gca,'Ytick',0:10:Pmin(imax))
ylabel('Prestressing force (MN)')
h12 = line(L,Pmin,'Color','r','Parent',ax2);
h13 = line(L,Pmax,'Color','black','Parent',ax2);
legend('Pmin','Pmax',1)

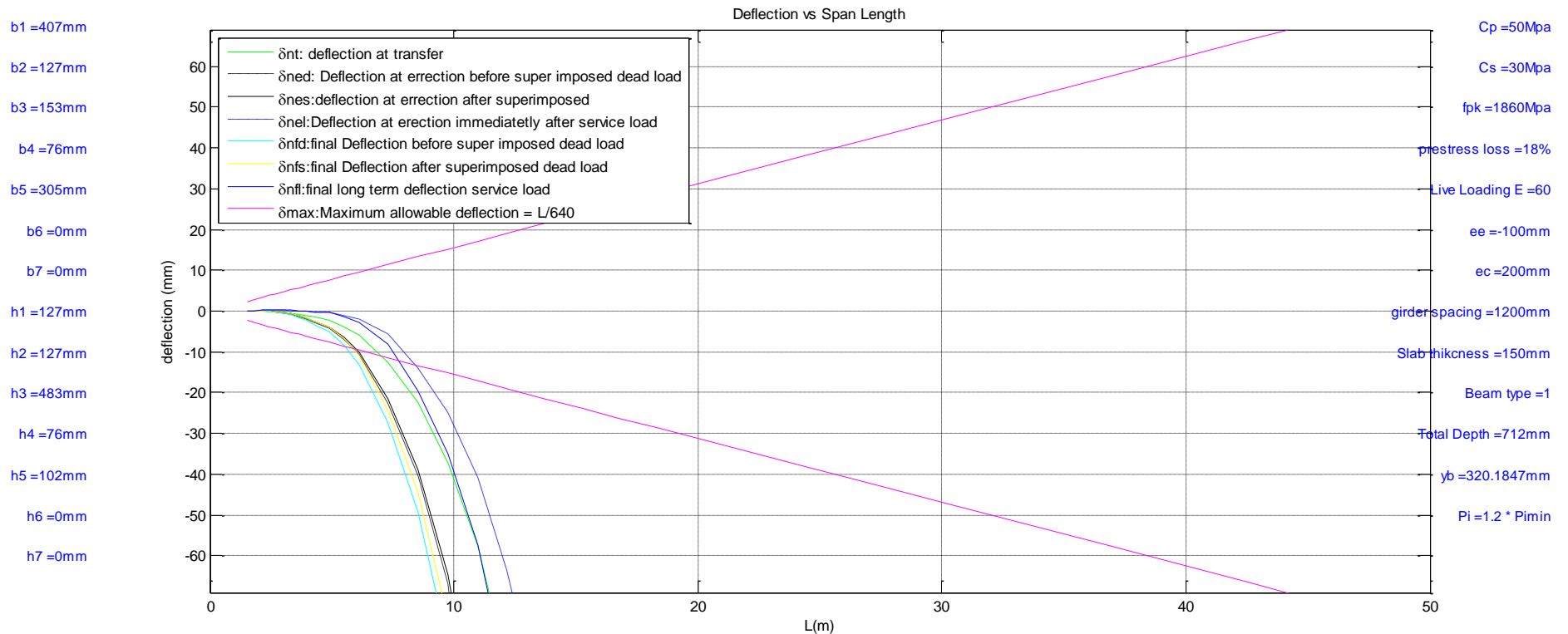
hold off

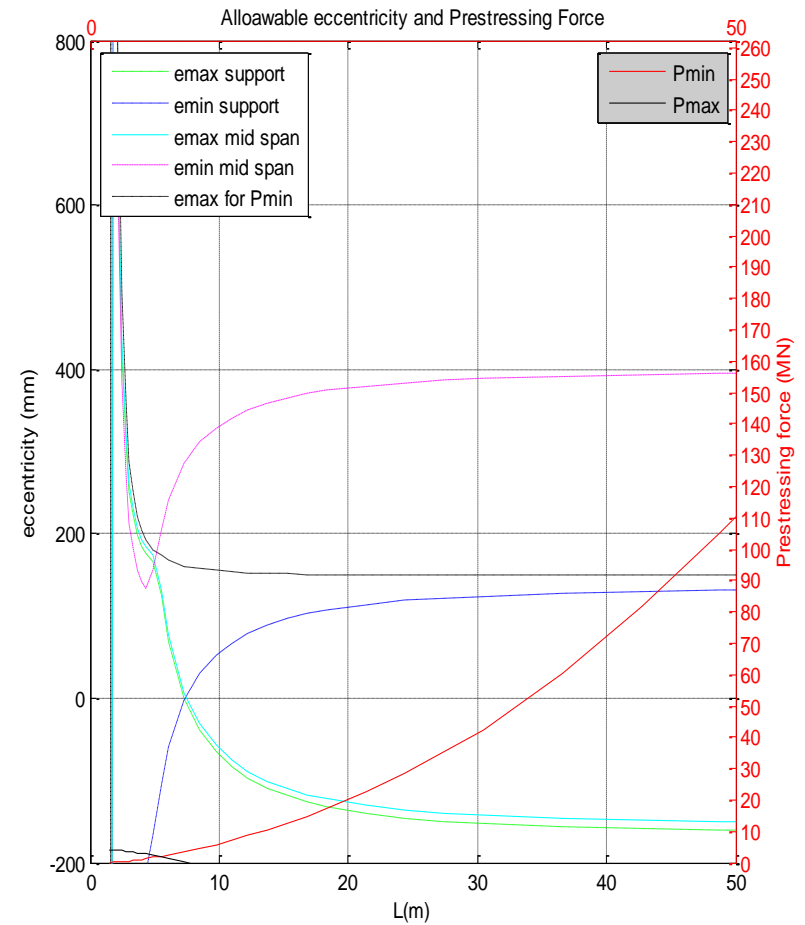
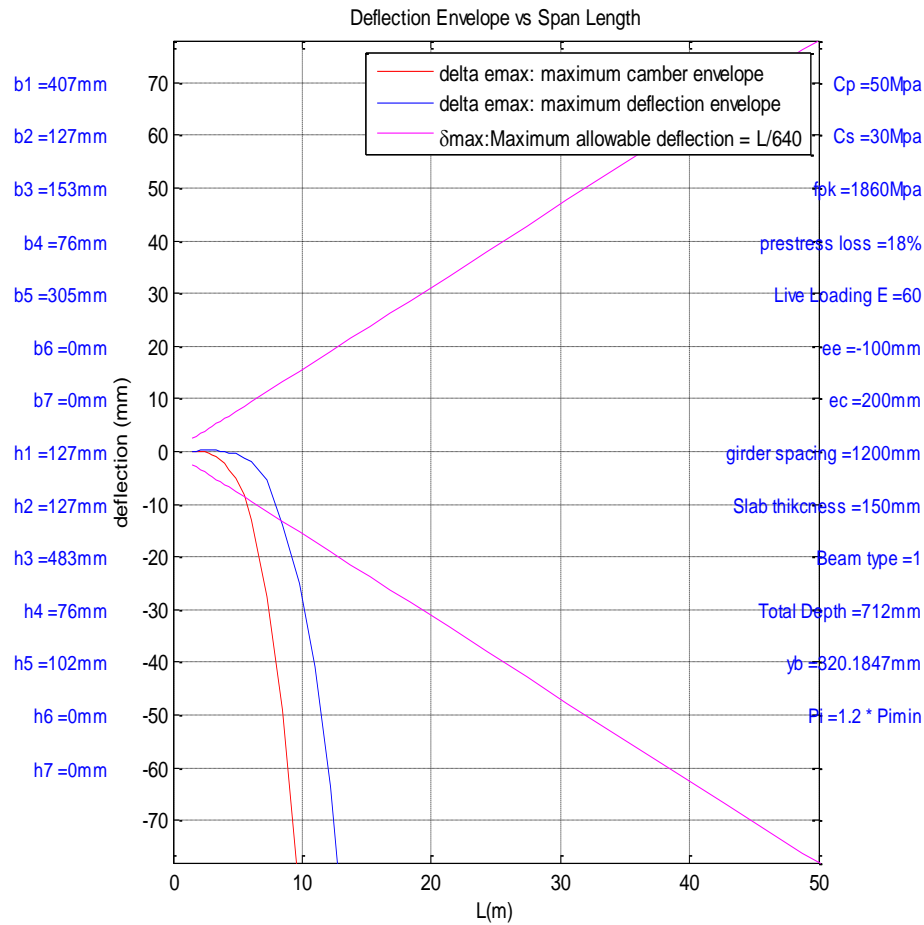
```

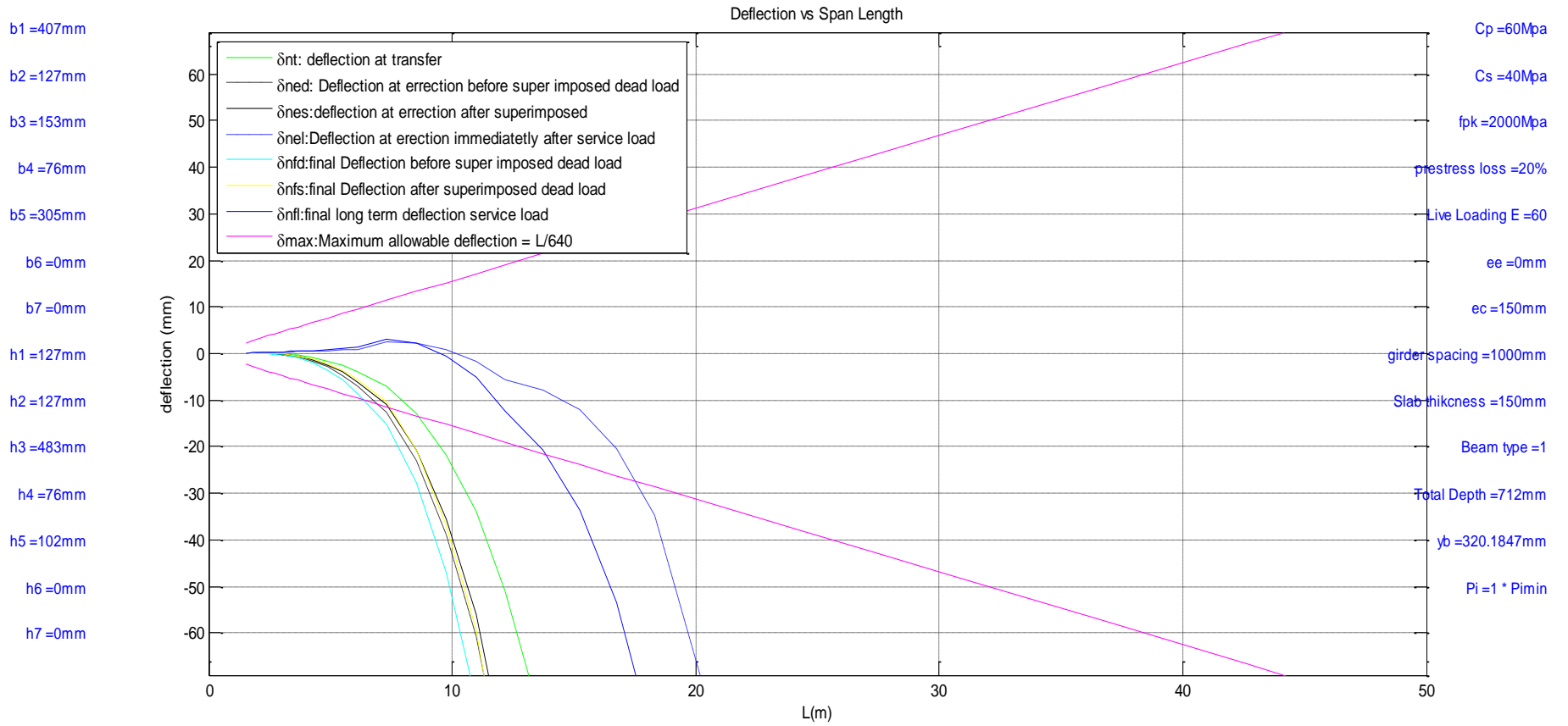
Appendix B: Sample Charts plotted using the program

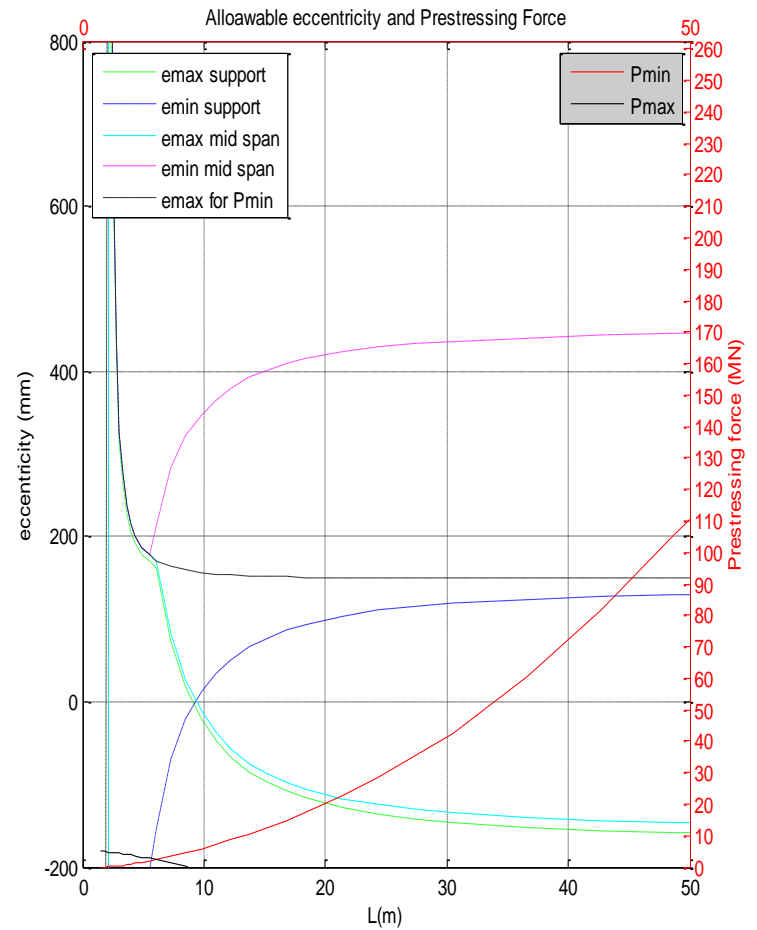
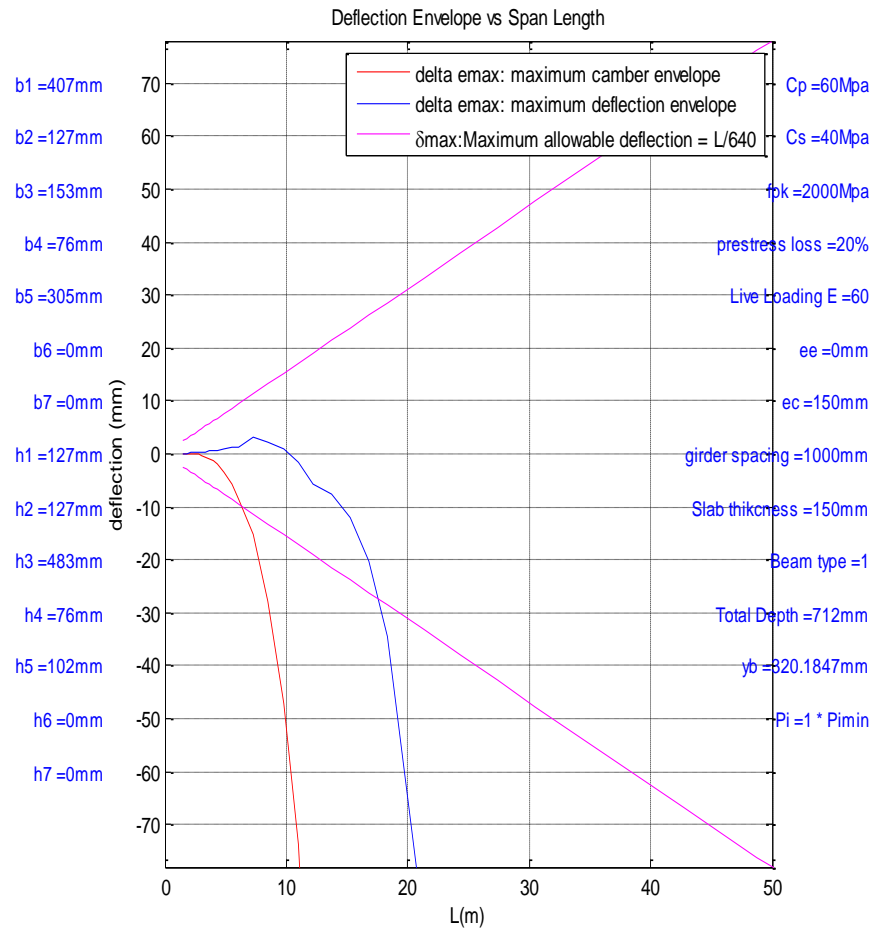
Note: - the deflection data after the break (after the minimum allowable eccentricity become higher than that of the maximum) is just numerical has no engineering value.

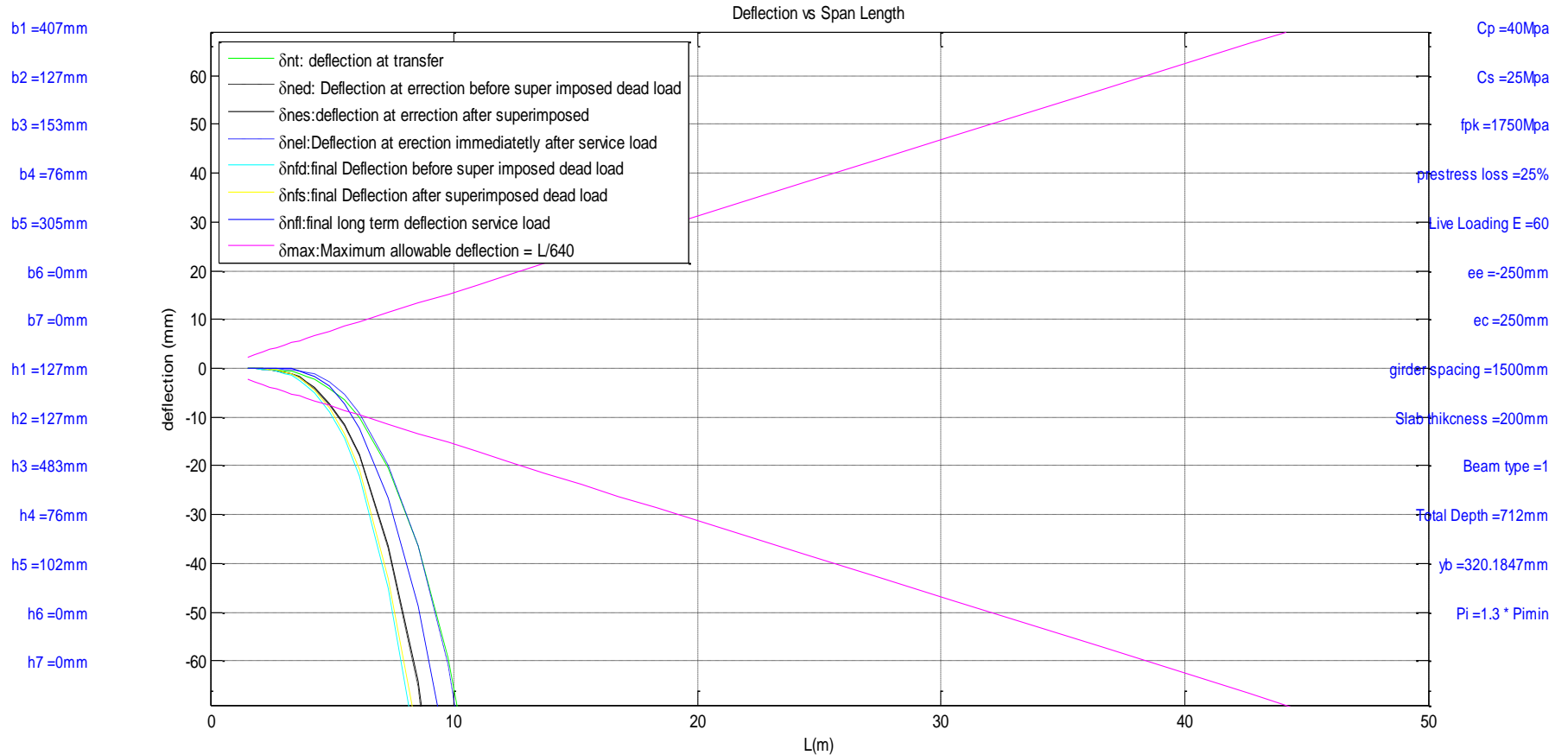
AASHTO/PCI I beam Type I

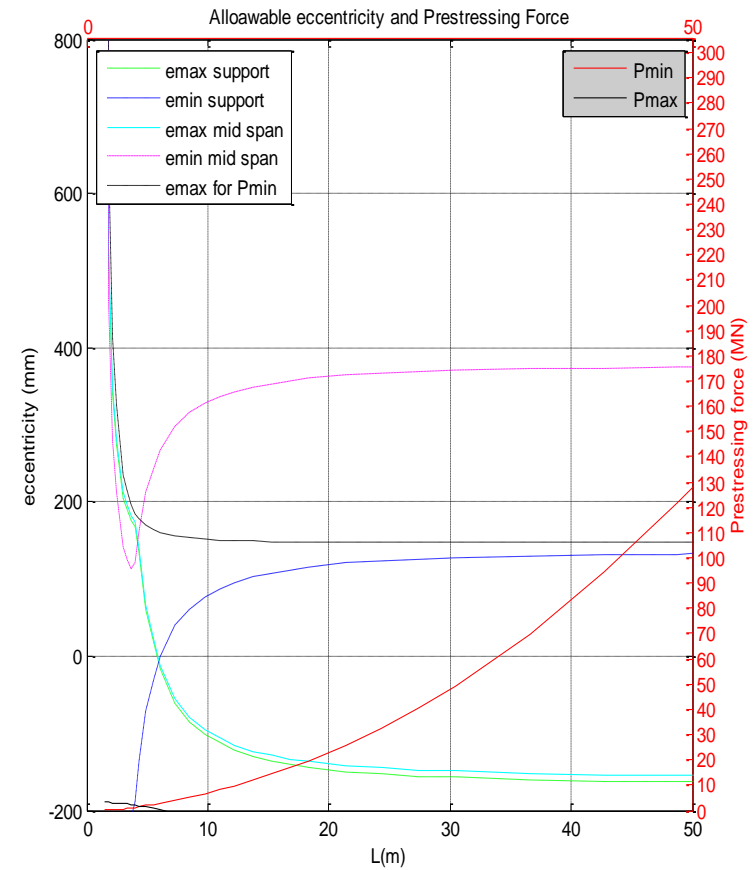
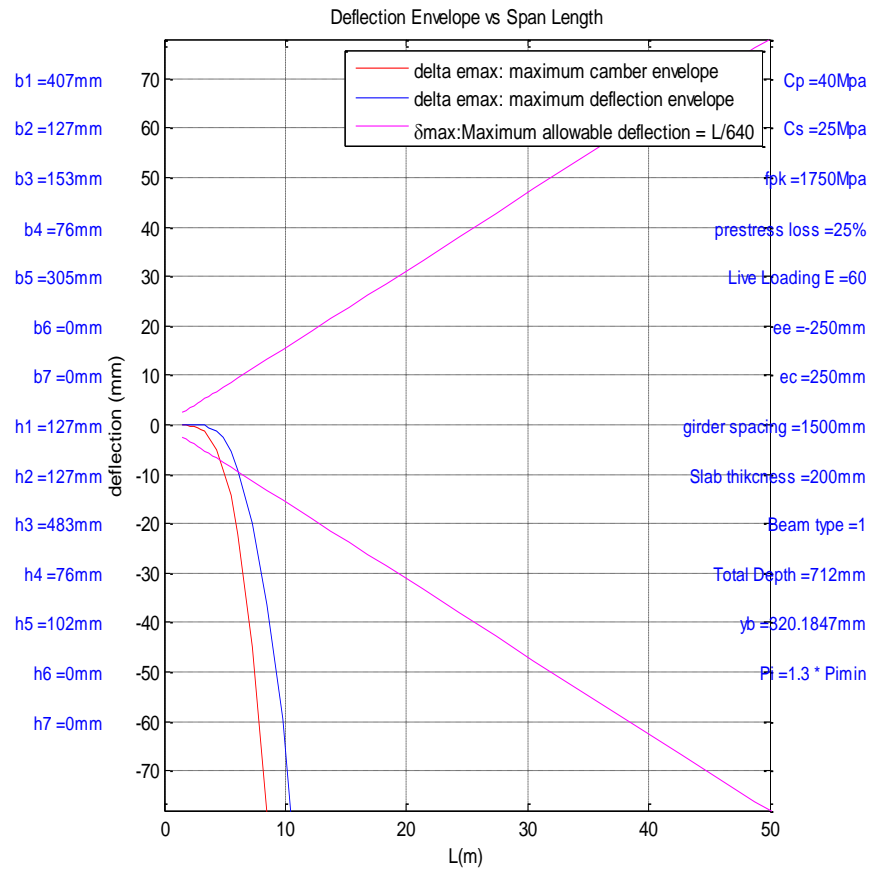






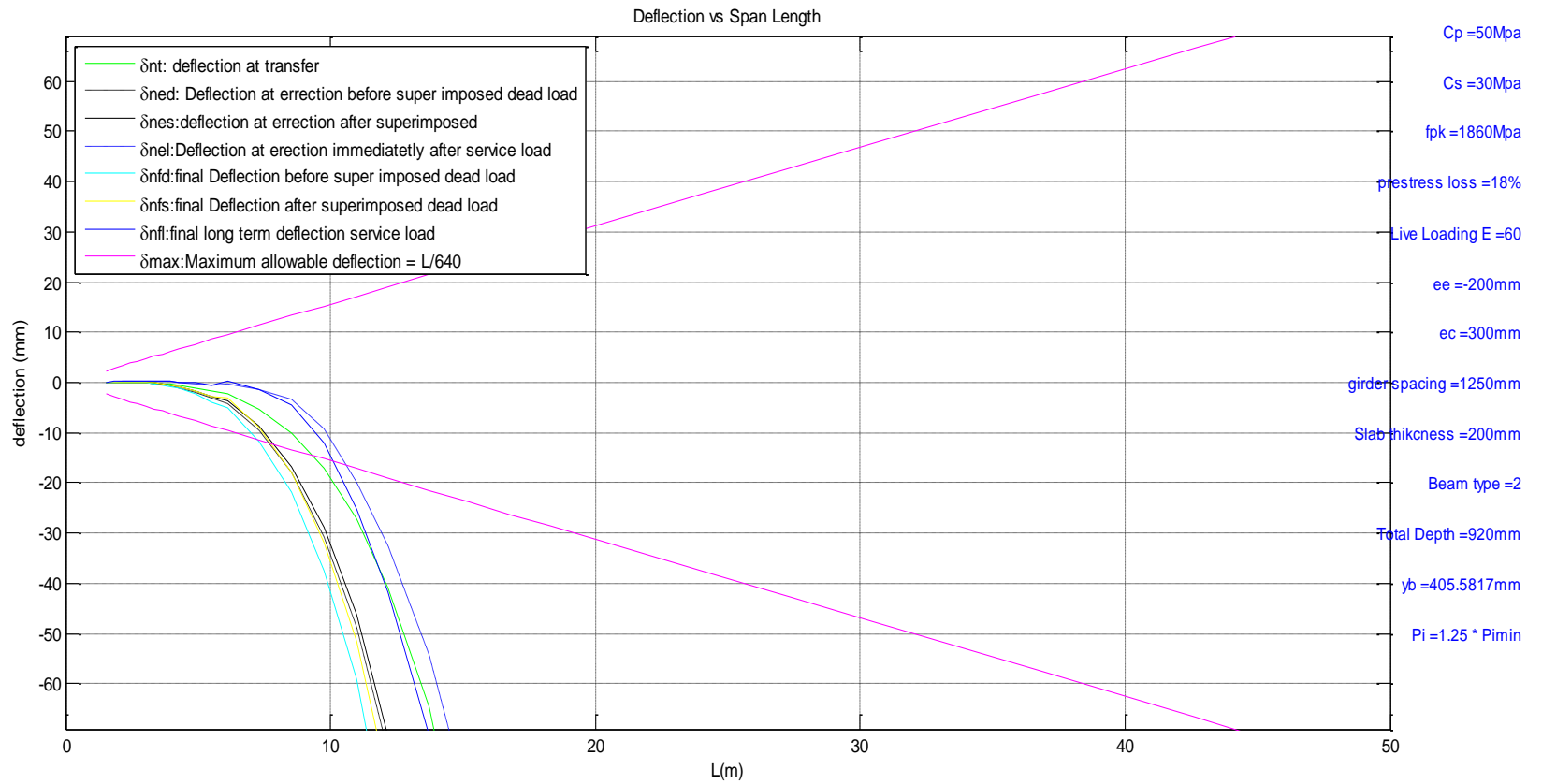


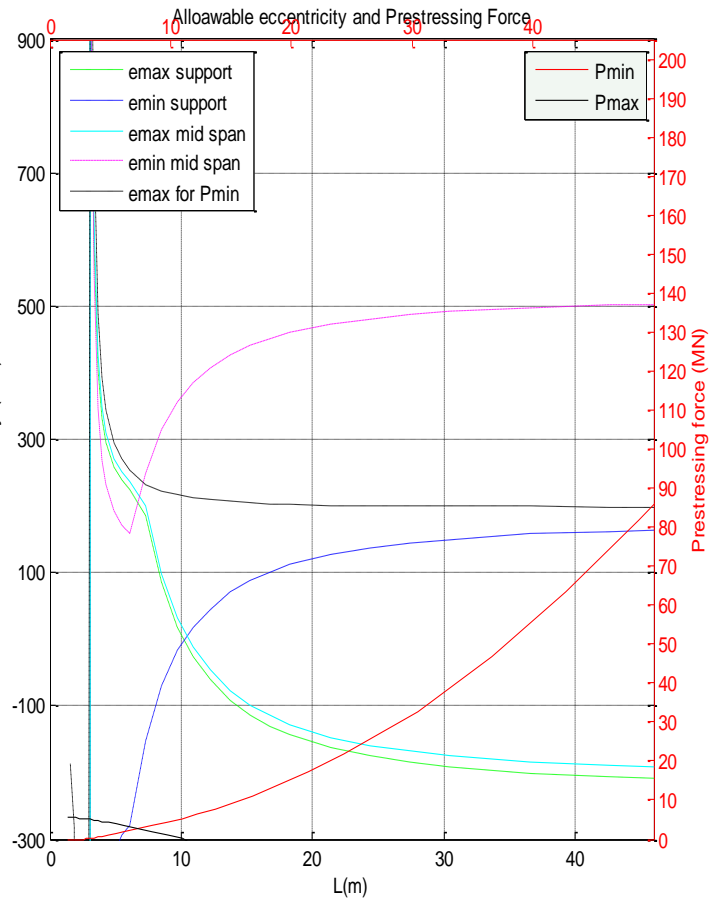
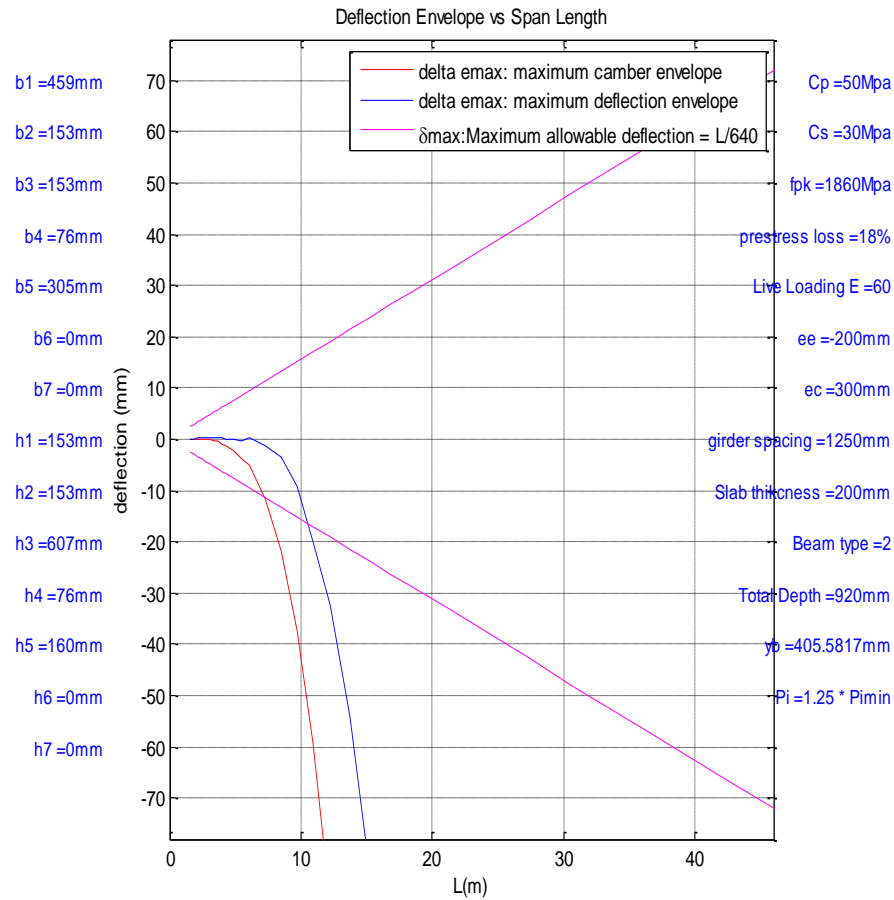


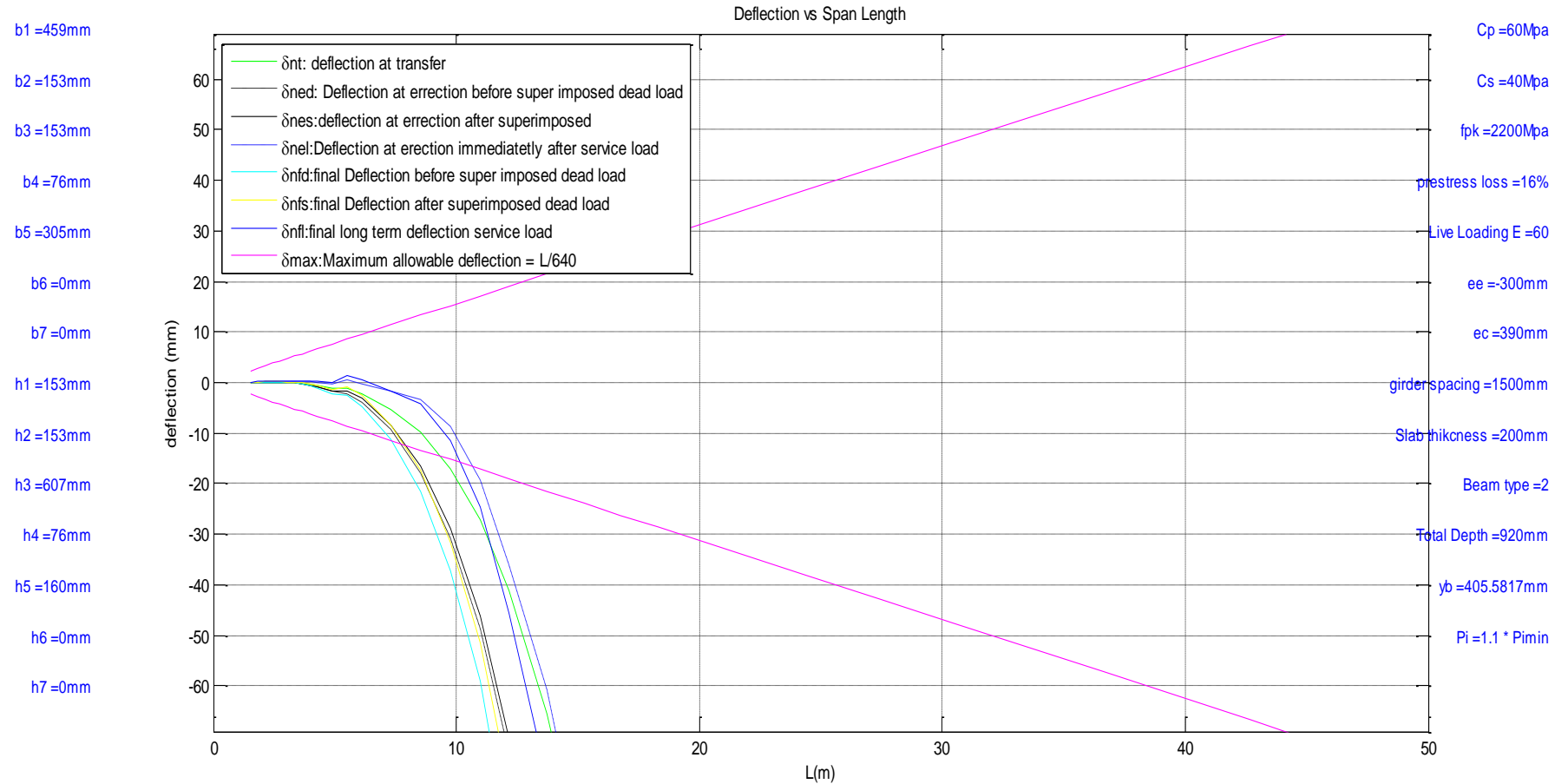


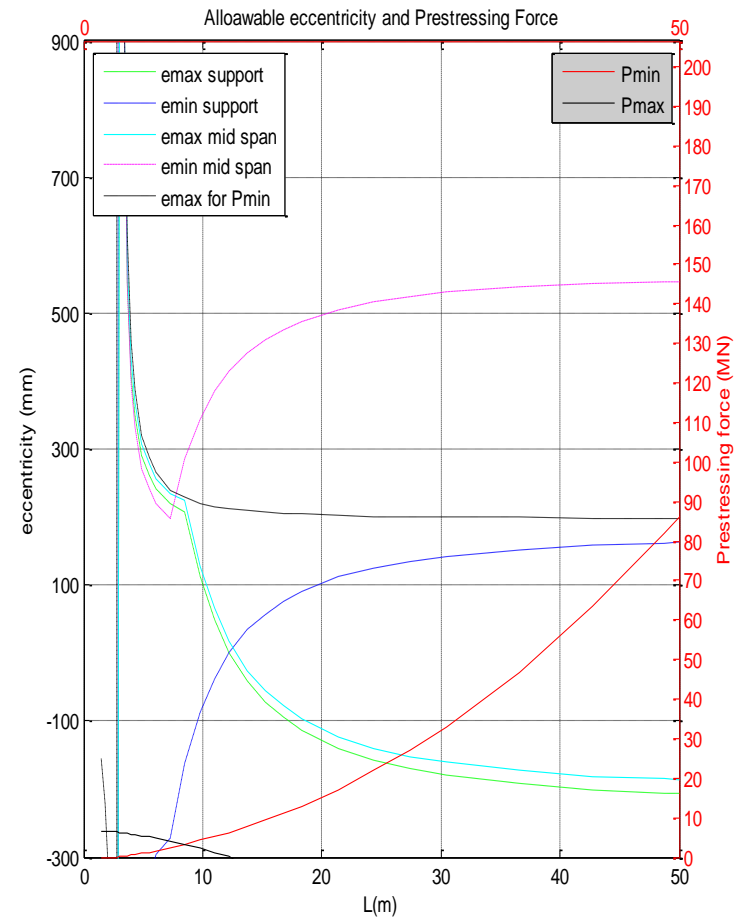
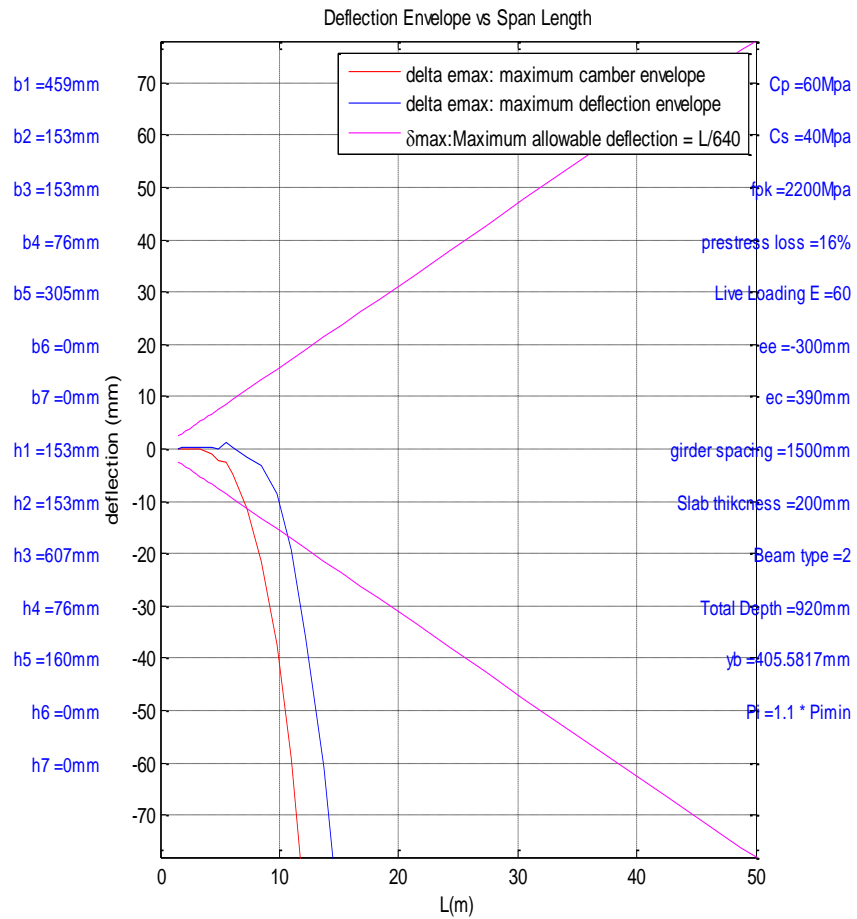
AASHTO/PCI I beam Type II

- b1 =459mm
- b2 =153mm
- b3 =153mm
- b4 =76mm
- b5 =305mm
- b6 =0mm
- b7 =0mm
- h1 =153mm
- h2 =153mm
- h3 =607mm
- h4 =76mm
- h5 =160mm
- h6 =0mm
- h7 =0mm

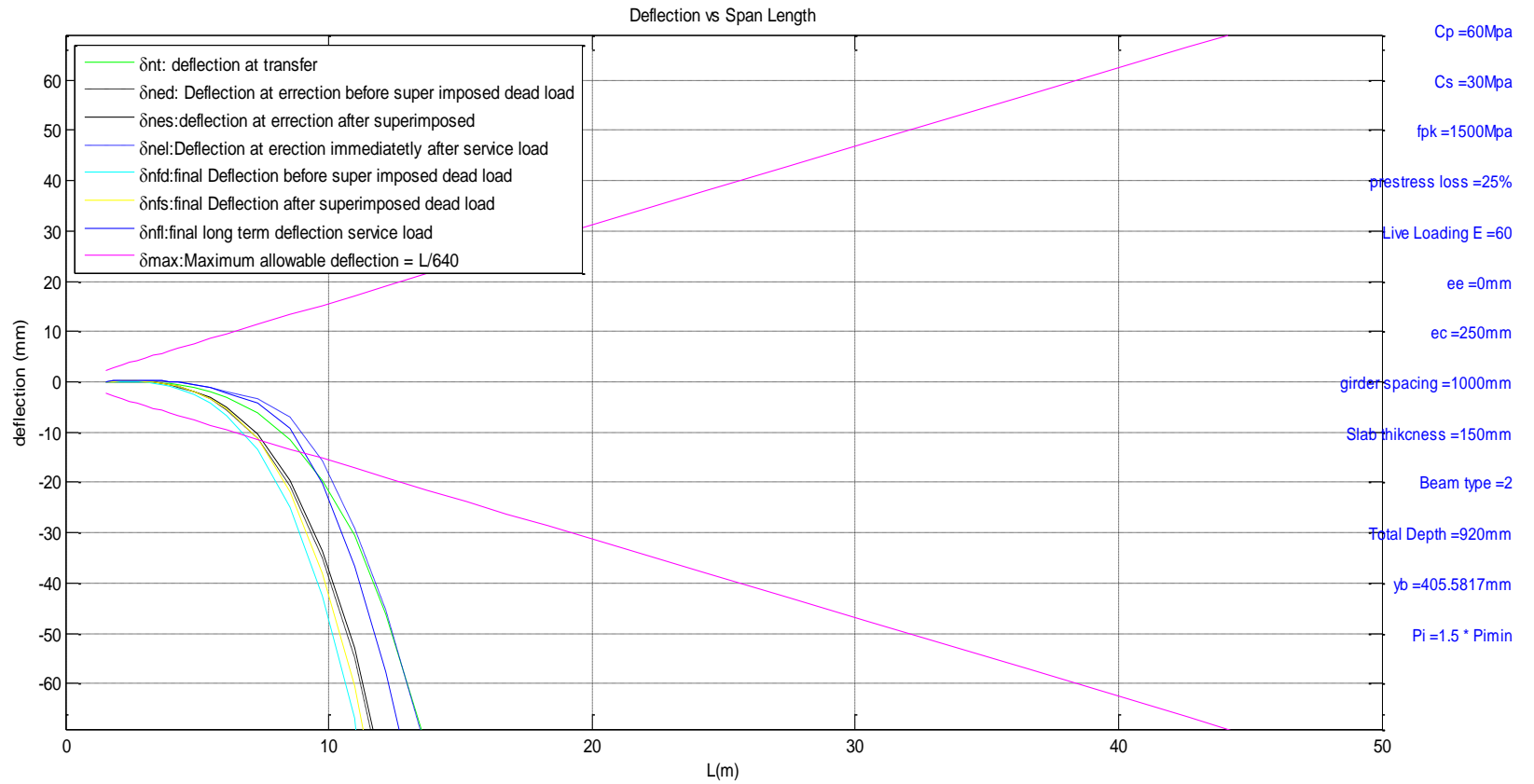


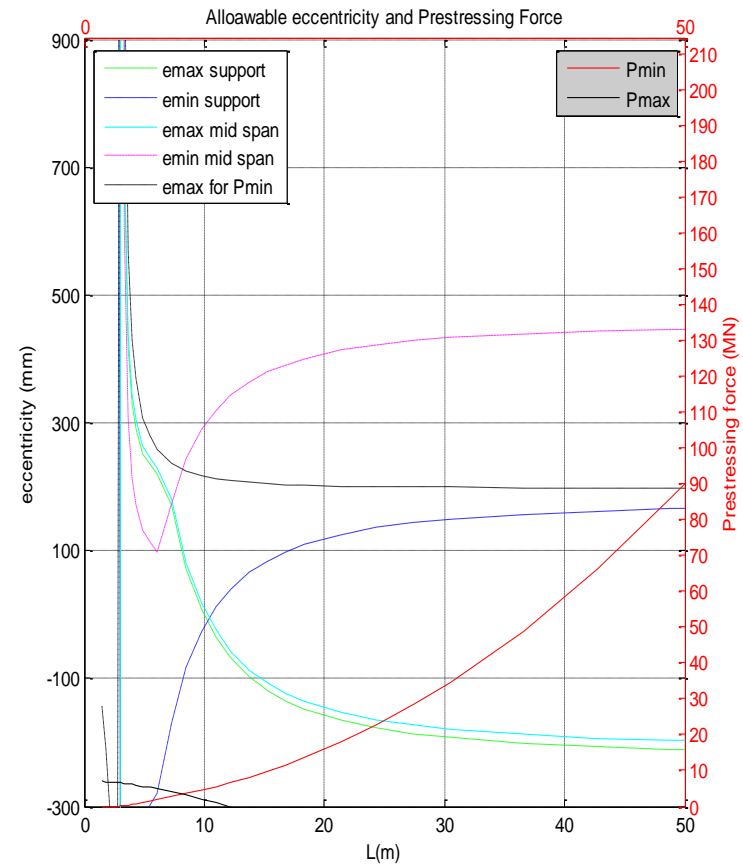
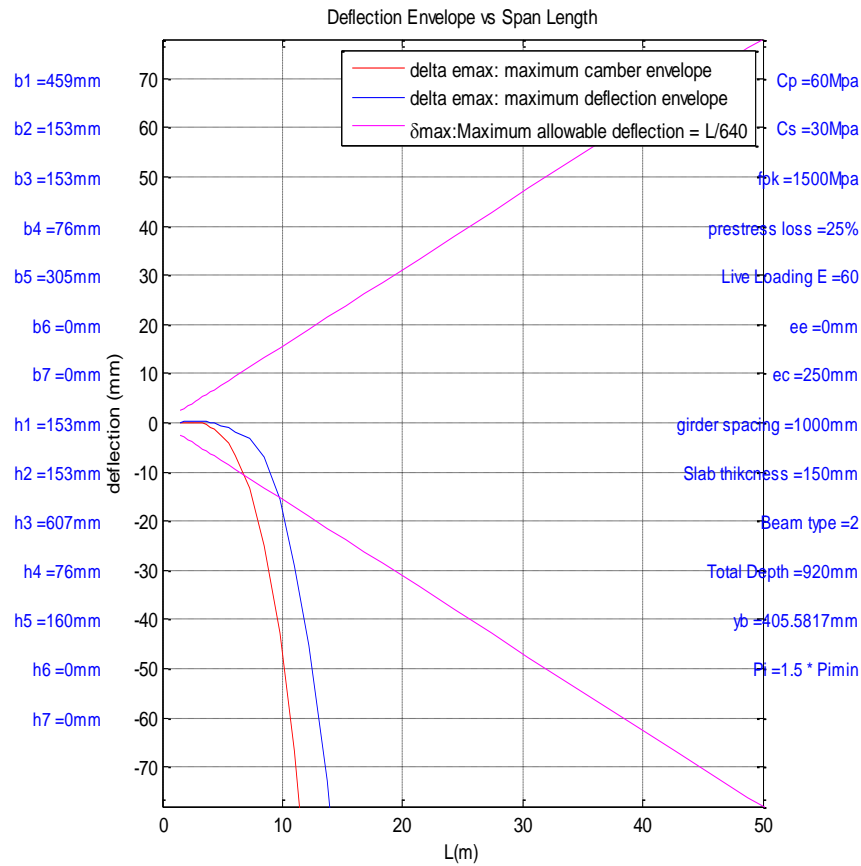




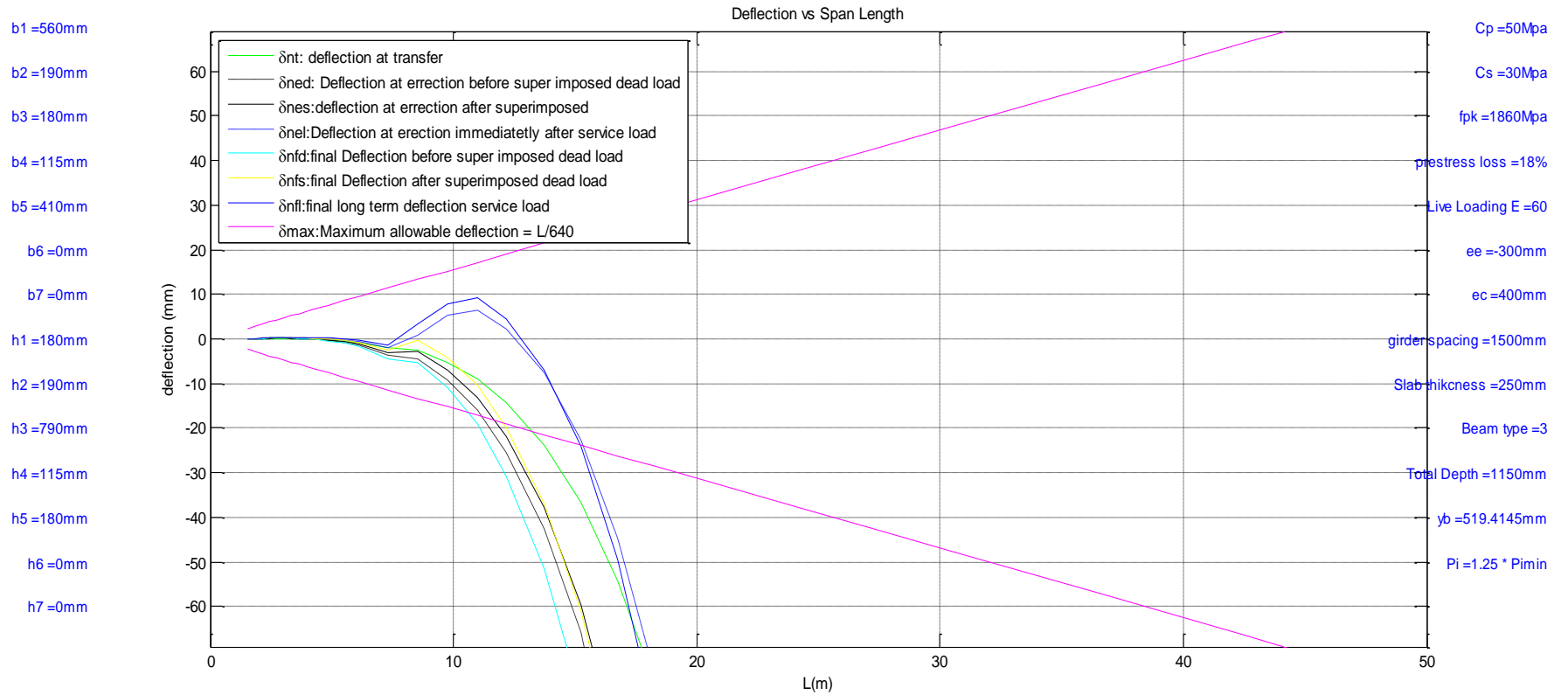


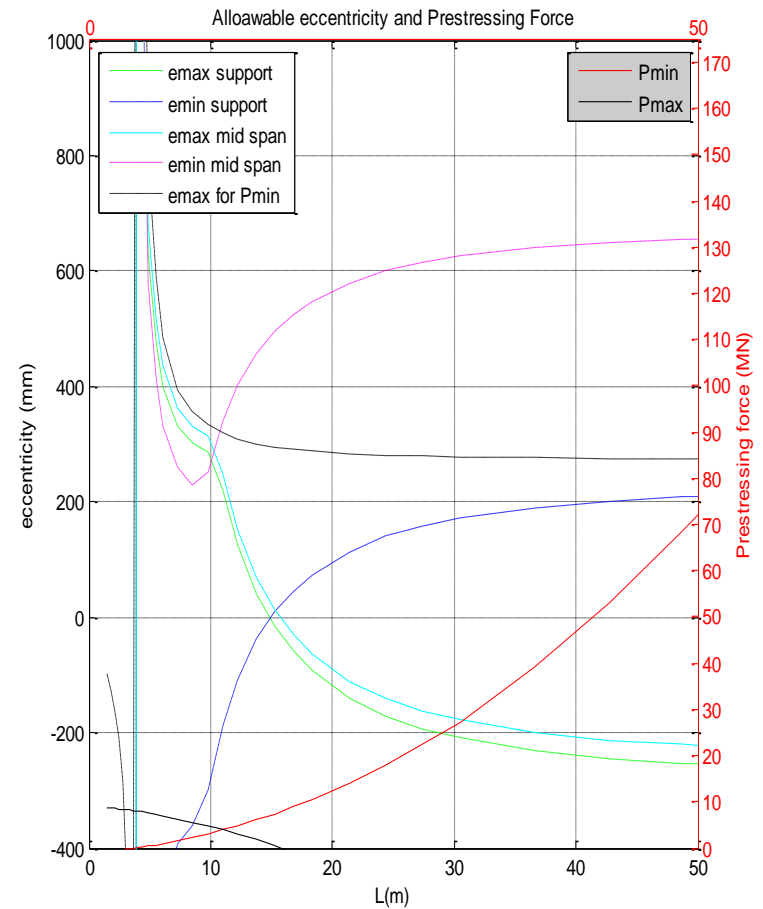
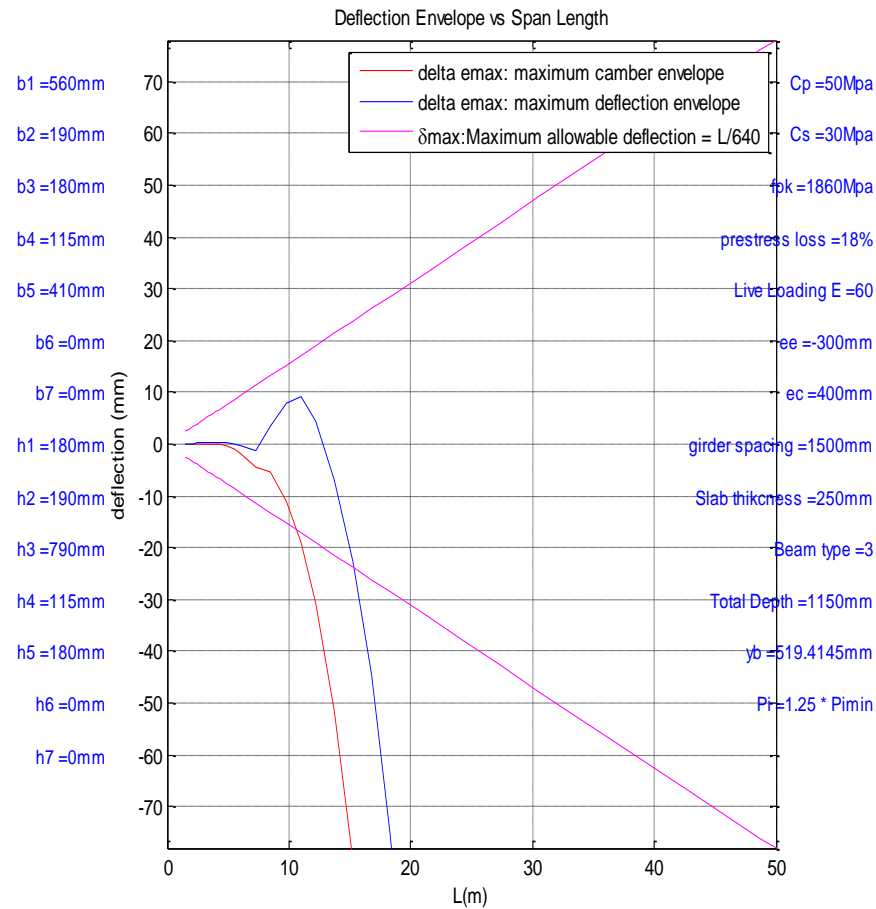
- b1 =459mm
- b2 =153mm
- b3 =153mm
- b4 =76mm
- b5 =305mm
- b6 =0mm
- b7 =0mm
- h1 =153mm
- h2 =153mm
- h3 =607mm
- h4 =76mm
- h5 =160mm
- h6 =0mm
- h7 =0mm

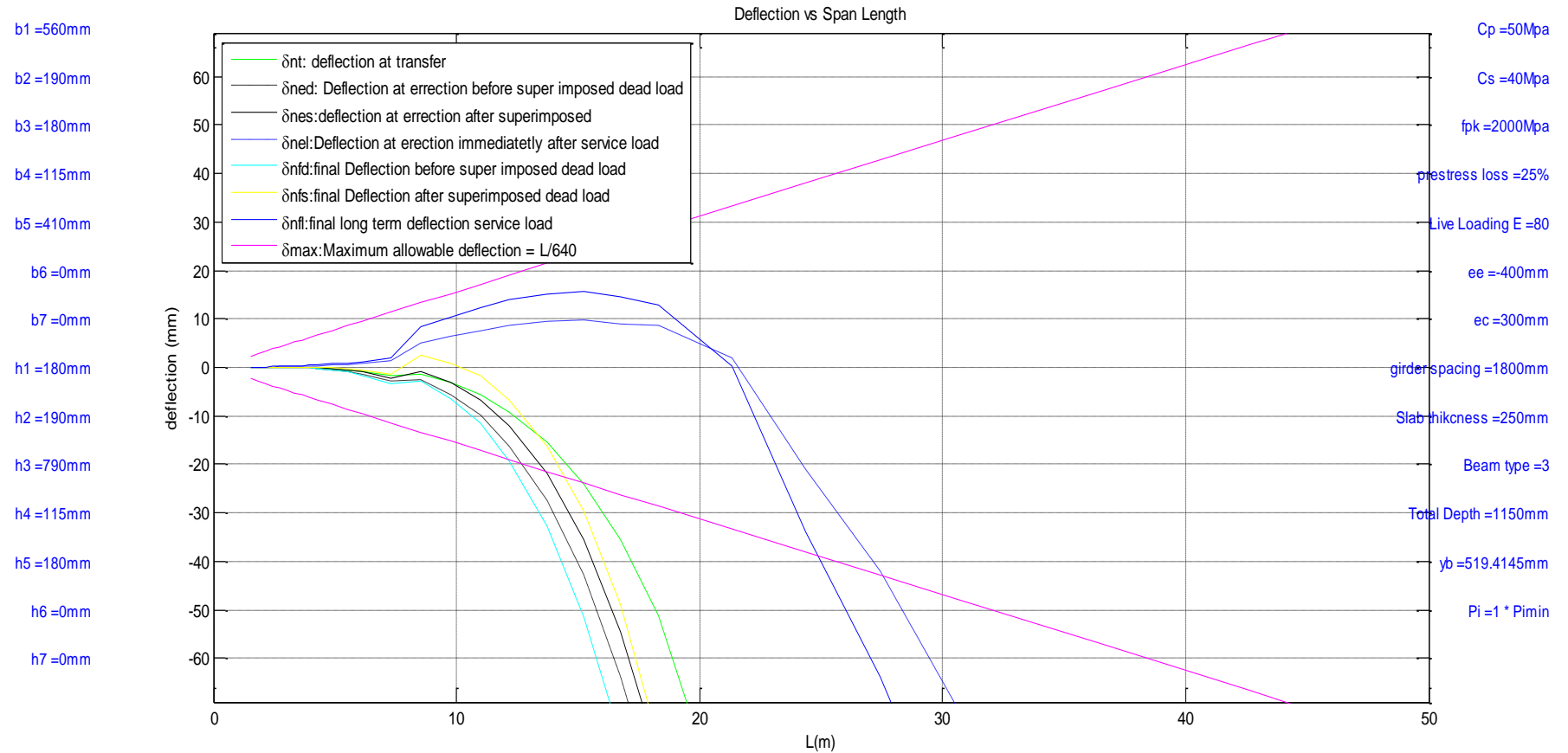


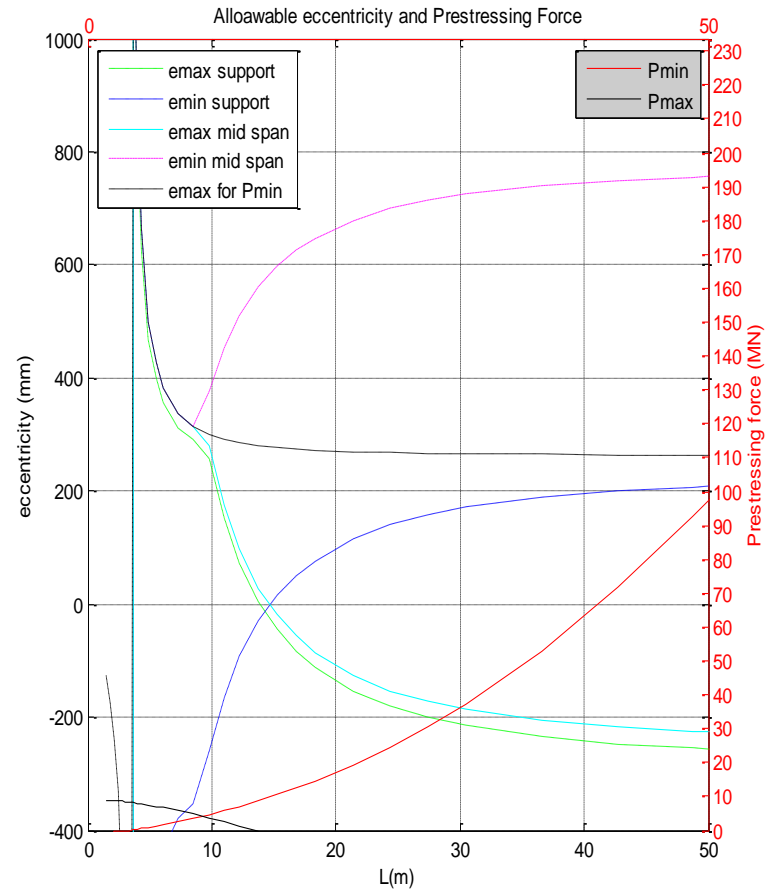
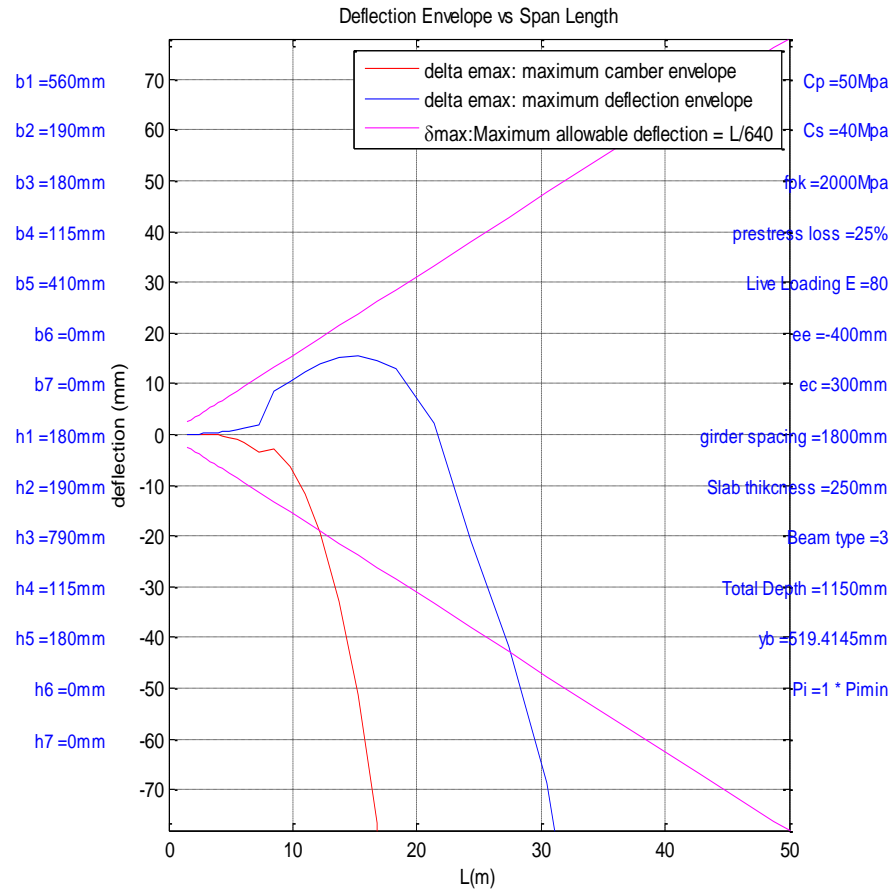


AASHTO/PCI I beam Type III

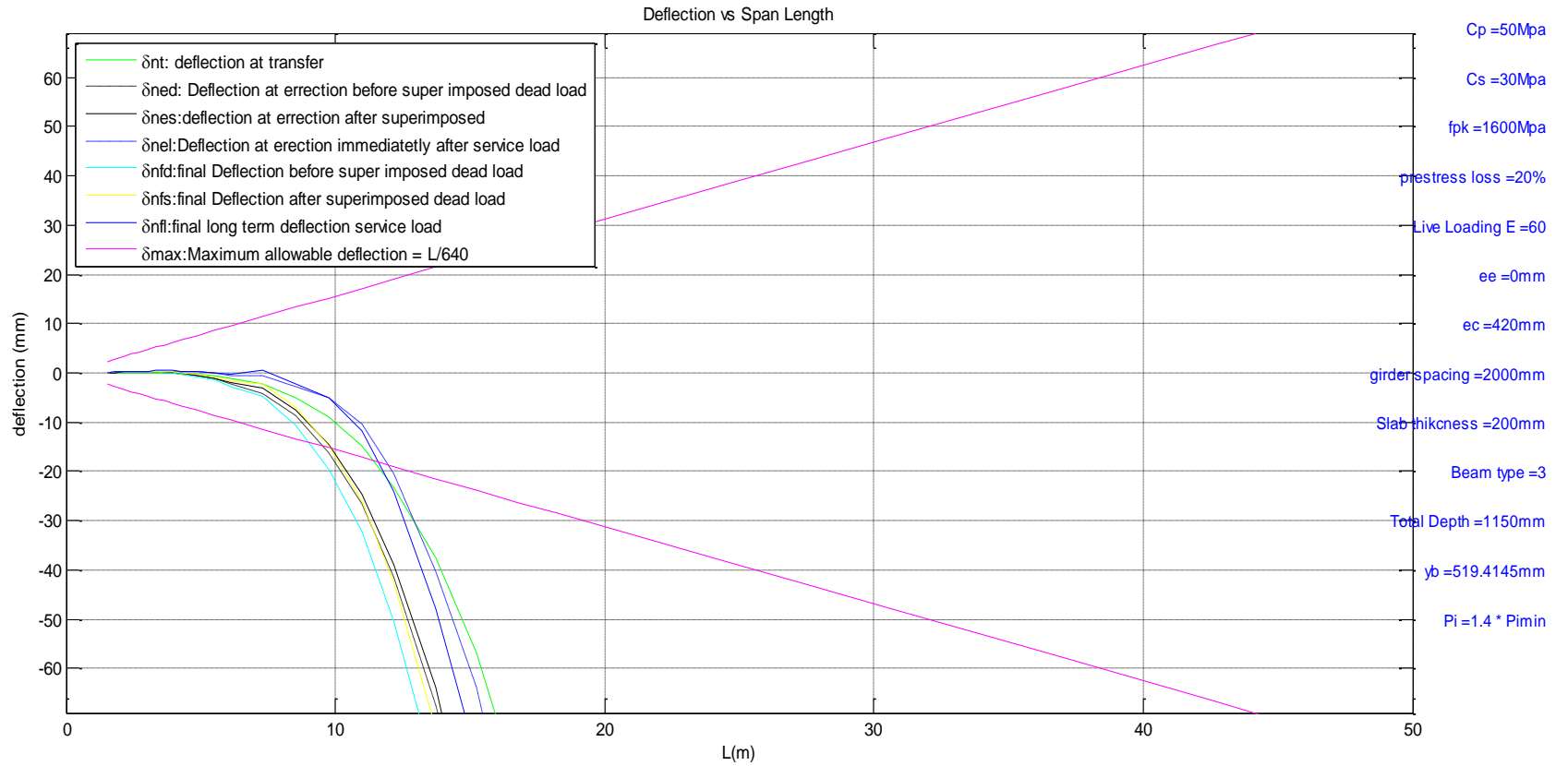


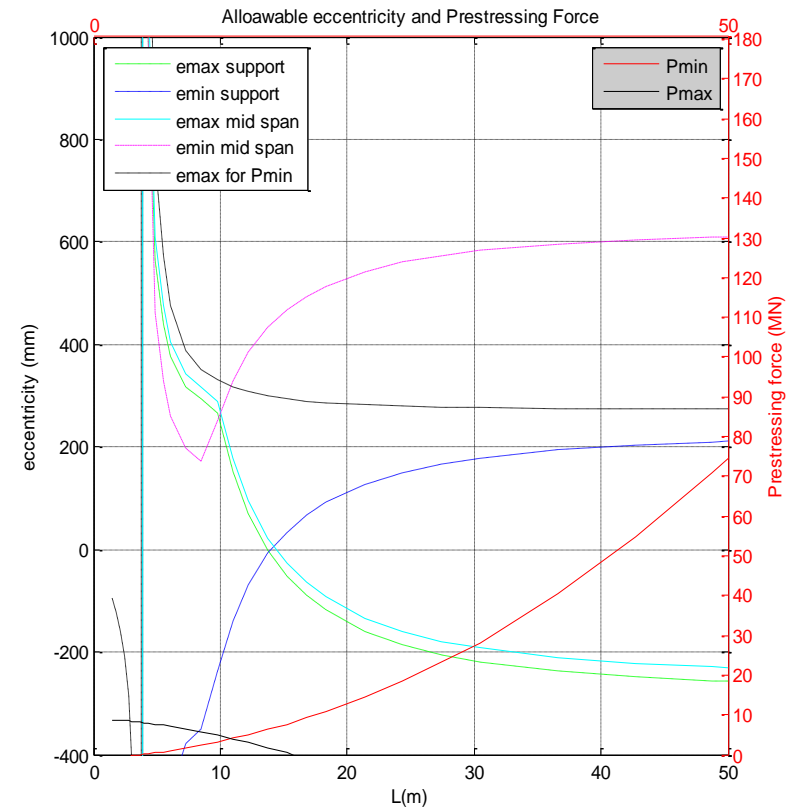
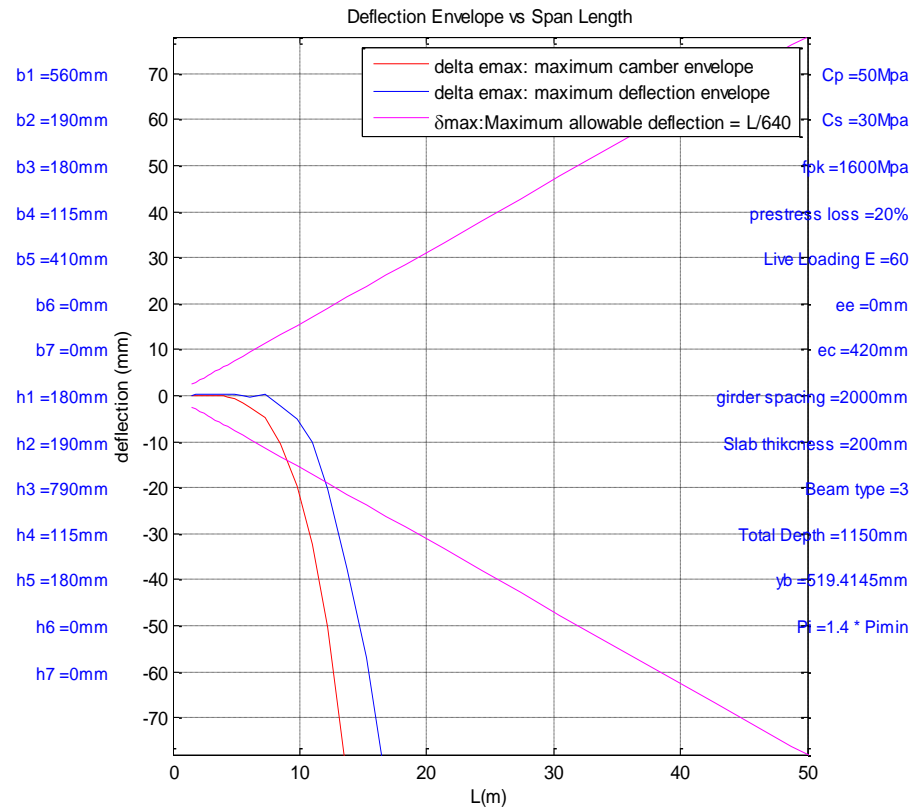






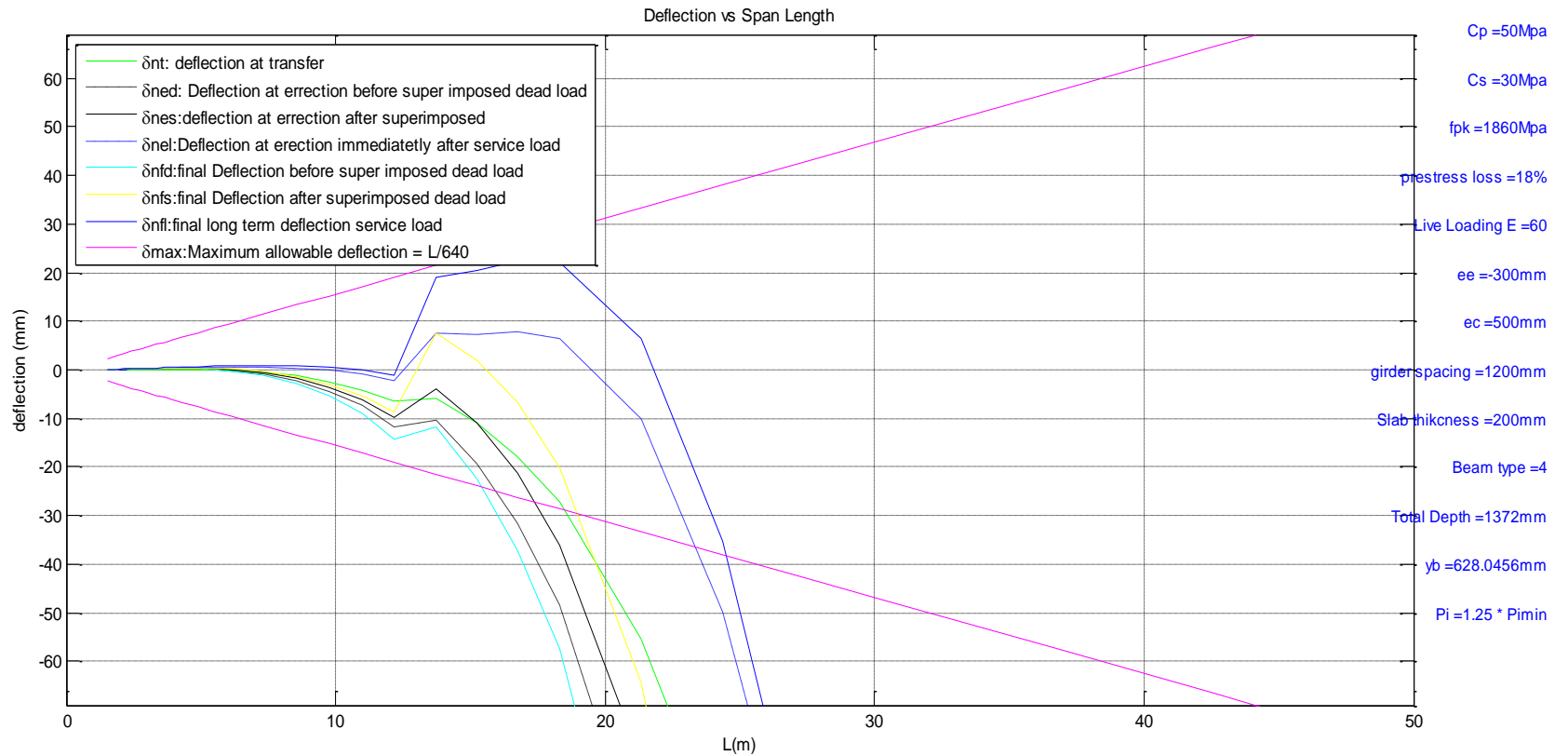
- b1 =560mm
- b2 =190mm
- b3 =180mm
- b4 =115mm
- b5 =410mm
- b6 =0mm
- b7 =0mm
- h1 =180mm
- h2 =190mm
- h3 =790mm
- h4 =115mm
- h5 =180mm
- h6 =0mm
- h7 =0mm

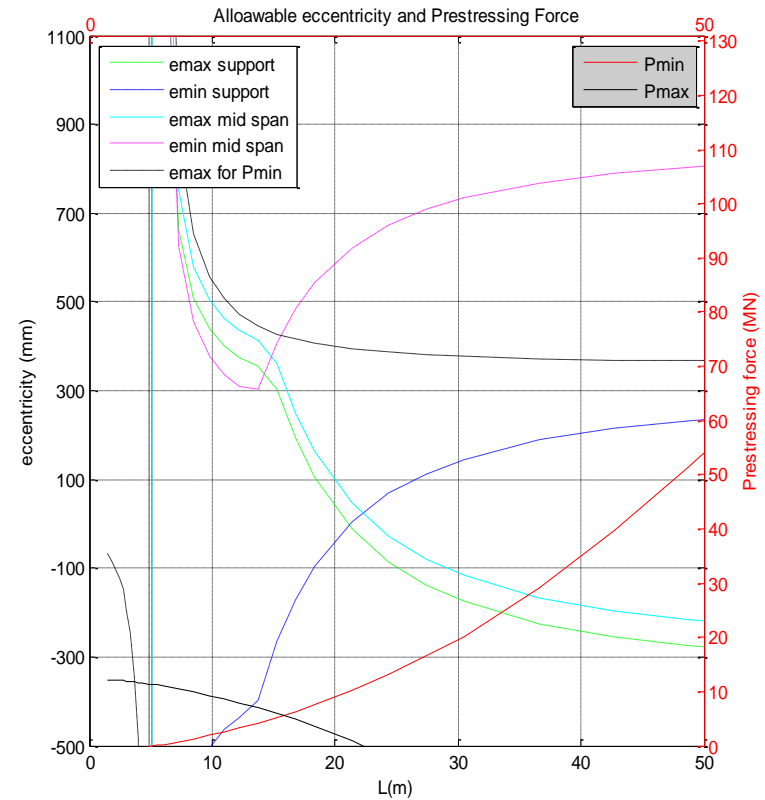
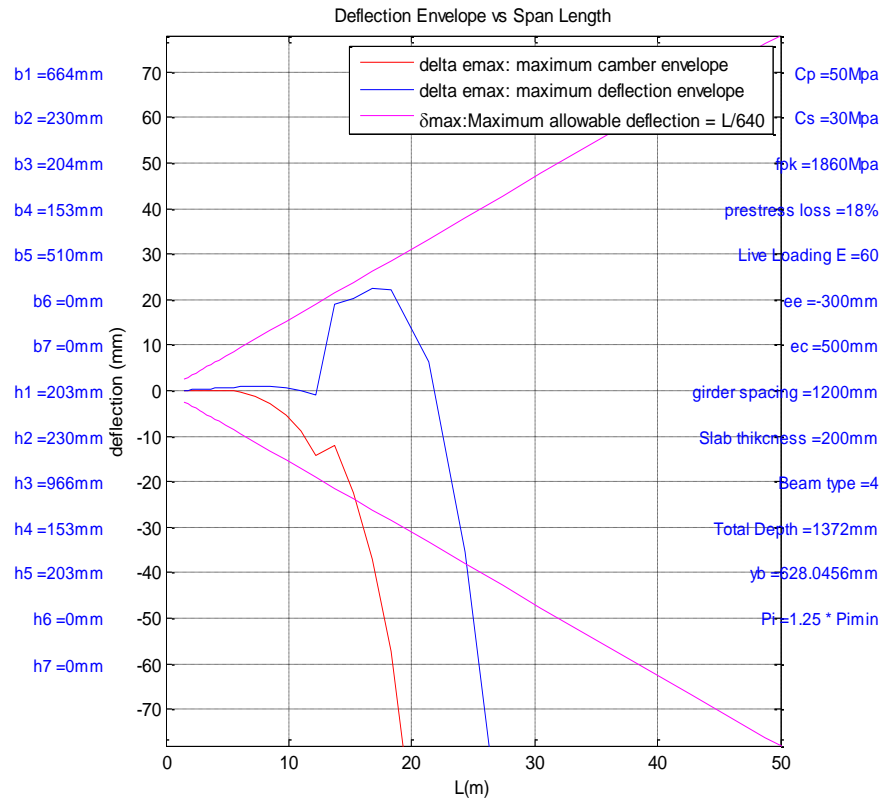


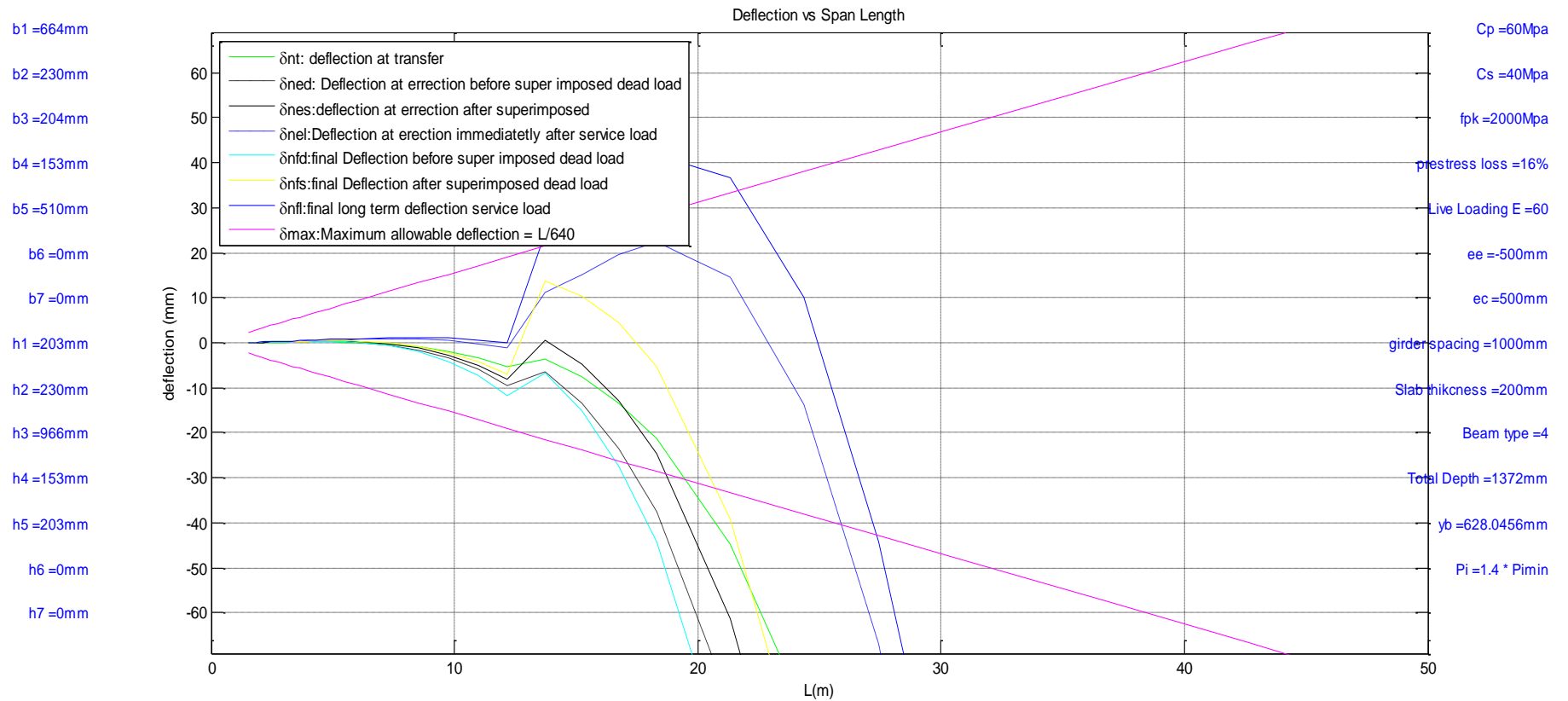


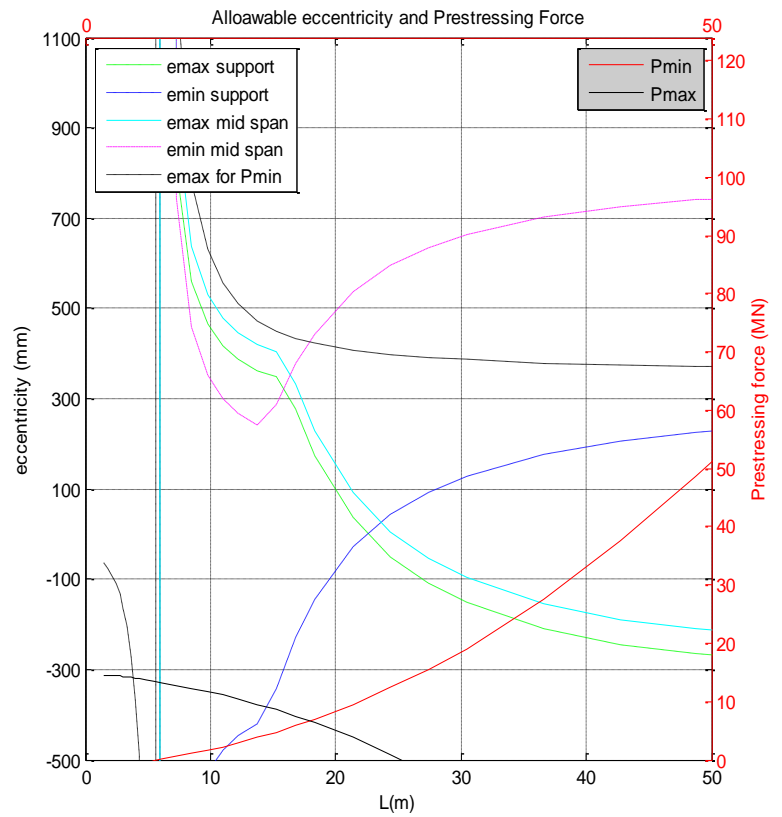
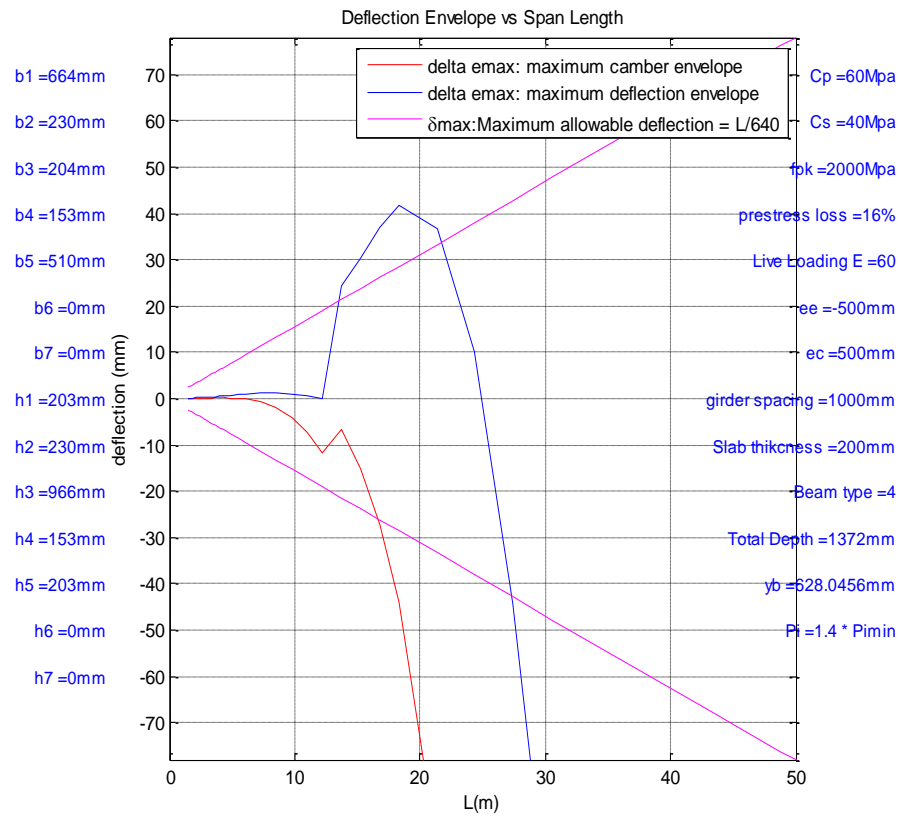
AASHTO/PCI I beam Type IV

- b1 =664mm
- b2 =230mm
- b3 =204mm
- b4 =153mm
- b5 =510mm
- b6 =0mm
- b7 =0mm
- h1 =203mm
- h2 =230mm
- h3 =966mm
- h4 =153mm
- h5 =203mm
- h6 =0mm
- h7 =0mm

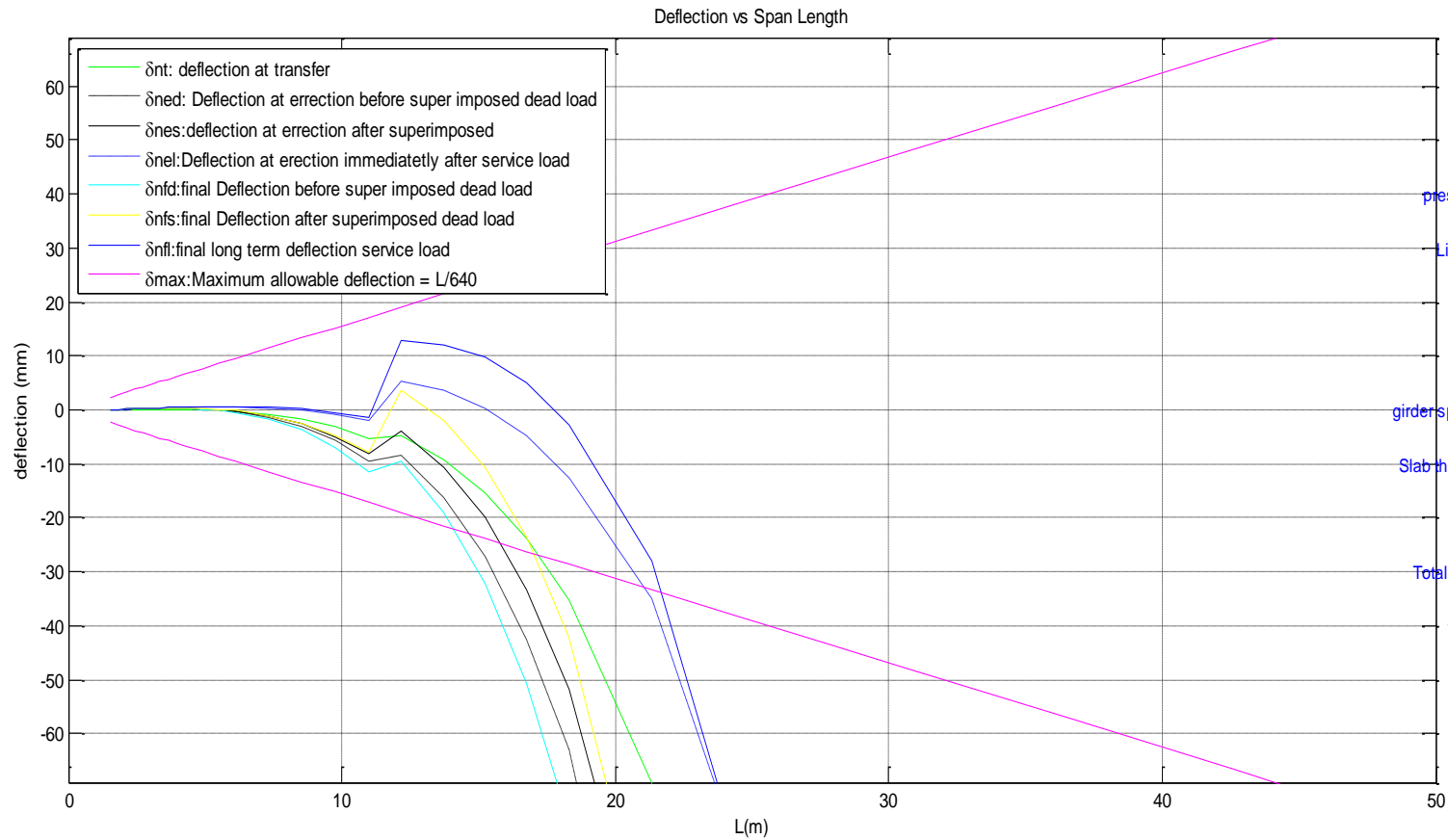


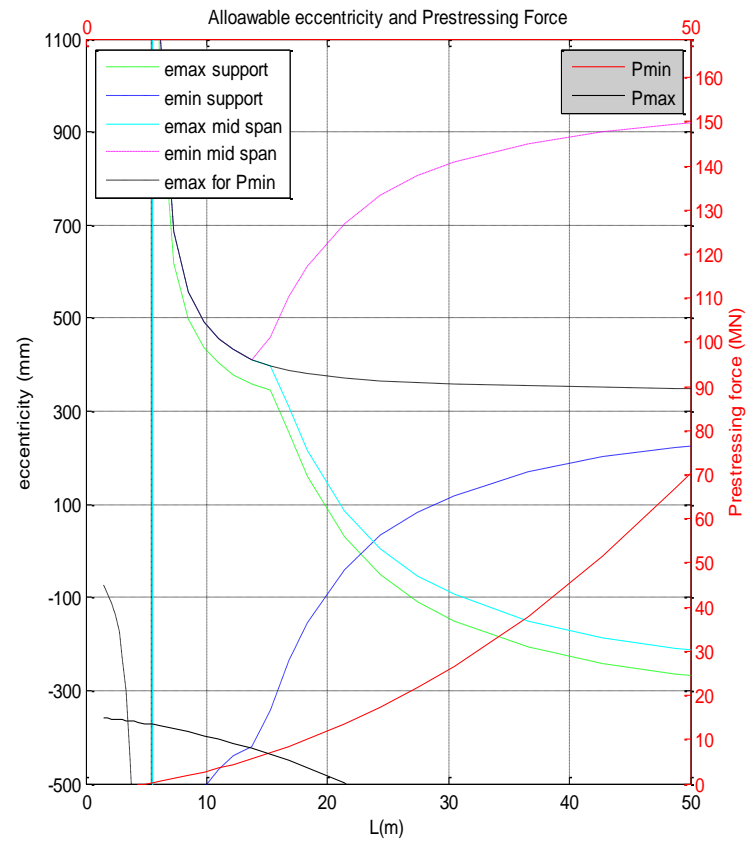
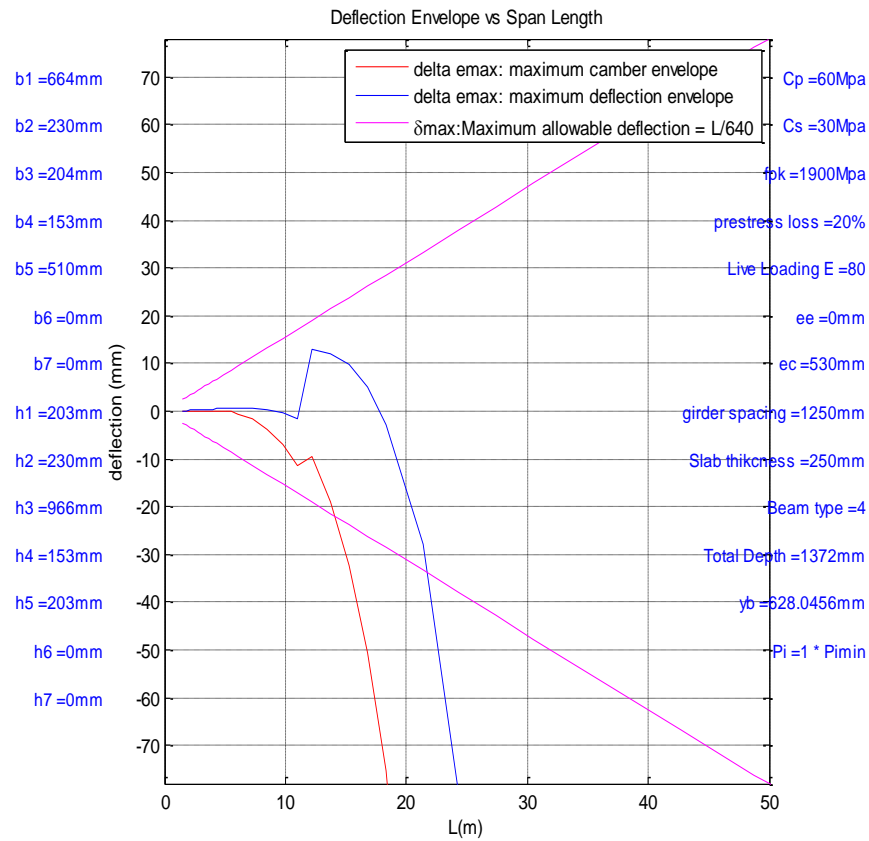






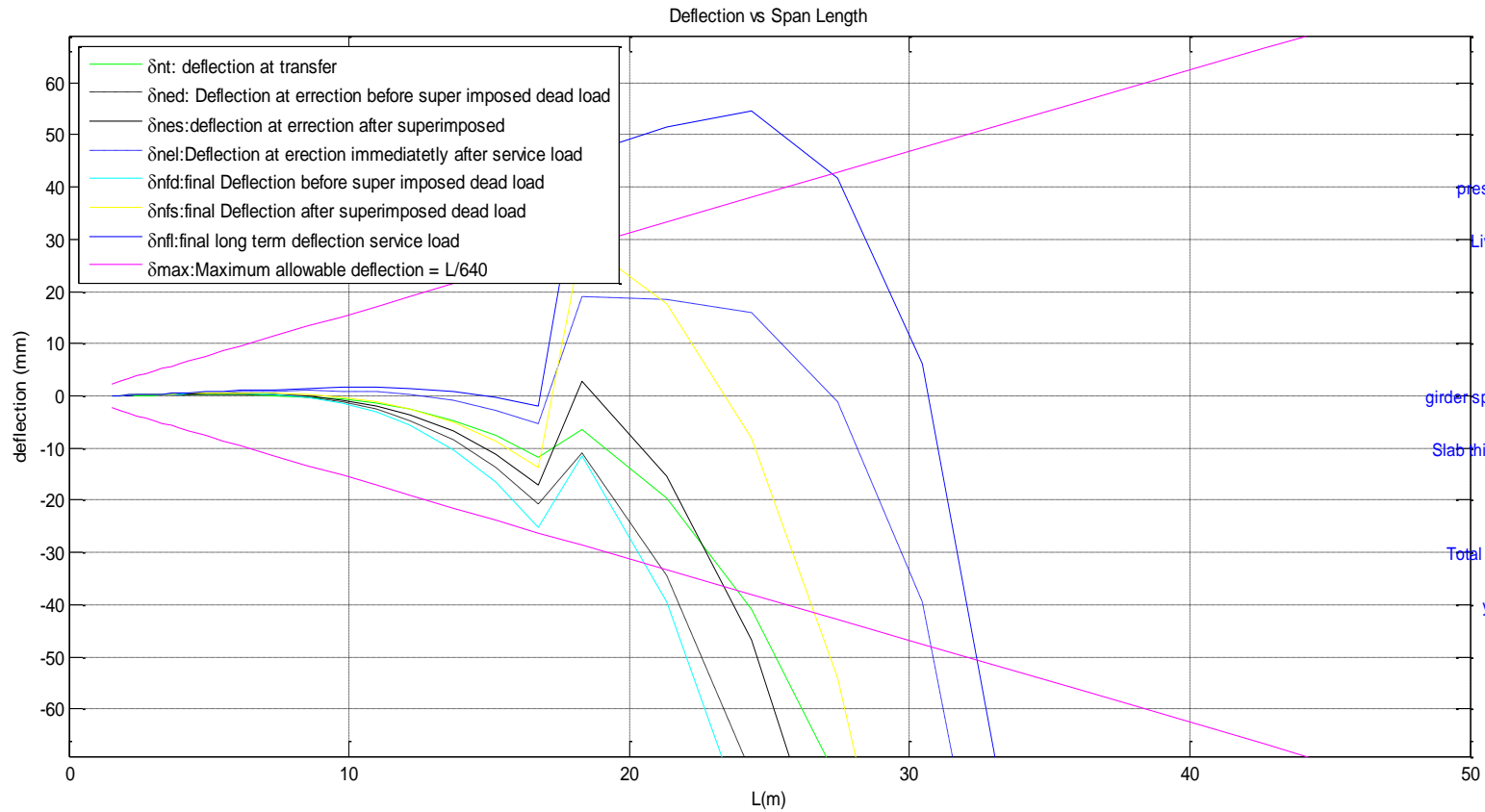
b1 =664mm
 b2 =230mm
 b3 =204mm
 b4 =153mm
 b5 =510mm
 b6 =0mm
 b7 =0mm
 h1 =203mm
 h2 =230mm
 h3 =966mm
 h4 =153mm
 h5 =203mm
 h6 =0mm
 h7 =0mm



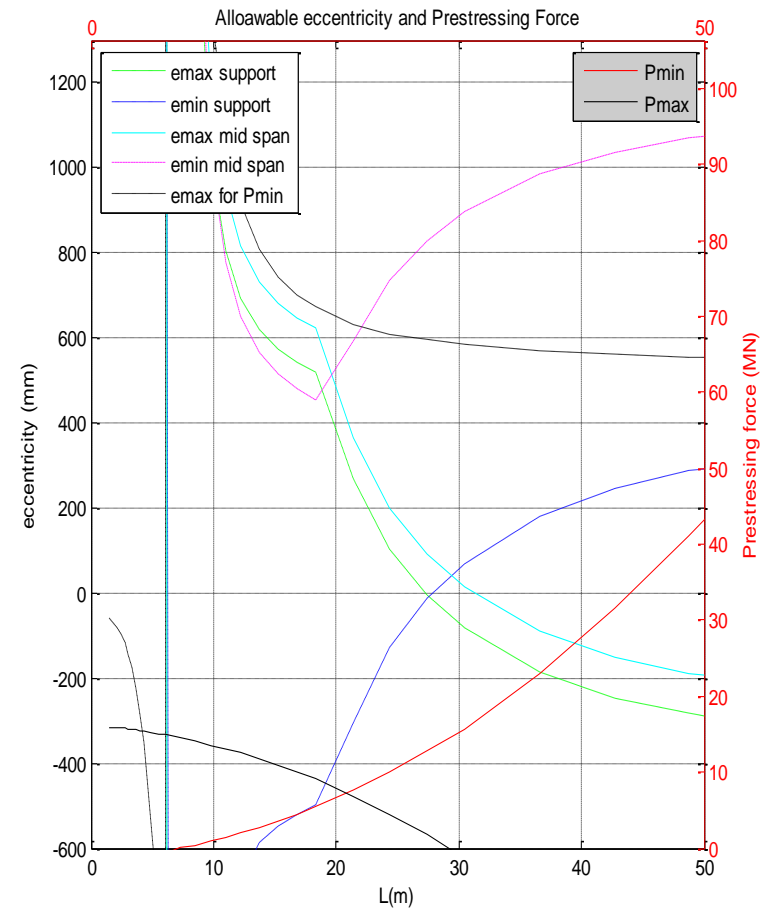
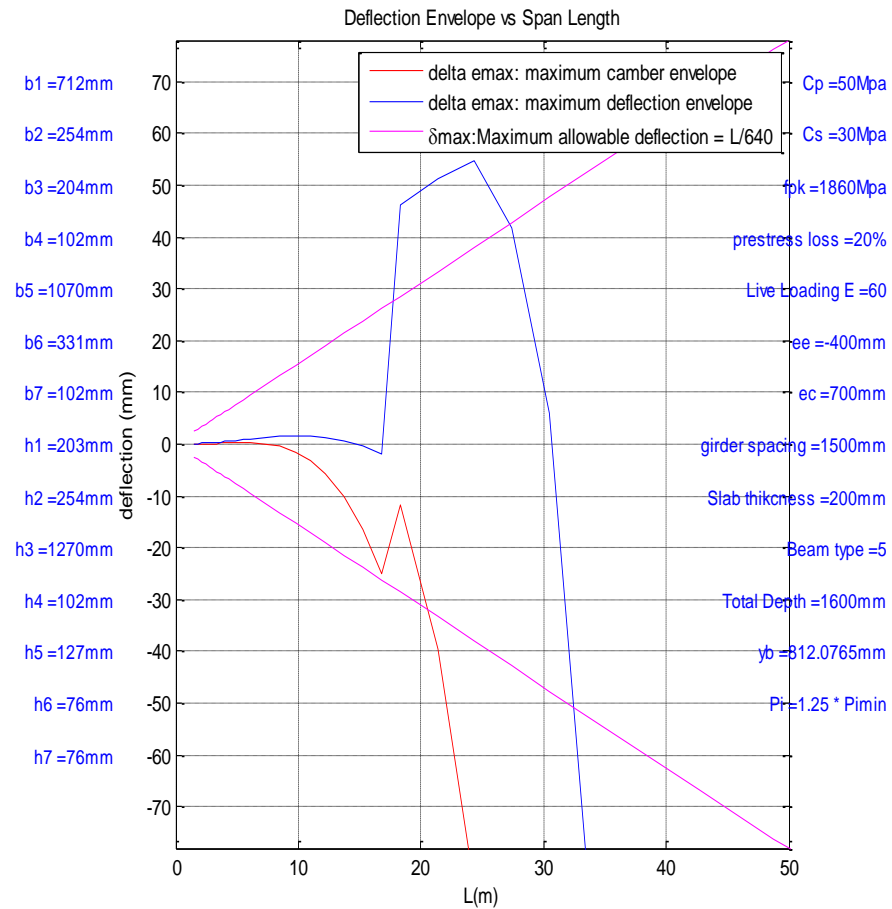


AASHTO/PCI I beam Type V

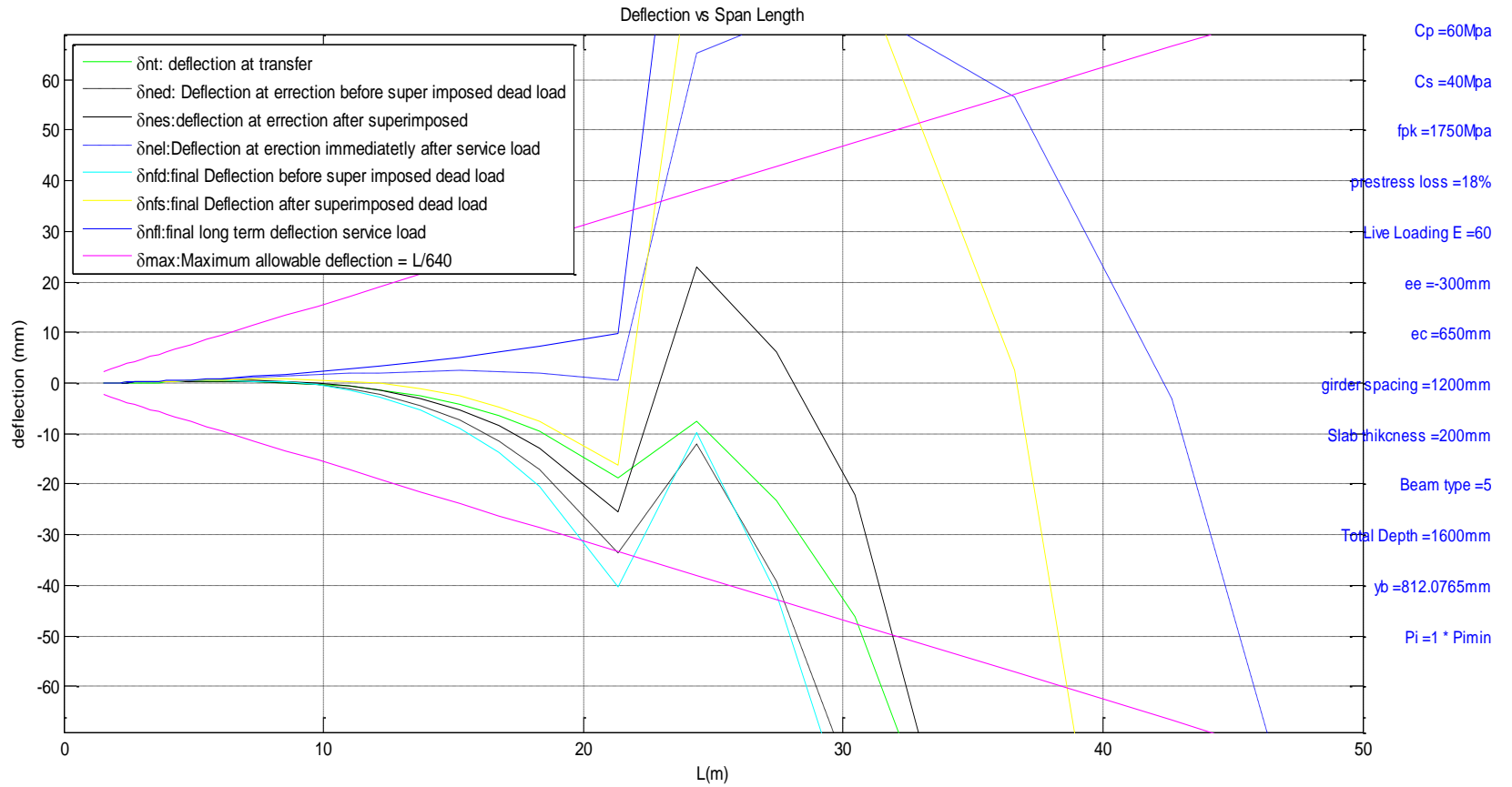
- b1 =712mm
- b2 =254mm
- b3 =204mm
- b4 =102mm
- s5 =1070mm
- b6 =331mm
- b7 =102mm
- h1 =203mm
- h2 =254mm
- s3 =1270mm
- h4 =102mm
- h5 =127mm
- h6 =76mm
- h7 =76mm

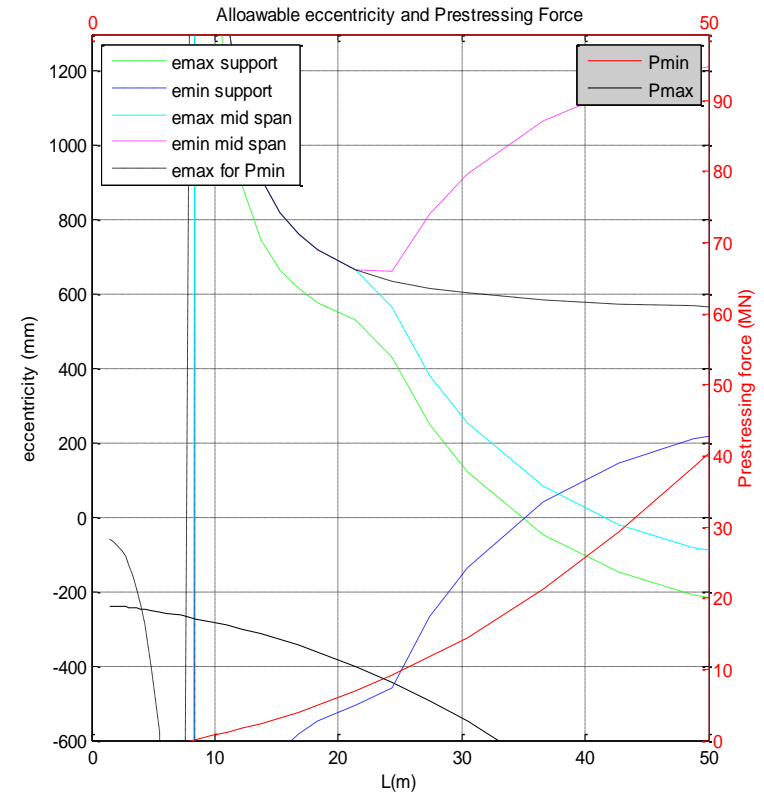
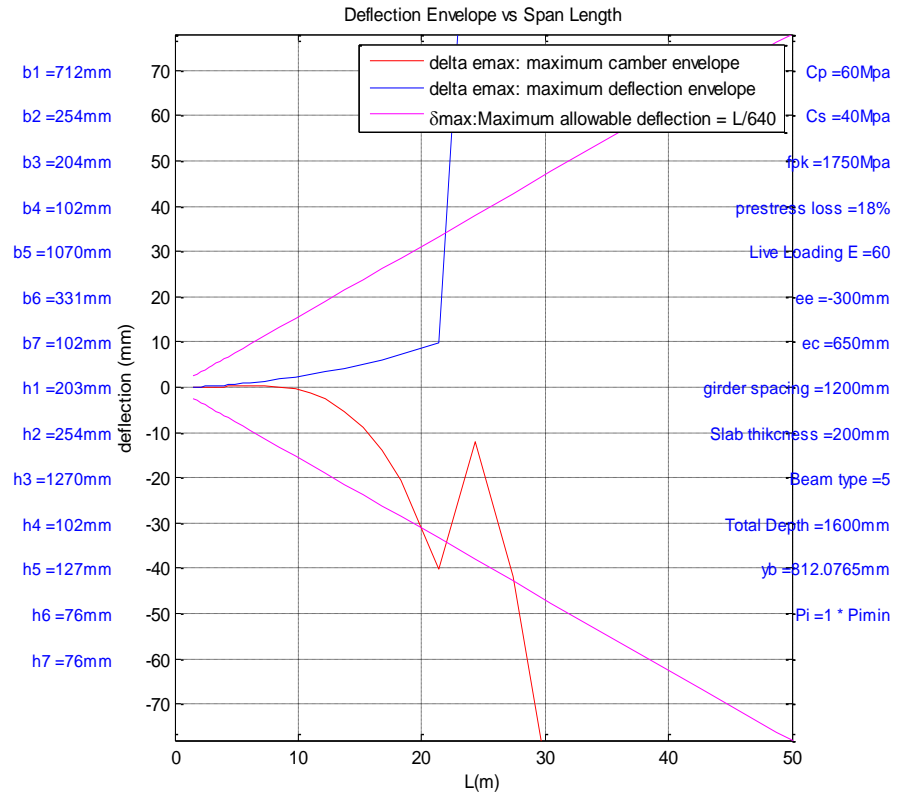


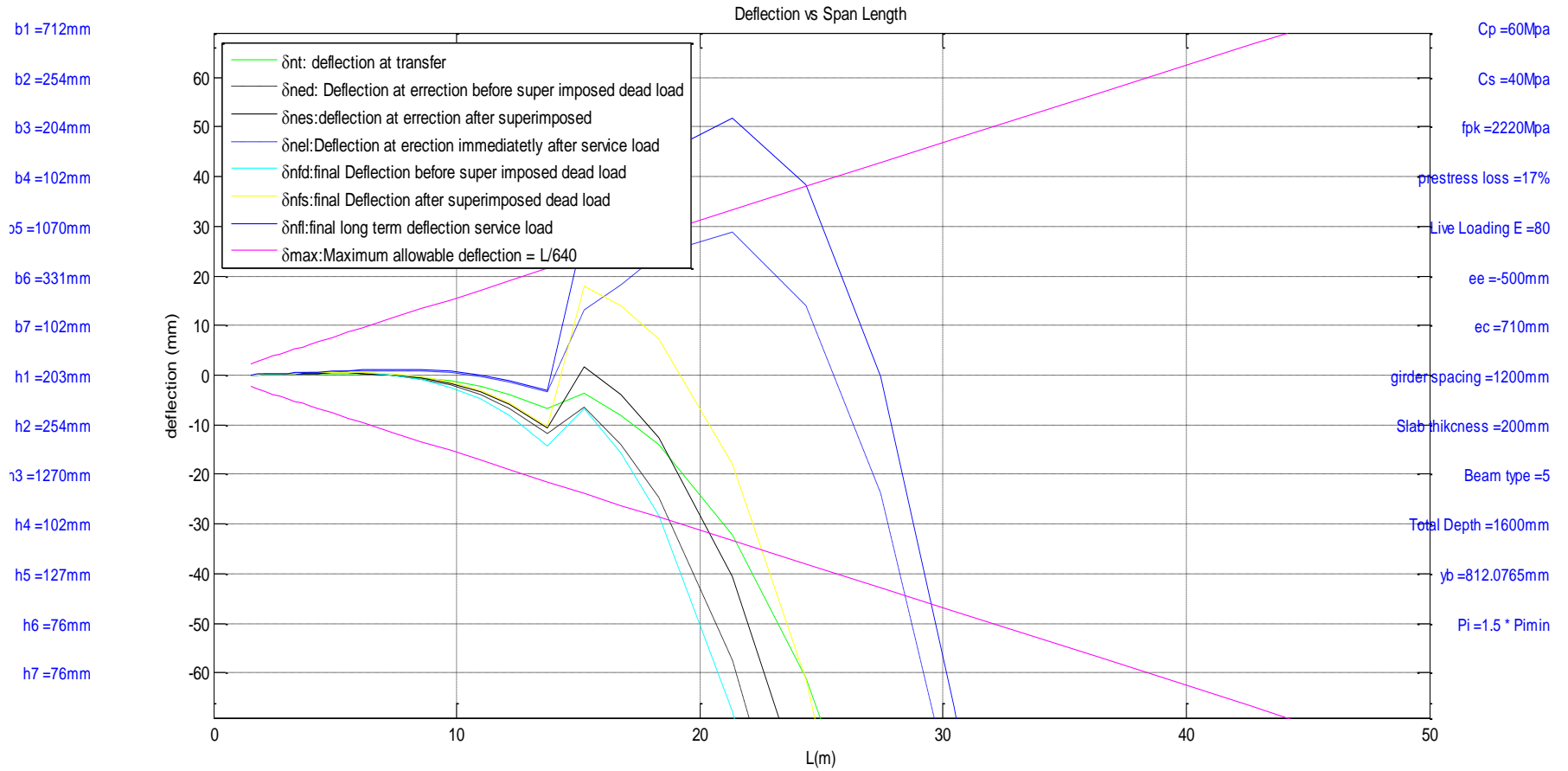
- $C_p = 50\text{Mpa}$
- $C_s = 30\text{Mpa}$
- $f_{pk} = 1860\text{Mpa}$
- prestress loss =20%
- Live Loading $E = 60$
- $e_e = -400\text{mm}$
- $e_c = 700\text{mm}$
- girders spacing =1500mm
- Slab thickness =200mm
- Beam type =5
- Total Depth =1600mm
- $y_b = 812.0765\text{mm}$
- $P_i = 1.25 * P_{imin}$

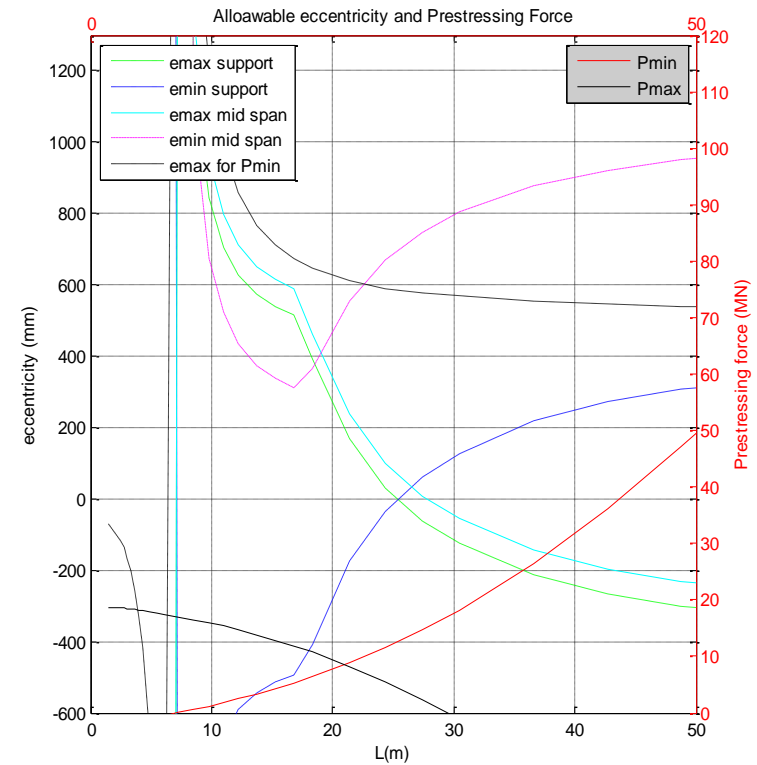
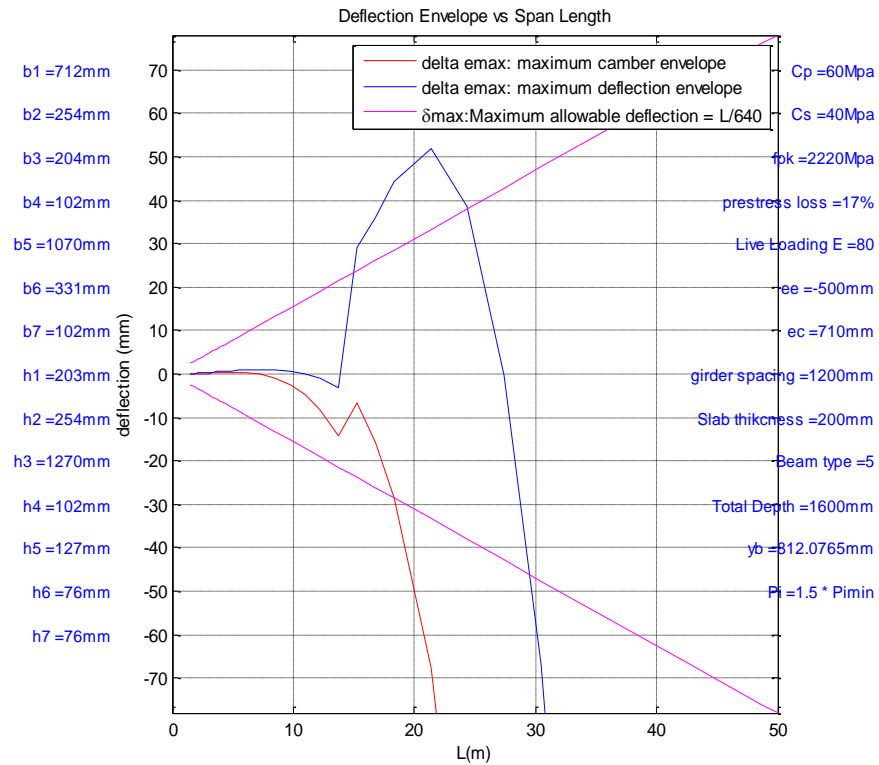


- b1 =712mm
- b2 =254mm
- b3 =204mm
- b4 =102mm
- b5 =1070mm
- b6 =331mm
- b7 =102mm
- h1 =203mm
- h2 =254mm
- h3 =1270mm
- h4 =102mm
- h5 =127mm
- h6 =76mm
- h7 =76mm

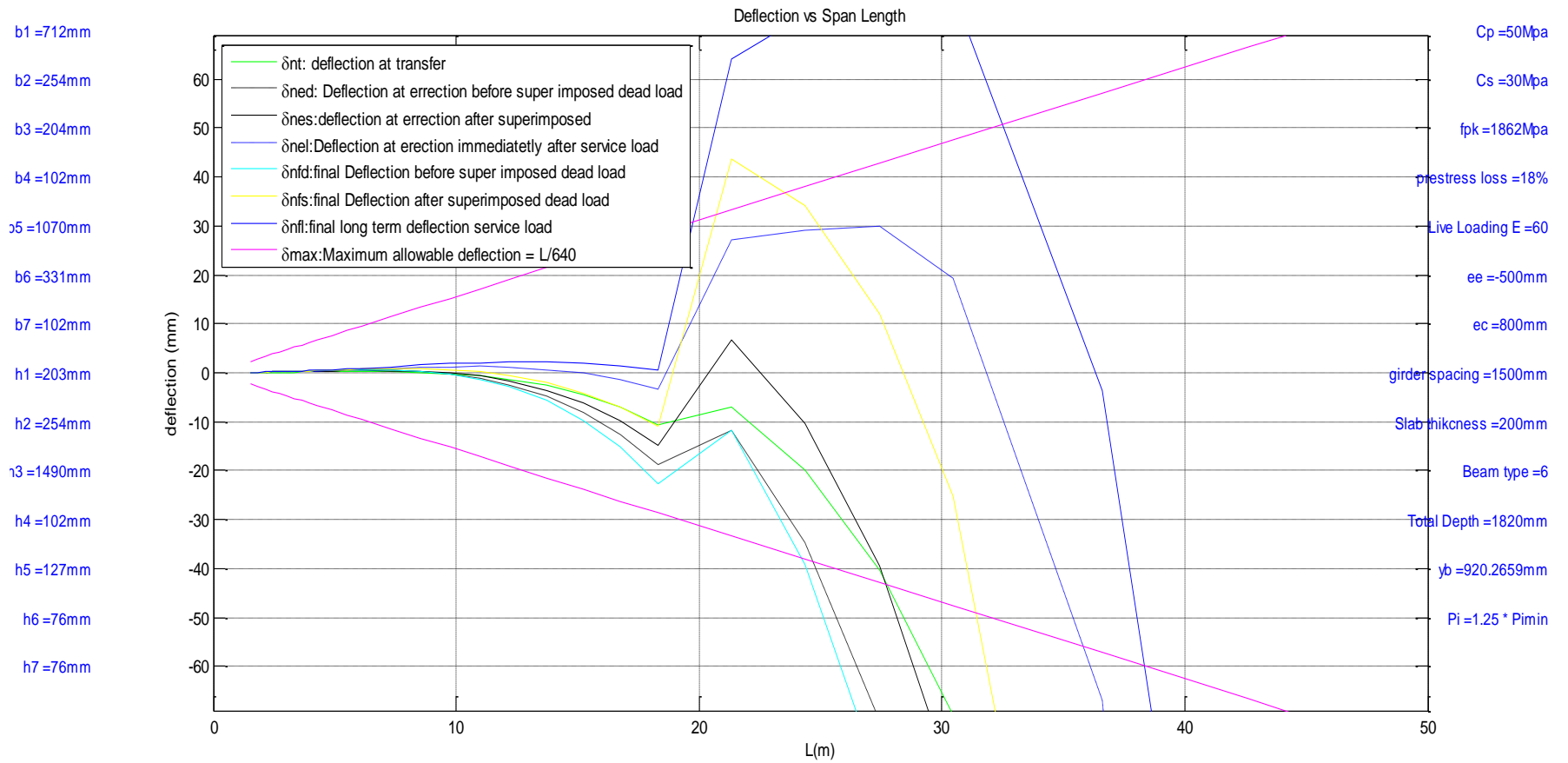


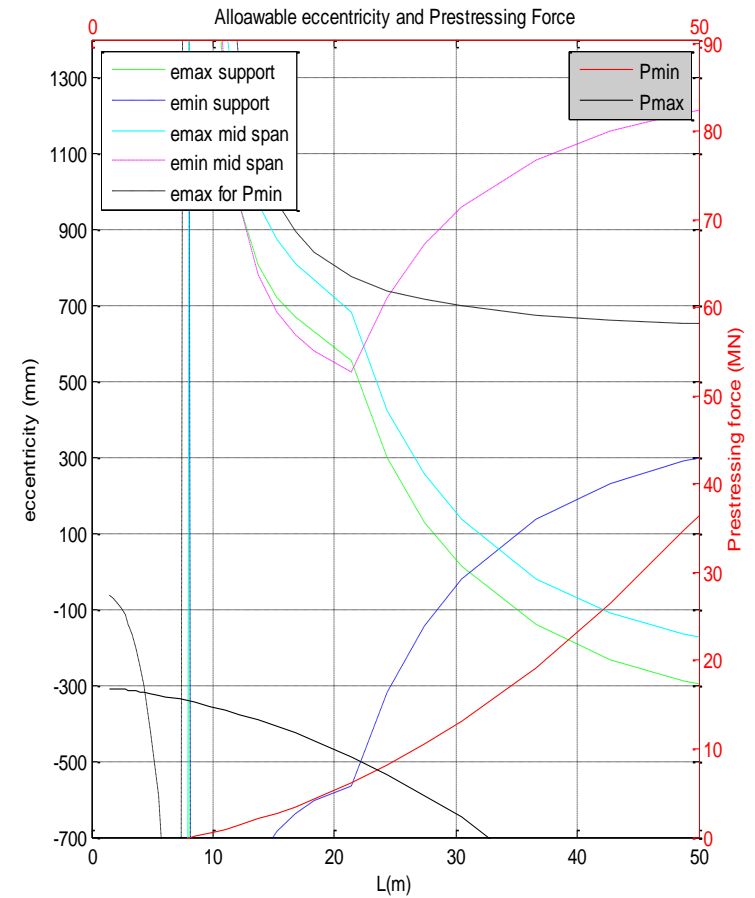
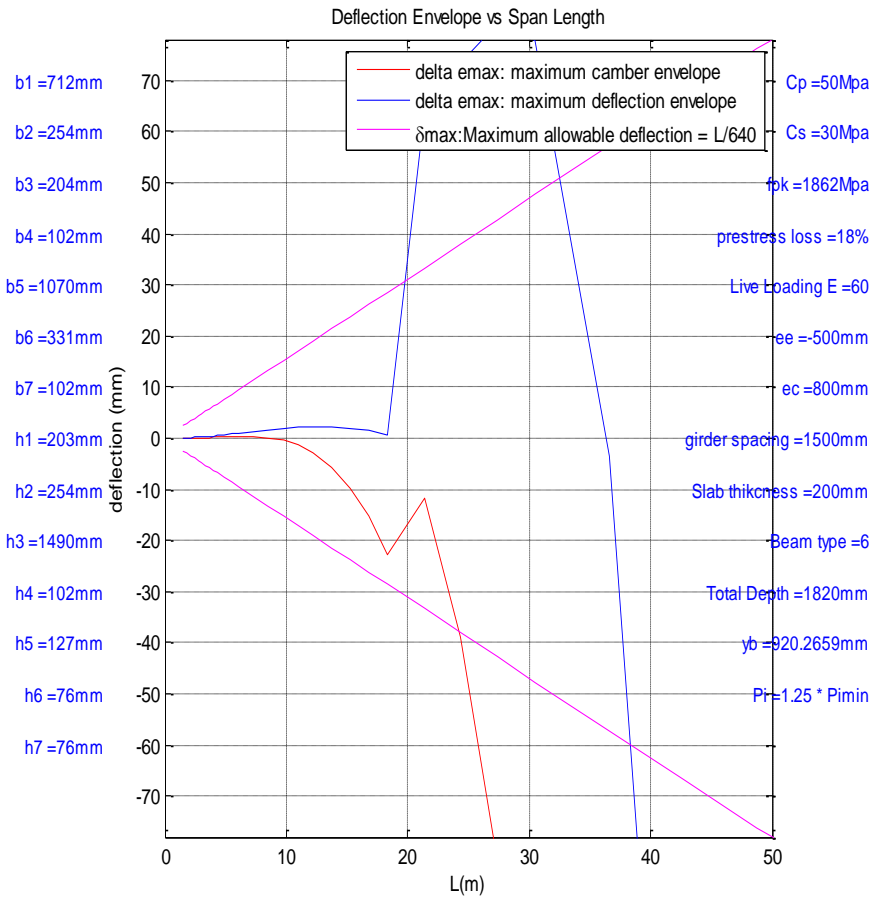


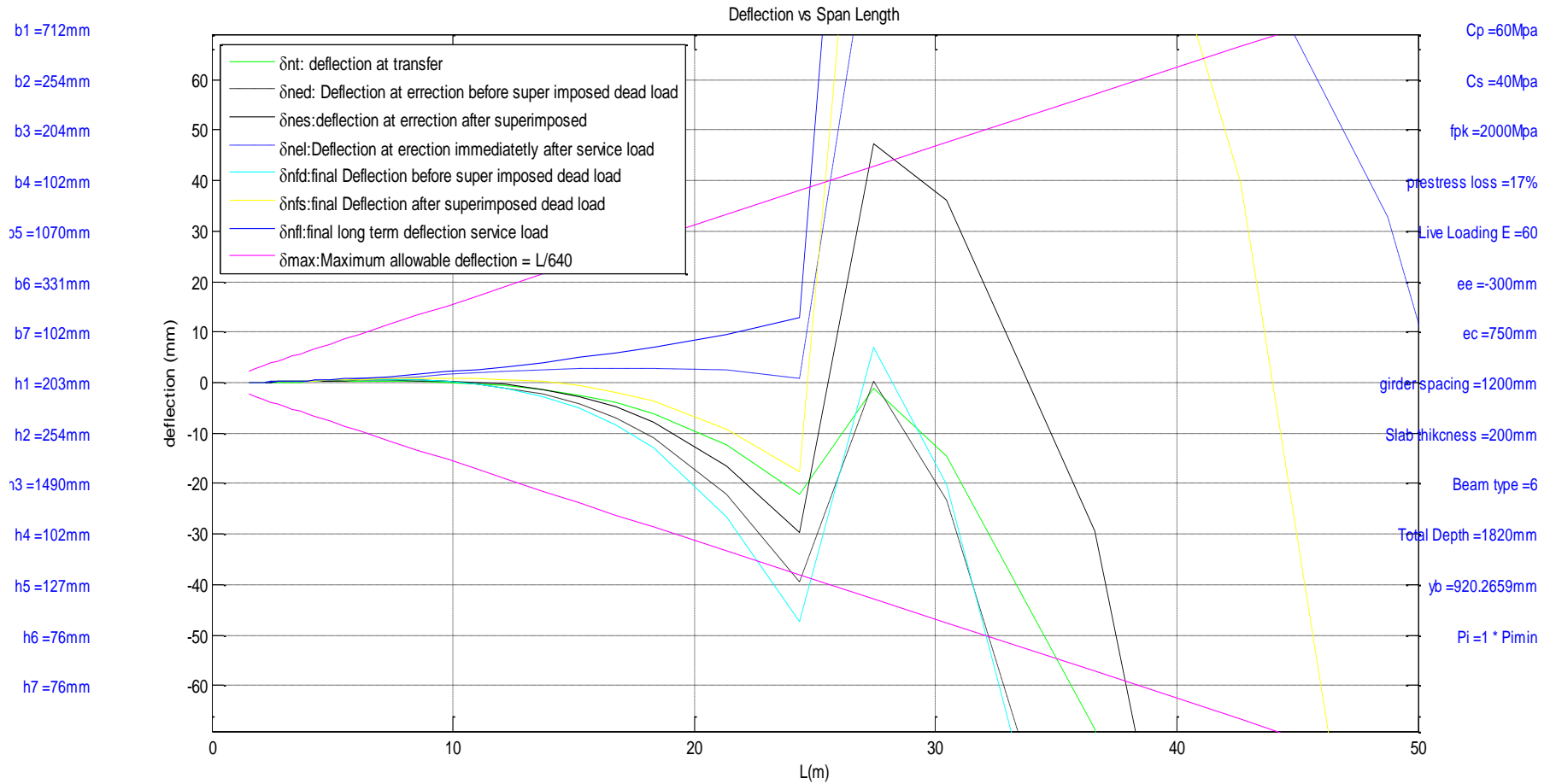


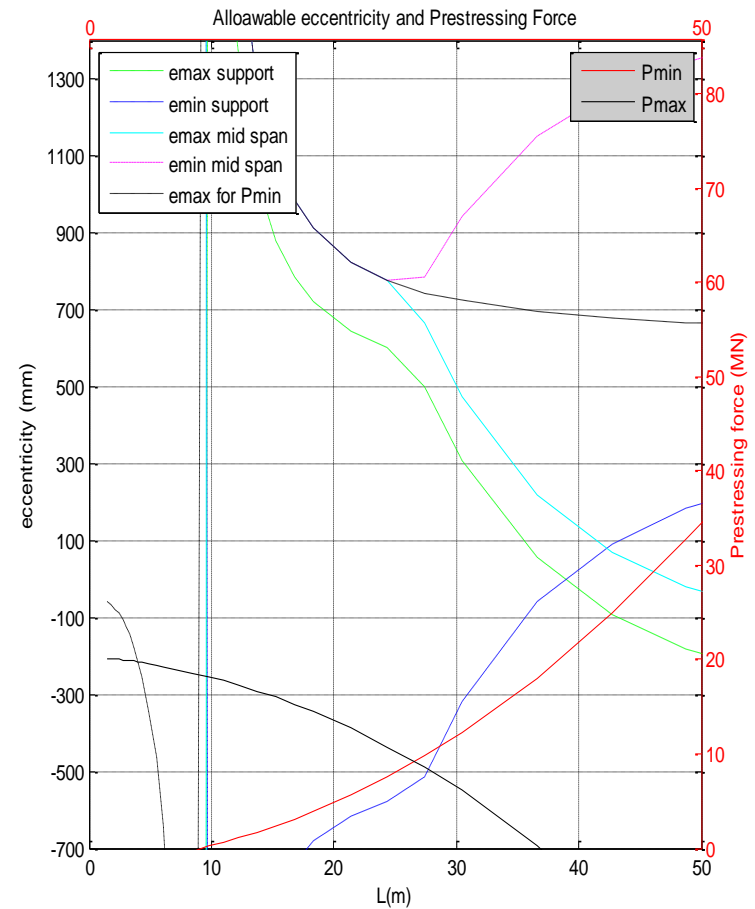
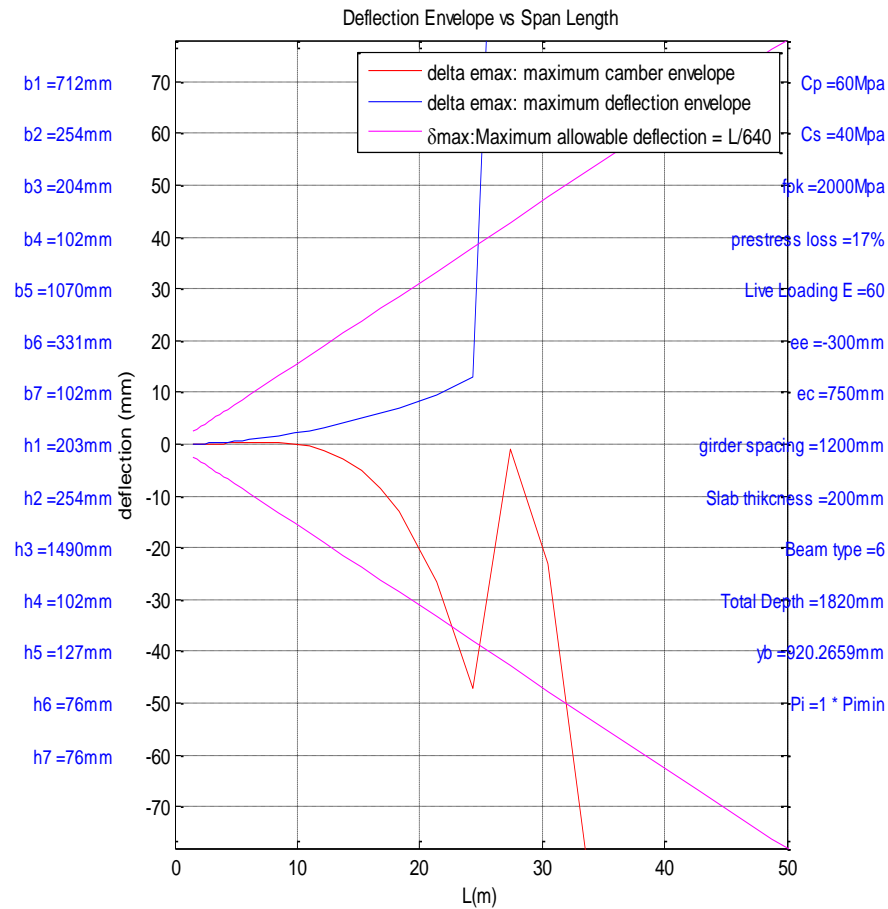


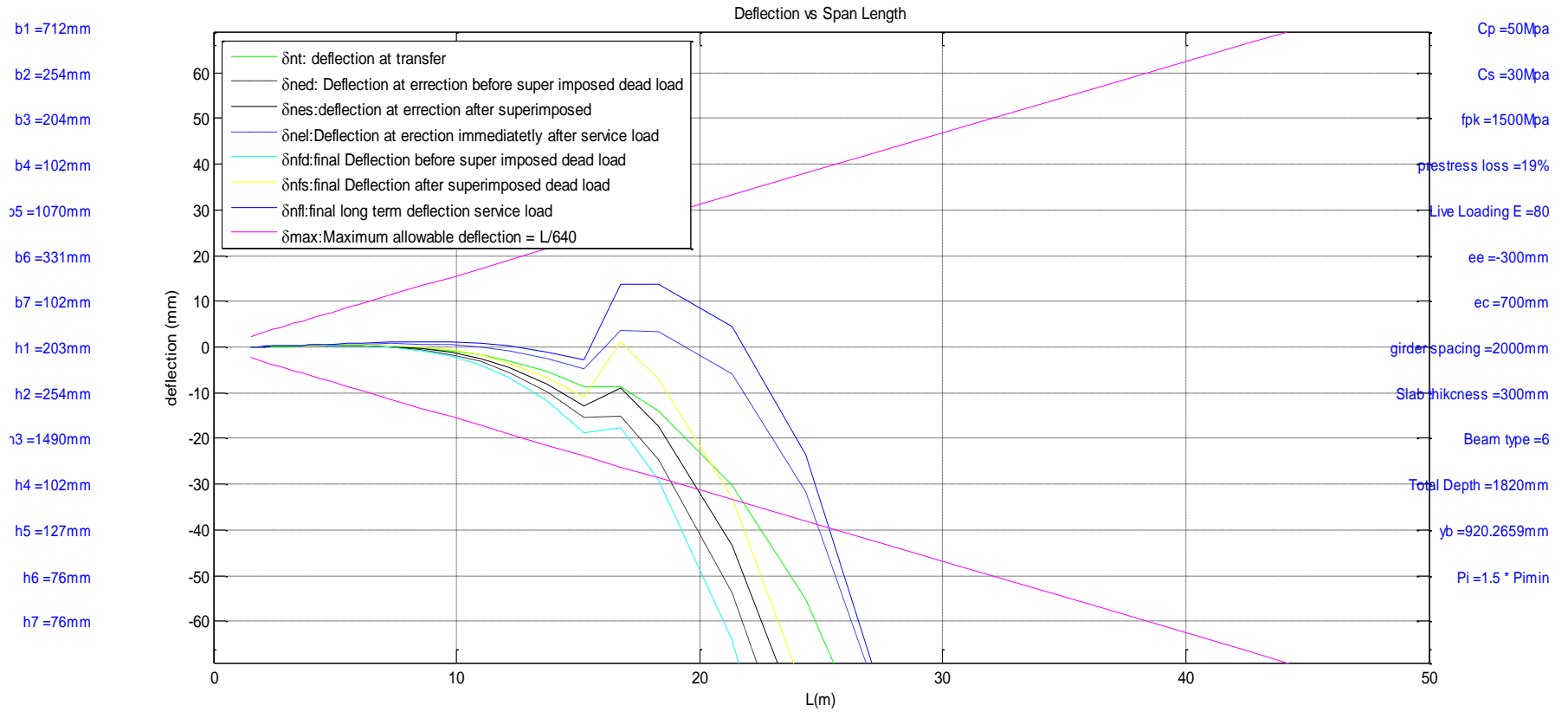
AASHTO/PCI I beam Type VI

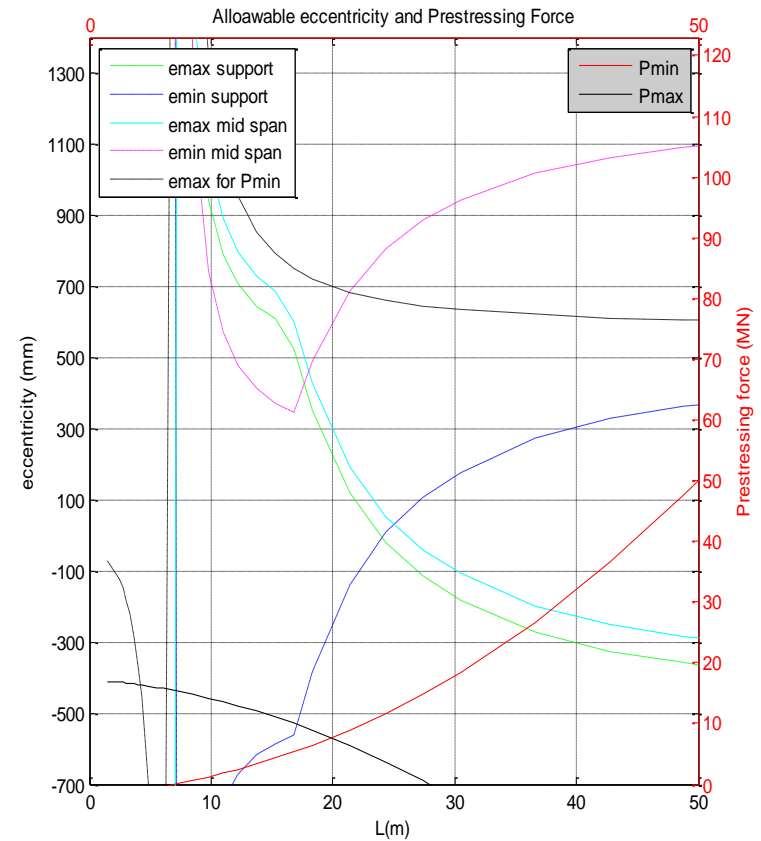
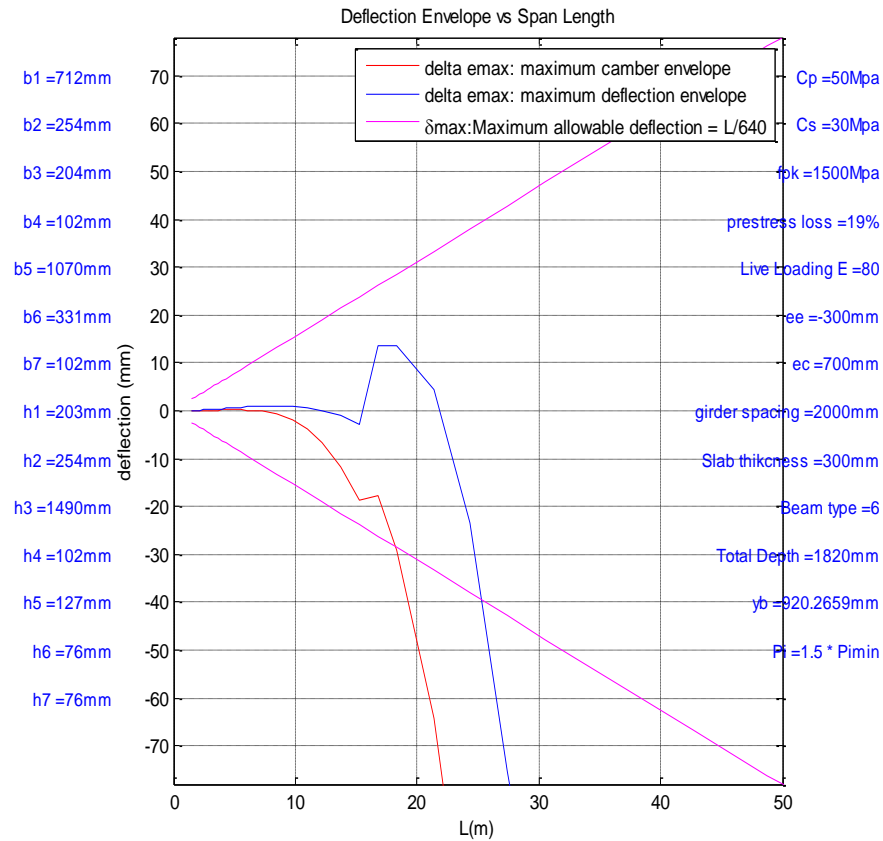












User Defined I beam

